2021 GALLIE DAY
ORAL PRESENTATIONS

1. Aadil Ali, Aizhou Wang, Rafaela V.P. Ribeiro, Cristina Baciu, Erika L. Beroncal, Marcos Galasso, Bruno Gomes, Olivia Hough, Etienne Abdelnour-Berchtold, Edson Brambate, Vinicius Michaelsen, Yu Zhang, Anajara Gazzalle, Tom Waddell, Mingyao Liu, Ana C. Andreazza, Shaf Keshavjee, Marcelo Cypel: EXTENDED COLD LUNG PRESERVATION WITH IMPROVED MITOCHONDRIAL HEALTH: PRE-CLINICAL STUDIES AND TRANSLATION TO HUMAN LUNG TRANSPLANTATION (TR)

2. David Burns (SSTP), Philip Boyer, Helen Razmjou, Robin Richards, Cari Whyne: IMPROVING PHYSIOTHERAPY ADHERENCE WITH WEARABLE DEVICES AND MACHINE LEARNING FROM CONCEPTION TO COMMERCIALIZATION

3. Jonathon Chon Teng Chio, Jian Wang, Vithushan Surendran, Lijun Li, Mohammad-Masoud Zavvarian, Kataryzna Pieczonka, Michael G. Fehlings: DELAYED ADMINISTRATION OF HIGH DOSE HUMAN IMMUNOGLOBULIN G REDUCES NEUROINFLAMMATION AND IMPROVES FUNCTIONAL RECOVERY AFTER TRAUMATIC CERVICAL SPINAL CORD INJURY (TR)

4. Benjamin Davidson (SSTP), Peter Giacobbe, Clement Hamani, Nir Lipsman: DEEP BRAIN STIMULATION OF THE NUCLEUS ACCUMBENS IN THE TREATMENT OF SEVERE ALCOHOL USE DISORDER: TARGETING THE BRAIN'S REWARD SYSTEM TO TREAT ADDICTION

5. Dhruvin H. Hirpara, Biniam Kidane, Alexandre Louie, Victoria Zuk, Gail Darling, Mathieu Rousseau, Tyler Chesney, Natalie Coburn, Julie Hallet : STEREOTACTIC BODY RADIOTHERAPY VERSUS SURGERY IN OLDER ADULTS WITH NON-SMALL CELL LUNG CANCER – A POPULATION-BASED, MATCHED ANALYSIS OF LONG-TERM DEPENDENCY OUTCOMES

6. Jethro C.C. Kwong, Adree Khondker, Christopher Tran, Emily Evans, Amna Ali, Munir Jamal, Thomas Short, Frank Papanikolaou, John R. Srigley, Andrew H. Feifer: USING EXPLAINABLE ARTIFICIAL INTELLIGENCE TO DEVELOP AN INTERPRETABLE MACHINE LEARNING MODEL TO PREDICT RISK OF SIDE-SPECIFIC EXTRAPROSTATIC EXTENSION IN MEN WITH PROSTATE CANCER

7. Deanna Ng, Karineh Kazazian, Olga Brashavitskaya, Kiera Lee, Aiman Ali, Karina Pacholczyk, Shelly Luu (SSTP), Michelle Lee, Monica Hasegan, Savtaj Brar, Marco Magalhaes, Carol J. Swallow: POLO-LIKE KINASE 4 (PLK4) PROMOTES PERITONEAL METASTASIS THROUGH ACTIVATION OF THE RAC1 GUANINE NUCLEOTIDE EXCHANGE FACTOR PREX2

8. Rafaela V.P. Ribeiro, Terrance Ku, Aizhou Wang, Layla Pires, Victor H. Ferreira, Vinicius Michaelsen, Aadil Ali, Marcos Galasso, Sajad Moshkelgosha, Anajara Gazzalle, Mingyao Liu, Lianne G. Singer, Deepali Kumar, Shaf Keshavjee, John Sinclair, Thomas Kledal, Atul Humar, Marcelo Cypel: EX VIVO TREATMENT OF CYTOMEGALOVIRUS IN HUMAN DONOR LUNGS USING A NOVEL CHEMOKINE-BASED IMMUNOTOXIN

9. Moaath Saggaf (SSTP), Aaron M. Drucker, Christine B. Novak, Larry R. Robinson, Dimitri J. Anastakis: THE CLINICAL PREDICTORS OF COLD SENSITIVITY AND THE IMPACT OF CARPAL TUNNEL RELEASE IN PATIENTS WITH CARPAL TUNNEL SYNDROME

10. Houman Tahmasebi, Arash Azin, Amanpreet Brar, Gary Ko, Sam Azin, Andrea Covelli, Tulin Cil: RACIAL AND SOCIOECONOMIC DISPARITIES IN BREAST CANCER DIAGNOSIS, TREATMENT, AND PROGNOSIS: A SEER-BASED POPULATION STUDY

11. Jeffrey A. Zuccato (SSTP), Vikas Patil, Sheila Mansouri, Jeffrey C. Liu, Farshad Nassiri (SSTP), Yasin Mamatjan, Ankur Chakravarthy, Shirin Karimi, Joao Paulo Almedia, Anne-Laure Bernat, Mohammed Hasen, Shahbaz Khan, Thomas Kislinger, Namita Sinha, Sébastien Froelich, Homa Adle-Biassette, Kenneth D Aldape, Daniel D De Carvalho, Gelareh Zadeh: METHYLATION BASED PROGNOSTIC SUBTYPES OF CHORDOMA TUMORS IN TISSUE AND PLASMA

12. Jesse Zuckerman (SSTP), Natalie Coburn, Jeannie Callum, Alyson L Mahar, Yulia Lin, Alexis F. Turgeon, Robin McLeod, Emily Pearsall, Guillaume Martel, Julie Hallet: EVALUATING VARIATION IN PERIOPERATIVE RED BLOOD CELL TRANSFUSION FOR PATIENTS UNDERGOING ELECTIVE GASTROINTESTINAL CANCER SURGERY: A POPULATION-BASED ANALYSIS

EXTENDED COLD LUNG PRESERVATION WITH IMPROVED MITOCHONDRIAL HEALTH: PRE-CLINICAL STUDIES AND TRANSLATION TO HUMAN LUNG TRANSPLANTATION

Aadil Ali[1], Aizhou Wang[1], Rafaela V.P. Ribeiro[1], Cristina Baciu[1], Erika L. Beroncal[2], Marcos Galasso[1], Bruno Gomes[1], Olivia Hough[1], Etienne Abdelnour-Berchtold[1], Edson Brambate[1], Vinicius Michaelsen[1], Yu Zhang[1], Anajara Gazzalle[1], Tom Waddell[1], Mingyao Liu[1], Ana C. Andreazza[2], Shaf Keshavjee[1], Marcelo Cypel (Supervisor)[1]

[1]Latner Thoracic Surgery Research Laboratories, Toronto, ON, Canada.[2]University of Toronto, Departments of Pharmacology & Toxicology and Psychiatry; The Canada Mitochondrial Network, Toronto, ON, Canada.

Background: For those with end-stage pulmonary disease, lung transplantation (LTx) is truly a lifesaving therapy. The advent of donor lung preservation practises has made LTx a clinical reality for patients around the world. The current clinical standard for the preservation of donor lungs involves cold flushing the organ with an extracellular low-potassium dextran solution (specialized solution to store lungs), and subsequently storing on ice (~4°C) until the beginning of the recipient transplant procedure.[1] Although significantly advancing the logistics of LTx practises, this preservation method remains limited by the amount of time the organ can be kept viable in this state. In a recent registry report from the International Society of Heart & Lung Transplantation (the largest lung transplant registry in the world), the median preservation times for lungs used for adult lung transplantation were found to be only 5.1h [range 2.6-8.5h].[2]

There remains a significant need to extend the preservation window beyond which is currently practiced. Longer preservation times will allow for the overcoming of geographic constraints faced in organ donation, allow for optimized immunological matching amongst donor and recipients, and notably- the opportunity to make lung transplantation a semi-elective procedure (in which overnight cases could be scheduled during typical working hours).

Transplantation during the daytime may lead to several advantages related to patient safety. Some of these advantages include the presence of rested staff performing optimally, a larger number of in-house professionals for emergency situations, and overall enhanced professional well-being. Recent literature has also suggested that the time of day has an influence on surgical procedure outcomes.[3] For example, retrospective data analysis has demonstrated a higher incidence of graft dysfunction in organs transplanted in the middle of the night versus those transplanted during the day.[4] The team from Washington University has confirmed these findings in the setting of LTx, showing improved survival outcomes for recipient surgeries performed in day hours.[5]

Preliminary studies published over 30 years ago have suggested lung storage at 10°C to be the optimal lung storage temperature.[6–8] Despite these reports, translation of these findings to clinical practice never occurred due to the previous constraints in precise temperature-controlled device technologies (as opposed to a simple ice cooler), and due to an incomplete understanding of the underlying biological mechanisms by which 10°C was functionally superior. Thus, the safety and suitability of 10°C for a prolonged storage period has not been explored.

Here, we aim to evaluate the suitability of 10°C lung static storage for prolonged pulmonary storage and provide mechanistic insights regarding the metabolic and biological impact of the different storage temperatures. Lastly, we report a proof-of-concept for the clinical use of 10°C in prolonging lung preservation, leading to semi-elective LTx in humans.

Methods and Results:

10°C lung preservation results in superior prolonged graft preservation. To evaluate 10°C preservation as a lung storage temperature, we elected to perform experiments using a large

animal pig model in which lung procurement followed that of current clinical practice.[9] Following explant, donor lungs (n = 5/group) were randomized to storage at either 10°C in a thermoelectric cooler (accuracy of ± 0.5°C) or 4°C in a walk-in cooler. Lung storage time was set to an extended period of 36h under these experimental conditions in order to maximize the opportunity to detect therapeutic differences. After 36h of cold static preservation, the lungs were subjected to 12h of assessment in the normothermic ex vivo lung perfusion (EVLP) platform in order to evaluate functional and biological differences amongst the groups (Fig 1A). A well-established protocol for EVLP was followed, referenced as the Toronto protocol.[10] This method has been used to evaluate over 600 human lungs at our center with excellent correlation with post-transplant outcomes.[11,12] No differences in baseline characteristics were found amongst the two experimental groups. After 36h of cold preservation, lungs stored at 10°C had a markedly better quality of preservation compared to those stored at 4°C as demonstrated by the following functional parameters: significantly lower airway pressures (Fig 1B & 1C, $p < 0.0001$), higher lung compliances (Fig 1D & E, $p < 0.0001$), and better oxygenation function (Fig 1F, $p < 0.0001$). In addition, lungs stored at 10°C developed less edema as reflected by a significantly lower lung weight gain during the perfusion period (Fig 1G, 30 ± 34.1 vs. 201 ± 33.2 grams, $p = 0.0159$). Importantly, lung function in the 10°C group after 36h of ischemia, faired similarly to lungs subjected to only 2h of ischemia in previous studies by our group.[13]

10ºC lung storage leads to the accumulation of cytoprotective metabolites. Temperature is known to play a key role in the alteration of cellular energetics and metabolism.[14] In order to have a high-fidelity view of the metabolome, we performed a global untargeted metabolomic analysis (Metabolon, Durhan, NC) of tissue samples collected during the experiments described above. Samples were obtained before and after the 36h cold preservation period. Of the metabolites identified, a total of 4 metabolites were found to be significantly different between the two groups after 36h of cold storage. Amongst these four metabolites, we identified significantly higher intensities of mitochondrial-related metabolites including itaconate, glutamate, and N-acetylglutamine. These metabolites have been previously described to promote innate anti-oxidative systems within the mitochondria.[15] Based on this information, we further hypothesized that 10°C storage may be advantageous due to the ability to sustain mitochondrial function during ischemia.

10ºC lung storage maintains mitochondrial function. Mitochondrial dysfunction states are characterized by changes in inflammatory, metabolic and oxidative function (Fig 3A). In order to evaluate the degree of oxidative protection amongst the two storage temperatures, we performed immunohistochemical staining for 8-hydroxy-2-deoxy Guanosine (8-OHdG), a known marker for DNA/RNA oxidation. Histological quantification of this marker in the tissue samples confirmed a trend towards less oxidative damage at 10°C versus 4°C during the cold storage period (Fig 3B, $p = 0.0952$). When under a significant amount of cellular stress, mitochondrial DNA (mtDNA) is released into both the intracellular and extracellular environment.[16] Therefore, to evaluate the level of mitochondrial damage amongst the groups, we measured the degree of mtDNA oxidation within the lung tissue, and the levels of circulating cell-free mtDNA during the perfusion period through qPCR analysis.[17] Results showed higher mtDNA oxidation rates (Fig 3C, $p=0.056$) in lung tissue at the end of the normothermic evaluation, and significantly more mtDNA release within the EVLP perfusate in the 4°C group as compared to 10°C (Fig 3D, $p=<0.0001$).

A well described consequence of intracellular mtDNA release is the activation of the intracellular inflammasome, and in turn, the release of the highly pro-inflammatory cytokine IL-1β through the NLRP-3 pathway.[18,19] Additionally, extracellular mtDNA release has been shown to aid in the production of pro-inflammatory cytokine IL-8, leading to neutrophil activation.[18,19] In order to measure the downstream effects of mtDNA release on cytokine production, we measured the levels of IL-1β and IL-8 within the EVLP perfusate using standard ELISA techniques. Results of

our analysis showed significantly lower levels of IL-1β (Fig 3E, p = <0.0001) and IL-8 (Fig 3F, p = <0.0001) in the EVLP perfusate for lungs stored at 10°C versus those stored at 4°C.

We then went on to determine the primary mode of cell death responsible for mtDNA release. In order to evaluate cellular necrosis, we measured levels of lactate dehydrogenase (LDH) activity within the EVLP perfusate and performed TUNEL staining on post-EVLP histological samples to quantify apoptosis. LDH activity was significantly higher when lungs were stored at 4°C versus 10°C (Fig 3G, p = 0.0065), while no differences were seen in levels of apoptosis after quantification. These results lead us to postulate that 10°C may be protective through pathways involving cellular necrosis, rather than apoptosis. Lastly, we hypothesized that if mitochondrial dysfunction were to occur during the preservation period, metabolic dysfunction would arise based on the mitochondria's important role in carrying out cellular respiration. To assess the degree of metabolic dysfunction, we measured perfusate glucose levels and lactate levels. Results showed that lung perfusate glucose consumption (Fig 3H, p = <0.0001) and lung lactate production (Fig 3I, p = <0.0001) were significantly higher at 4°C in comparison to 10°C.

Proof of concept 10°C prolonged lung storage followed by transplantation in humans. Under a clinical protocol with research ethics board approval, we investigated the suitability of extended lung preservation using 10°C. In this specific pilot study, the prolongation of preservation was aimed at moving night transplants to the morning (Fig 3A). Lungs retrieved overnight (cross clamp after 6:00pm) meeting criteria for transplantation based on standard assessments transported in usual fashion to our hospital. Upon arrival, lungs were then immediately stored at 10°C within a temperature-controlled incubator with an earliest planned recipient anesthesia time of 6:00am allowed. Five patients received bilateral lung transplants. The mean recipient age for patients transplanted was 70 years old and 4/5 of the recipients had a diagnosis of pulmonary fibrosis. Three of the five donors involved donation after neurologic determination of death (NDD), while the other two were donation after circulatory determination of death (DCD). The median total preservation time for the first implanted lung was 10.4h [9.92h – 14.8h] and second lung was 12.1h [10.9h – 16.5h]. No patients had primary graft dysfunction grade 3 (PGD 3) at 72h nor required post-operative extracorporeal membrane oxygenation (ECMO) or post-transplant nitric oxide (NO) usage. In clinical LTx, PGD3 at 72h is a commonly referenced indicator for early mortality and poor outcomes post-transplantation.[21] The median time on the ventilator post-LTx was 2 days (range 0 – 7 days) and the median time to hospital discharge was 17 days (range 14 – 26 days). For comparison, the approximate median hospital length of stay after LTx at our center is 24 days.[22] The 30-day survival was 100% and none of the patients required any use of oxygen for exertion at that time. Figure 3B shows chest x-ray images taken from the donor, during admission to the ICU post-transplantation, at 24h post-transplantation, 48h post-transplantation, and 72h post-transplantation.

Conclusions:

In conclusion, the results of this study demonstrate that 10°C is a superior storage temperature compared to the current clinical gold standard of an ice cooler (4°C). Using today's technology, 10°C preservation is easily achievable and logistically simple for those who wish to adopt this approach. In our biological analysis, we describe a novel underlying mechanism of lung protection using this approach which appears to be related to improved mitochondrial preservation. Development of therapeutic strategies to further enhance mitochondrial protection during the preservation period may lead to further optimization of donor lung preservation and may have implications in the setting of lung injury. 10°C preservation could be the new standard of care for prolonged pulmonary preservation allowing transplants to be performed in a semi-elective fashion with benefits to patients and health care teams. An international multi-center clinical trial is currently underway to confirm these findings (ClinicalTrials.gov identifier: NCT04616365). Further studies should be performed evaluating 10°C preservation for other solid organ preservation.

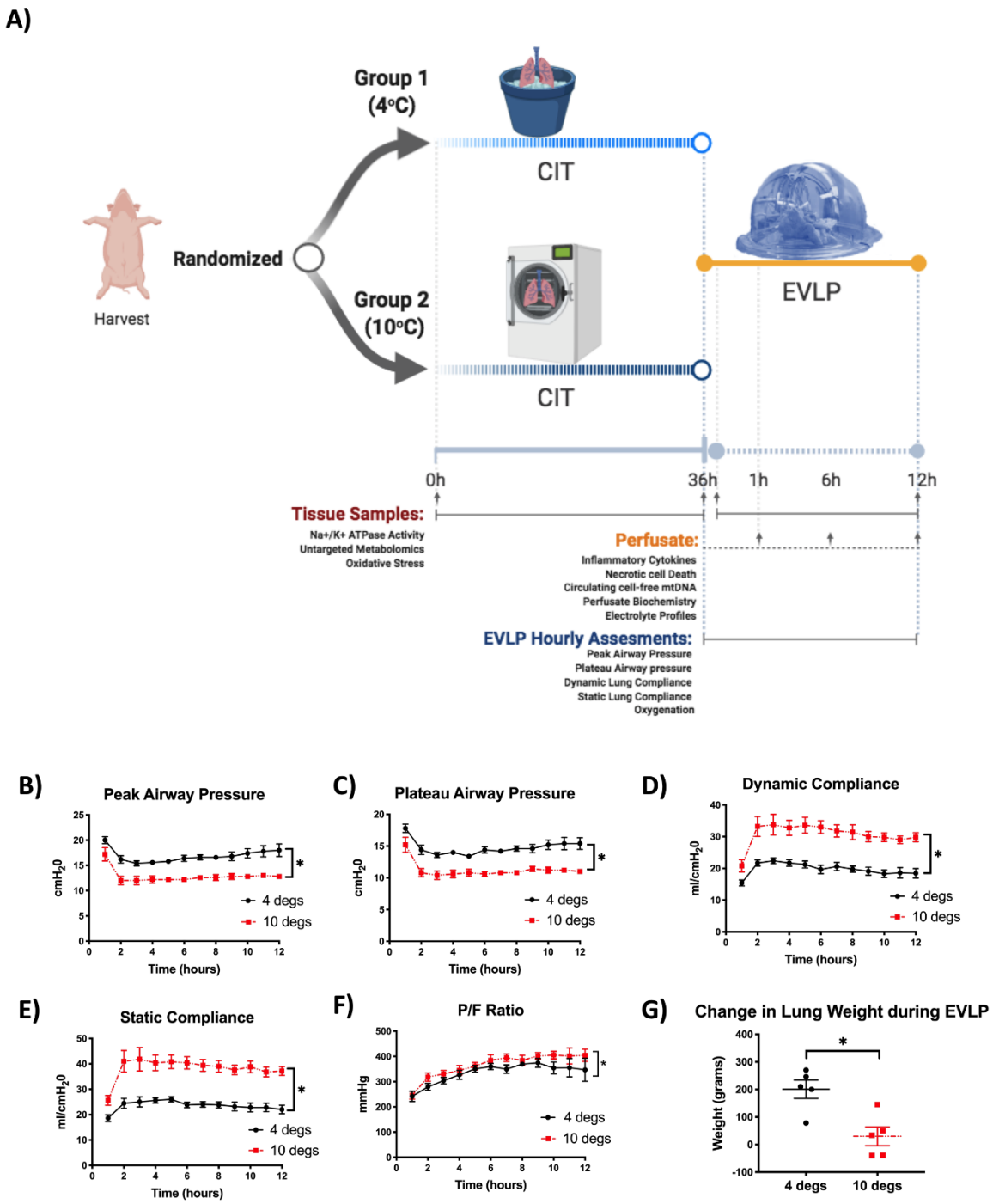

Figure 1. Functional evaluation of 10°C versus 4°C lung storage after an extended period of cold storage. **(A)** Donor pig lungs were retrieved and randomized to be stored at either 4°C or 10°C for 36h (n=5/group), followed by 12h of normothermic ex vivo lung perfusion (EVLP) evaluation. Scheme created with BioRender.com **B-G)** Results of physiologic evaluation during EVLP (Two-way ANOVA performed for all figures involving a time component and Mann-Whittney test for comparison of two groups. Results are expressed as mean ± SEM). P/F ratio: ratio of oxygen partial pressure to fraction of inspired oxygen, (* $p<0.05$).

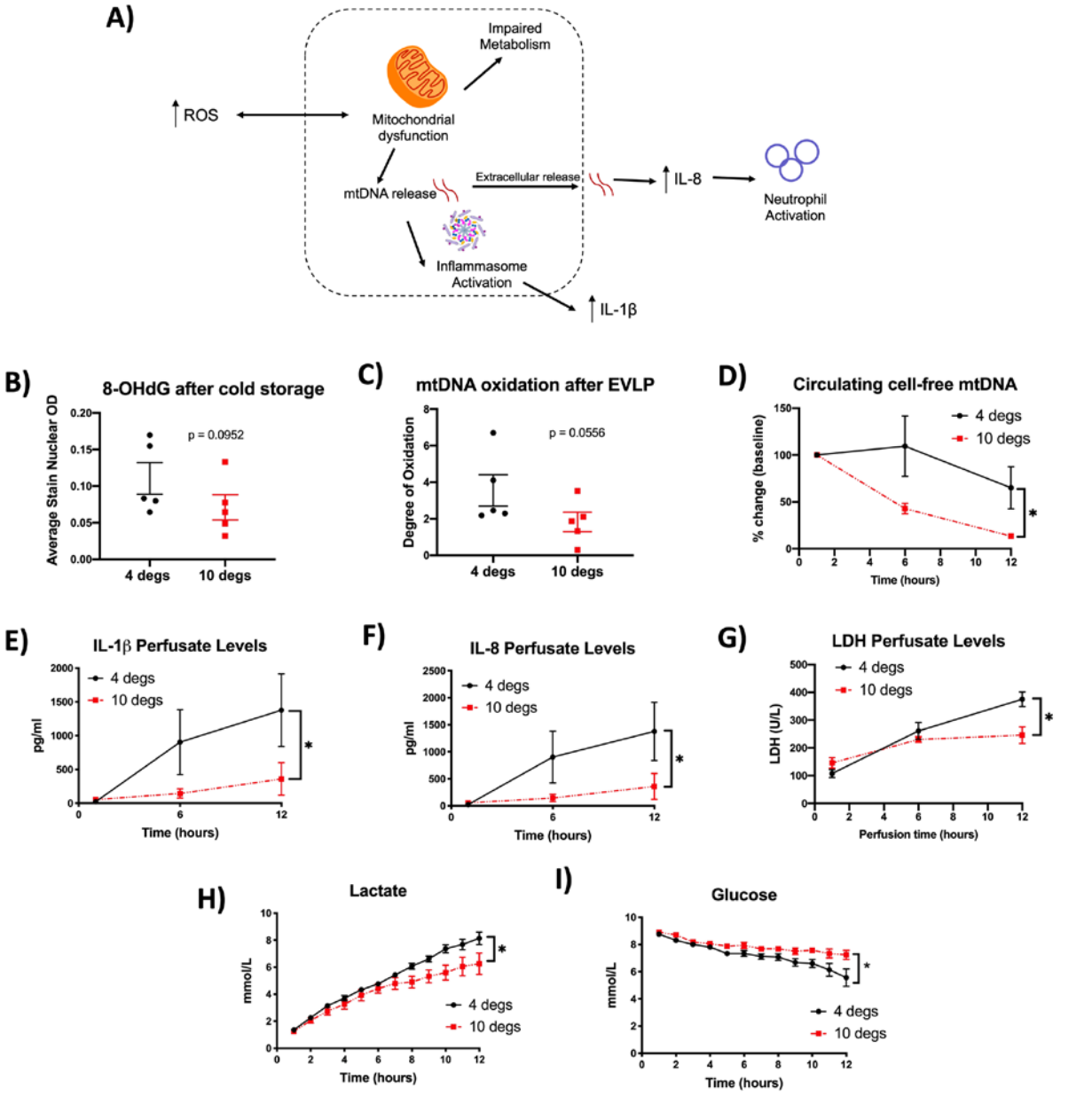

Figure 2. Assessment of mitochondrial health between 4ºC and 10ºC lung storage. **(A)** Graphical representation of biological consequences of mitochondrial dysfunction. Increased oxidative stress leads to mitochondrial dysfunction, in turn leading to mtDNA release and metabolic impairment. mtDNA can lead to increased production of IL1-β through inflammasome activation and as well as increased release of IL-8. **(B)** DNA/RNA oxidation of histological tissue samples taken after the cold preservation period measured through 8-hydroxy-2-deoxy guanosine (8-OHdG) immunohistochemistry staining. Oxidative stress marker levels were measured through quantification of average stain nuclear optical density. (Mann-Whittney test, results are expressed as mean ± SEM).
(C) Calculated mtDNA oxidation rates found within the lung tissue after EVLP (Mann-Whittney test, results are expressed as mean ± SEM). **(D)** Circulating cell-free mtDNA extracted from EVLP perfusate and quantified using qPCR during lung perfusion. Fold changes from baseline levels (1h perfusion) were calculated and plotted. (Two-way ANOVA; data expressed as mean ± SEM). E-F) Perfusate inflammatory cytokine profiles (Two-way ANOVA; data expressed as mean ± SEM) **(G)** Lactate dehydrogenase (LDH) activity levels within EVLP perfusate, a measure of cellular necrosis (Two-way ANOVA; data expressed as mean ± SEM). **(H-I)** Perfusate glucose and lactate levels (Two-way ANOVA; data expressed as mean ± SEM). mtDNA: mitochondrial DNA, EVLP: ex vivo lung perfusion, IL: interleukin, ROS: Reactive oxidative species, (* $p<0.05$).

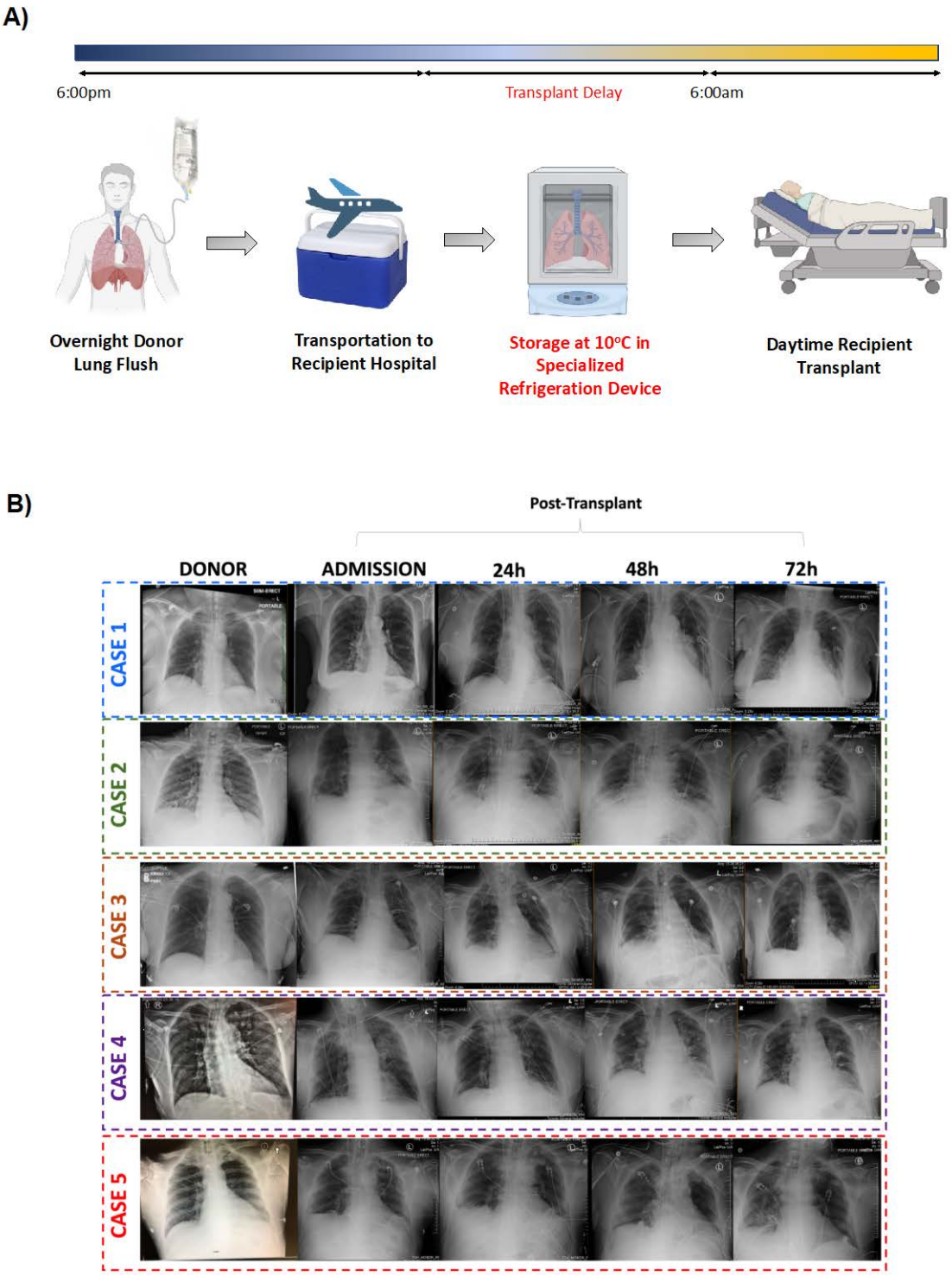

Figure 3. Pilot clinical study for semi-elective lung transplantation. **(A)** Clinical pilot study design schema. **(B)** Chest X-ray images taken in the donor, at the time of admission to the intensive care unit, and at the 24, 48, and 72 hour-recipient follow-up for the 5 patients transplanted using 10°C for semi-elective transplantation. Side labels outline each individual case number.

References

1. Keshavjee SH, Yamazaki F, Cardoso PF, McRitchie DI, Patterson GA, Cooper JD. A method for safe twelve-hour pulmonary preservation. *J Thorac Cardiovasc Surg*. 1989;98(4):529-534.
2. Chambers DC, Cherikh WS, Goldfarb SB, et al. The International Thoracic Organ Transplant Registry of the International Society for Heart and Lung Transplantation: Thirty-fifth adult lung and heart-lung transplant report—2018; Focus theme: Multiorgan Transplantation. *J Hear Lung Transplant*. 2018. doi:10.1016/j.healun.2018.07.020
3. Dalton MK, McDonald E, Bhatia P, Davis KA, Schuster KM. Outcomes of acute care surgical cases performed at night. *Am J Surg*. 2016. doi:10.1016/j.amjsurg.2016.02.024
4. Cunningham PS, Maidstone R, Durrington HJ, et al. Incidence of primary graft dysfunction after lung transplantation is altered by timing of allograft implantation. *Thorax*. 2019. doi:10.1136/thoraxjnl-2018-212021
5. Yang Z, Takahashi T, Gerull WD, et al. Impact of Nighttime Lung Transplantation on Outcomes and Costs. *Ann Thorac Surg*. 2020. doi:10.1016/j.athoracsur.2020.07.060
6. Wang LS, Yoshikawa K, Miyoshi S, et al. The effect of ischemic time and temperature on lung preservation in a simple ex vivo rabbit model used for functional assessment. *J Thorac Cardiovasc Surg*. 1989.
7. Date H, Lima O, Matsumura A, Tsuji H, d'Avignon DA, Cooper JD. In a canine model, lung preservation at 10 degrees C is superior to that at 4 degrees C. A comparison of two preservation temperatures on lung function and on adenosine triphosphate level measured by phosphorus 31-nuclear magnetic resonance. *J Thorac Cardiovasc Surg*. 1992;103(4):773-780.
8. Nakamoto K, Maeda M, Taniguchi K, Tsubota N, Kawashima Y. A study on optimal temperature for isolated lung preservation. *Ann Thorac Surg*. 1992. doi:10.1016/0003-4975(92)90766-W
9. Mariscal A, Caldarone L, Tikkanen J, et al. Pig lung transplant survival model. *Nat Protoc*. 2018. doi:10.1038/s41596-018-0019-4
10. Cypel M, Yeung JC, Hirayama S, et al. Technique for Prolonged Normothermic Ex Vivo Lung Perfusion. *J Hear Lung Transplant*. 2008;27(12):1319-1325. doi:10.1016/j.healun.2008.09.003
11. Tikkanen JM, Cypel M, Machuca TN, et al. Functional outcomes and quality of life after normothermic ex vivo lung perfusion lung transplantation. *J Hear Lung Transplant*. 2014;34(4):1-10. doi:10.1016/j.healun.2014.09.044
12. Divithotawela C, Cypel M, Martinu T, et al. Long-term Outcomes of Lung Transplant with Ex Vivo Lung Perfusion. *JAMA Surg*. 2019. doi:10.1001/jamasurg.2019.4079
13. Cypel M, Yeung JC, Hirayama S, et al. Technique for prolonged normothermic ex vivo lung perfusion. *J Hear Lung Transpl*. 2008;27(12):1319-1325. doi:10.1016/j.healun.2008.09.003
14. Jing L, Yao L, Zhao M, Peng LP, Liu M. Organ preservation: From the past to the future. *Acta Pharmacol Sin*. 2018. doi:10.1038/aps.2017.182
15. Cordes T, Lucas A, Divakaruni AS, Murphy AN, Cabrales P, Metallo CM. Itaconate modulates tricarboxylic acid and redox metabolism to mitigate reperfusion injury. *Mol Metab*. 2020. doi:10.1016/j.molmet.2019.11.019
16. Shimada K, Crother TR, Karlin J, et al. Oxidized Mitochondrial DNA Activates the NLRP3 Inflammasome during Apoptosis. *Immunity*. 2012. doi:10.1016/j.immuni.2012.01.009
17. Jeong H, Dimick MK, Sultan A, et al. Peripheral biomarkers of mitochondrial dysfunction in adolescents with bipolar disorder. *J Psychiatr Res*. 2020. doi:10.1016/j.jpsychires.2020.02.009

18. Dias I, Milic I, Heiss C, et al. Inflammation, lipid (per)oxidation and redox regulation. *Antioxid Redox Signal*. 2020. doi:10.1089/ars.2020.8022
19. Yabal M, Calleja DJ, Simpson DS, Lawlor KE. Stressing out the mitochondria: Mechanistic insights into NLRP3 inflammasome activation. *J Leukoc Biol*. 2019. doi:10.1002/JLB.MR0318-124R
20. D. VR, M.G. H, M.I. H, et al. Report of the ISHLT Working Group on primary lung graft dysfunction Part IV: Prevention and treatment: A 2016 Consensus Group statement of the International Society for Heart and Lung Transplantation. *J Hear Lung Transplant*. 2017;36(10):1121-1136. doi:http://dx.doi.org/10.1016/j.healun.2017.07.013
21. De Perrot M, Bonser RS, Dark J, et al. Report of the ISHLT Working Group on Primary Lung Graft Dysfunction part III: Donor-related risk factors and markers. *J Hear Lung Transplant*. 2005. doi:10.1016/j.healun.2005.02.017
22. Yeung JC, Krueger T, Yasufuku K, et al. Outcomes after transplantation of lungs preserved for more than 12 h: a retrospective study. *Lancet Respir Med*. 2016;2600(16):1-6. doi:10.1016/S2213-2600(16)30323-X

Letter of submission for the **McMurrich oral presentation competition in consideration for the Translational Research Award**

Project title: Extended cold lung preservation with improved mitochondrial health: Pre-clinical studies and translation to human lung transplantation

This work was performed entirely at the Toronto General Hospital Research Institute, MaRS building, University Health Network (UHN) between **June 2019 and February 2021**

Author Contributions
AA led the data acquisition and model development

AA and MC were involved in the conception and experimental design of the study and participated in writing and reviewing the extended abstract

MC was the study supervisor

Translation Research

IMPROVING PHYSIOTHERAPY ADHERENCE WITH WEARABLE DEVICES AND MACHINE LEARNING FROM CONCEPTION TO COMMERCIALIZATION

David Burns[1,2] (SSTP), Philip Boyer[2], Helen Razmjou[2,3,4], Robin Richards[1,5], Cari Whyne[1,2]
[1]Division of Orthopaedic Surgery, Department of Surgery, University of Toronto, Toronto, ON, Canada.
[2]Sunnybrook Research Institute, Toronto, ON, Canada.
[3]Working Condition Program, Holland Orthopedic and Arthritic Centre, Toronto, ON, Canada.
[4]Department of Physical Therapy, University of Toronto, Toronto, ON, Canada.
[5]Sunnybrook Health Sciences Centre, Toronto, ON, Canada

BACKGROUND: Exercise-based physical therapy is important in the treatment of a wide-range of pathologies across the life-span including illness, injury, and disabilities involving the musculoskeletal, cardiopulmonary, vascular, and neurological systems[1]. Physical therapy is considered essential both as a primary treatment, and in post-operative rehabilitation[1]. In the context of musculoskeletal care, surgical management is often offered secondary to a failed course of pharmacological management and physiotherapy[2,3].

In the Canadian health care context, and in most of the developed world, patients are assessed and then receive training from their physiotherapist on their required activities but are responsible for performing the majority of the therapy (>90%) independently at home. A significant challenge with this paradigm of treatment delivery, is that does not guarantee the successful and complete delivery of the prescribed therapy.

Studies based on patient-self report indicate that patients struggle to adhere to prescribed exercise programs with estimates of non- or partial non-adherence varying between 50-70%[4,5]. There is evidence to suggest that low baseline levels of physical activity, low self-efficacy, depression, anxiety, helplessness, poor social support, and increased pain during exercise are all significant barriers to physiotherapy adherence[6]. Of all medically prescribed treatments, physiotherapy calls for one of the greatest levels of independent patient engagement.

Patient adherence to prescribed physical therapy has been shown to be an important predictor for successful management of musculoskeletal disorders[4]. However, the impact of poor patient physiotherapy adherence to individual patient outcomes and the health care system has never been fully quantified.

A significant gap in understanding and addressing the problem of poor physical therapy adherence, has been an inability to accurately and objectively quantify adherence in the home setting. Any effort to tackle adherence barriers and improve adherence depends first on the capacity for its measurement.

The purpose of this research was to develop a system for better engaging patients in their physiotherapy, beginning first with the technology to measure participation and performance objectively. Presented herein is the journey taken from proof-of-concept, to clinical trial and commercialization.

METHODS AND RESULTS

Translation Research

Proof of Concept and Pilot: We determined early on that adherence tracking technology must be affordable, unobtrusive, and easy to use by patients in any age group. The increasing adoption and performance of wearables presented an opportunity to leverage robust and accessible devices that patients already own and use in their day to day lives: smart watches. These devices have been used for basic activity tracking including walking, running, swimming, cycling, but not for physiotherapy.

Our work began with a proof-of-concept laboratory study where we sought to determine if the inertial sensors (accelerometer and gyroscope) on a smart watch could be used to classify and track shoulder physiotherapy exercise.

We recruited twenty healthy subjects to perform 20 repetitions of seven rotator cuff exercises bilaterally while inertial data was recorded from an Apple Watch. The inertial data was pre-processed using a sliding window segmentation, and four supervised learning algorithms were trained and optimized to classify the exercises: k-nearest neighbor, random forest, support vector machine classifier, and a convolutional recurrent neural network. This study demonstrated the superiority of modern neural network architectures for activity recognition and supported the potential feasibility of physiotherapy adherence tracking with greater than 90% accuracy[7].

Based on this work, a Python software package for time series machine learning (seglearn[8]) was initially developed to support our ongoing collaborative technical developments. Seglearn was later released as an open source toolkit on Github and has gathered international contributors and has been downloaded more than 135,000 times.

Building the Research Program: Based on the successful pilot research, we assembled a multi-disciplinary team of academic bioengineers, data scientists, physiotherapists, ethicists, and physicians to further develop and translate this technology into the clinical context. We formed a clinical partnership with a key knowledge user, the Sunnybrook Working Condition Program, that a large provider of physiotherapy services to injured workers in Ontario. We then successfully applied for and obtained more than $1.1 million dollars of industry and federal academic grant funding to carry out the next phase of this project.

Our first goal was to validate our physiotherapy adherence tracking solution in the clinical context, and leverage it to answer previously unanswerable questions: what are the rate and patterns of physiotherapy adherence? What is the impact of adherence on recovery? What patient factors and barriers contribute to poor physiotherapy adherence?

Clinical Validation and New Insights: A robust clinical prototype was developed for recording and labelling smart watch inertial data in the clinic and home setting. We developed custom mobile and wearable android applications with a Google cloud backend for data storage. To facilitate the use of our technology through a range of demographic groups including elderly, inertial data recording was implemented as a stand-alone smart watch application such that our patients would only be required to don their smart watch during physiotherapy exercise for inertial data collection.

The clinical validation study (ongoing) is a prospective longitudinal cohort study of 120 patients undergoing physiotherapy for rotator cuff pathology[9]. Baseline demographic data and 23 potential adherence predictors are recorded for each patient. The patients each receive at least 3 months of physiotherapy and are followed to one year from treatment onset. The primary and secondary study outcomes include objective and validated clinical outcomes: work status, numeric pain rating scale, Disabilities of the Arm Shoulder and Hand (DASH) score, rotator cuff strength measured by dynamometer, and shoulder active range of motion. These outcomes are recorded at baseline, monthly through treatment, and at final follow-up. Throughout treatment,

the patients' clinic and independent physiotherapy are tracked using a smart watch. Both patients and clinicians are blinded to the tracking data for this non-interventional study.

Although the outbreak of the COVID-19 pandemic impacted our ability to carry out this work, we conducted a preliminary analysis of 42 patients who completed at least one month of treatment[10]. Using a fully convolution neural network architecture, we tracked home and in-clinic patient physiotherapy participation from smart watch inertial sensors with an accuracy of 95%[10] (Figure 1). We observed that patients participated in physiotherapy on 41% of days assigned treatment (Figure 2), with a significant (P=0.03) decline in home participation over time (Figure 3). We also found there was a statistically significant and clinically meaningful relationship between cumulative physiotherapy participation and recovery in pain and disability scores at 8 weeks and 12 weeks follow-up ($P < 0.05$). Low patient expectations for recovery, low self-efficacy, low income and greater anxiety were associated with low rates of physiotherapy participation. The findings established the scope and impact of the adherence problem, and gave us some early clues to help tackle it.

Advancing State-of-the-Art: Concurrent to the ongoing clinical validation, we further developed the underlying technology to enable personalized adherence tracking. It was apparent in our pre-clinical work that algorithm performance was not uniform across subjects, and most errors produced by the algorithms occur across a minority of the test group. This result is due to the differences in how individuals perform different exercises, depending on their inherent capabilities and even how they were instructed. We developed a novel approach to activity recognition whereby we collect sample data under supervision for each subject, and utilize this baseline data to better inform future predictions of their physiotherapy activity. This was accomplished using a triplet neural network architecture, leveraging advances developed primarily for facial recognition[11] where adaptation to new individuals is essential. In this way, our algorithms can compensate for individual differences in the performance of the same activity. We demonstrated state-of-the results of a personalized approach on several open activity recognition data sets and improved our physiotherapy tracking accuracy to 99%[12].

Changing Patient Behaviour: Our next challenge lies in the development and validation of a physiotherapy engagement platform that can change behaviour and patient outcomes. We are engaging with key stakeholder groups including policy experts, physiotherapists, clinicians, and patients in a conscientious user-centered design process to examine user needs, motivations, and ethical and policy challenges with the deployment of physiotherapy adherence tracking in the Canadian health care context. The goal is to integrate the underlying technology into a system that promotes physiotherapy engagement and allows for early detection and intervention for patients unable to appropriately participate in their home program. In addition to development of the required patient and clinician interfaces and applications, this work also involves determining how best to utilize objective adherence data to better inform patient care. Development of the patient and clinician applications is complete, with a clinical pilot (N=30) planned to start in Q2 2021.

Commercialization: In order to achieve our objectives on a broader scale, we determined that commercial translation of the technology would be necessary for business development, to provide ongoing support, technical development, and scaling. A startup company, Halterix, was formed to first develop a business case and lead the commercialization efforts. The related intellectual property was successfully negotiated from the institution and inventors, and provisional patents were filed at the commercialization company which now has three full-time employees and is hiring a fourth.

CONCLUSION

A significant limitation to the successful delivery of physical therapy is poor patient engagement in home exercise programs, and a lack of objective means to track and promote better engagement. Poor home shoulder physiotherapy is correlated with inferior pain and disability treatment outcomes for patients with rotator cuff pathology. While participation is correlated with higher expectations for recovery, better self-efficacy, lower anxiety and higher income, further work is required to better understand the reasons for poor participation and develop methods to optimize home physiotherapy adherence.

Translation Research

References

1. Martinello N, Bhandari A, Santos J, Dinh T. The Role of Physiotherapy in Canada: Contributing to a Stronger Health Care System. Ottawa: The Conference Board of Canada; 2017.

2. Wu PI-K, Meleger A, Witkower A, Mondale T, Borg-Stein J. Nonpharmacologic Options for Treating Acute and Chronic Pain. PM R. 2015 Nov;7(11 Suppl):S278–94.

3. Pieters L, Lewis J, Kuppens K, Jochems J, Bruijstens T, Joossens L, et al. An Update of Systematic Reviews Examining the Effectiveness of Conservative Physiotherapy Interventions for Subacromial Shoulder Pain. J Orthop Sports Phys Ther. 2019 Nov 15;1–33.

4. Holden MA, Haywood KL, Potia TA, Gee M, McLean S. Recommendations for exercise adherence measures in musculoskeletal settings: a systematic review and consensus meeting (protocol). Syst Rev. 2014 Feb 10;3:10.

5. Peek K, Sanson-Fisher R, Mackenzie L, Carey M. Interventions to aid patient adherence to physiotherapist prescribed self-management strategies: a systematic review. Physiotherapy. 2016 Jun;102(2):127–35.

6. Jack K, McLean SM, Moffett JK, Gardiner E. Barriers to treatment adherence in physiotherapy outpatient clinics: A systematic review. Man Ther. 2010 Jun;15(3–2):220–8.

7. Burns D, Leung N, Hardisty M, Whyne C, Henry P, McLachlin S. Shoulder Physiotherapy Exercise Recognition: Machine Learning the Inertial Signals from a Smartwatch. Physiol Meas. 2018 Jul 23;39(7):075007.

8. Burns DM, Whyne CM. Seglearn: A Python Package for Learning Sequences and Time Series. J Mach Learn Res. 2018;19(83):1–7.

9. Shifting the Paradigm in Home Physiotherapy: Implementation and Implications of Adherence Monitoring with Artificial Intelligence And Wearable Sensors [Internet]. JMIR Preprints. Available from: https://preprints.jmir.org/preprint/17841

10. Adherence Patterns and Dose Response of Physiotherapy For Rotator Cuff Pathology: A Longitudinal Cohort Study. JMIR Preprints.

11. Schroff F, Kalenichenko D, Philbin J. FaceNet: A Unified Embedding for Face Recognition and Clustering. 2015 IEEE Conf Comput Vis Pattern Recognit CVPR. 2015 Jun;815–23.

12. Burns DM, Whyne CM. Personalized Activity Recognition with Deep Triplet Embeddings. ArXiv200105517 Cs Stat. 2020 Jan 15;

Translation Research

Figures

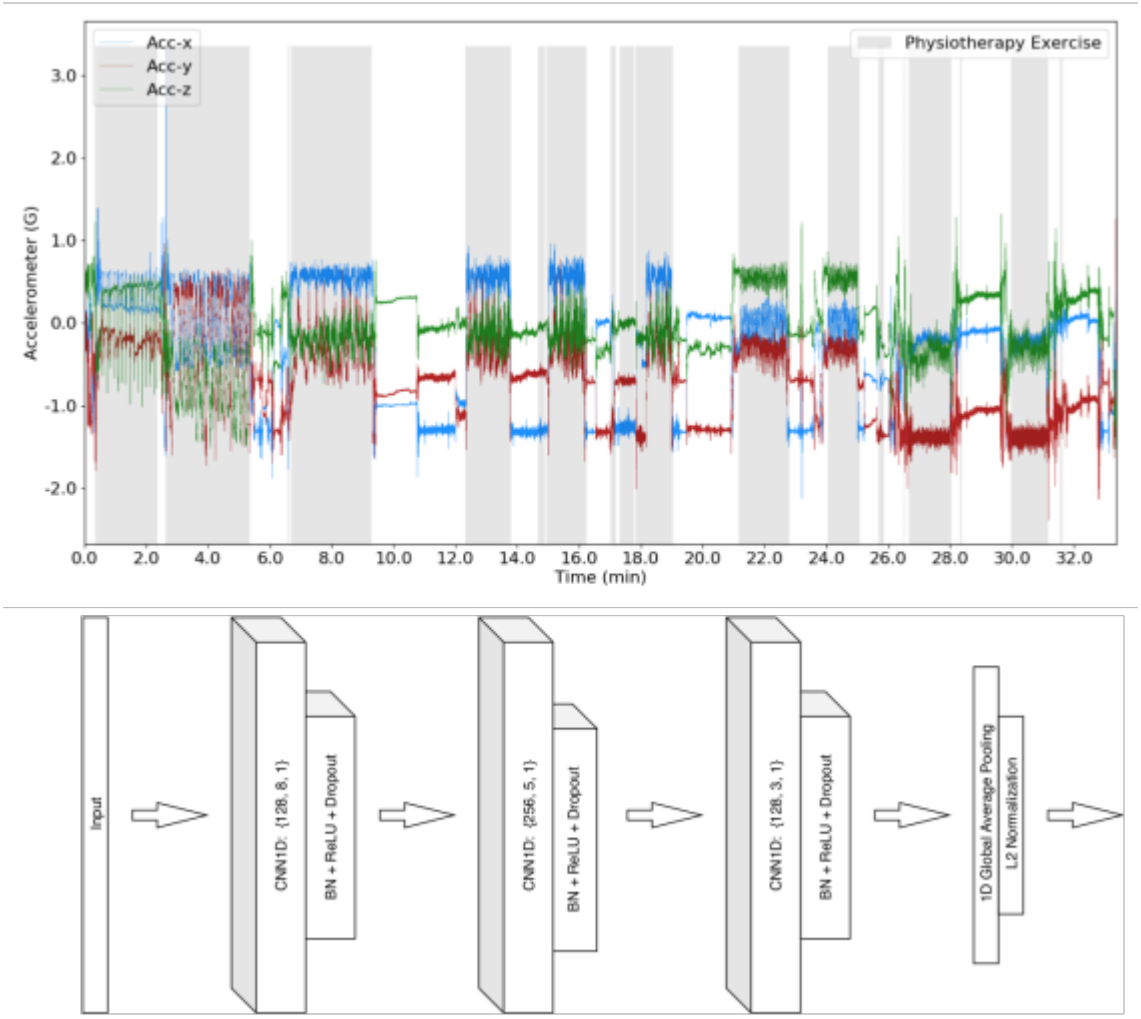

Figure 1: Predicted binary classification of physiotherapy exercise activity and inter-exercise rest periods overlaid on 3-axis accelerometer data. The repetitive oscillatory patterns of exercise are correctly identified by the fully convolutional neural network model.

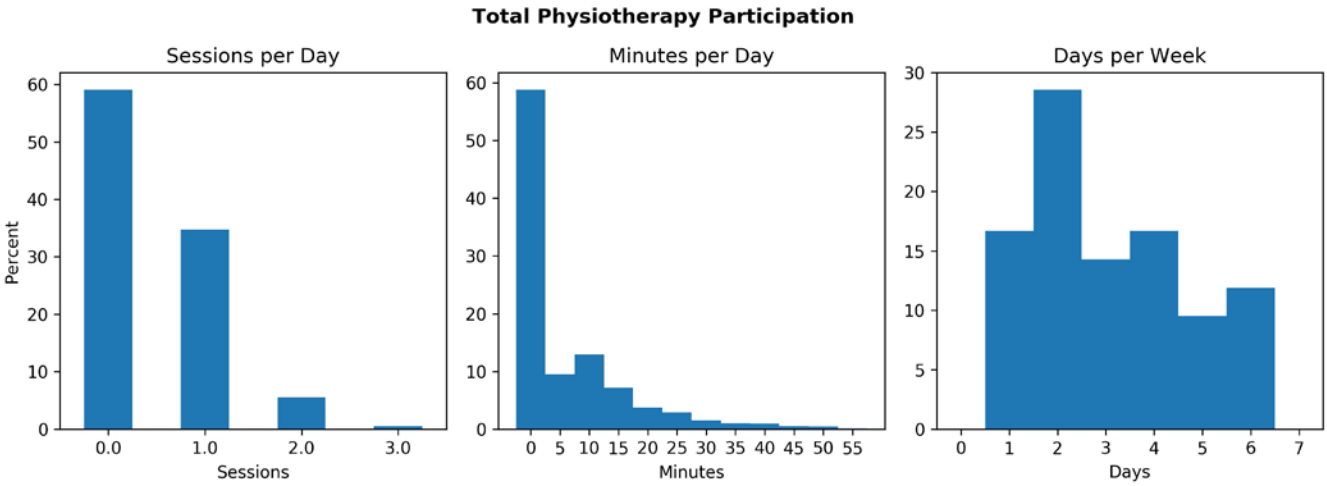

Figure 2: Distribution of daily and weekly total physiotherapy participation based on 3386 patient-days of tracking data. Patients performed some physiotherapy on 41% of days in treatment, which typically lasted between 5-15 minutes.

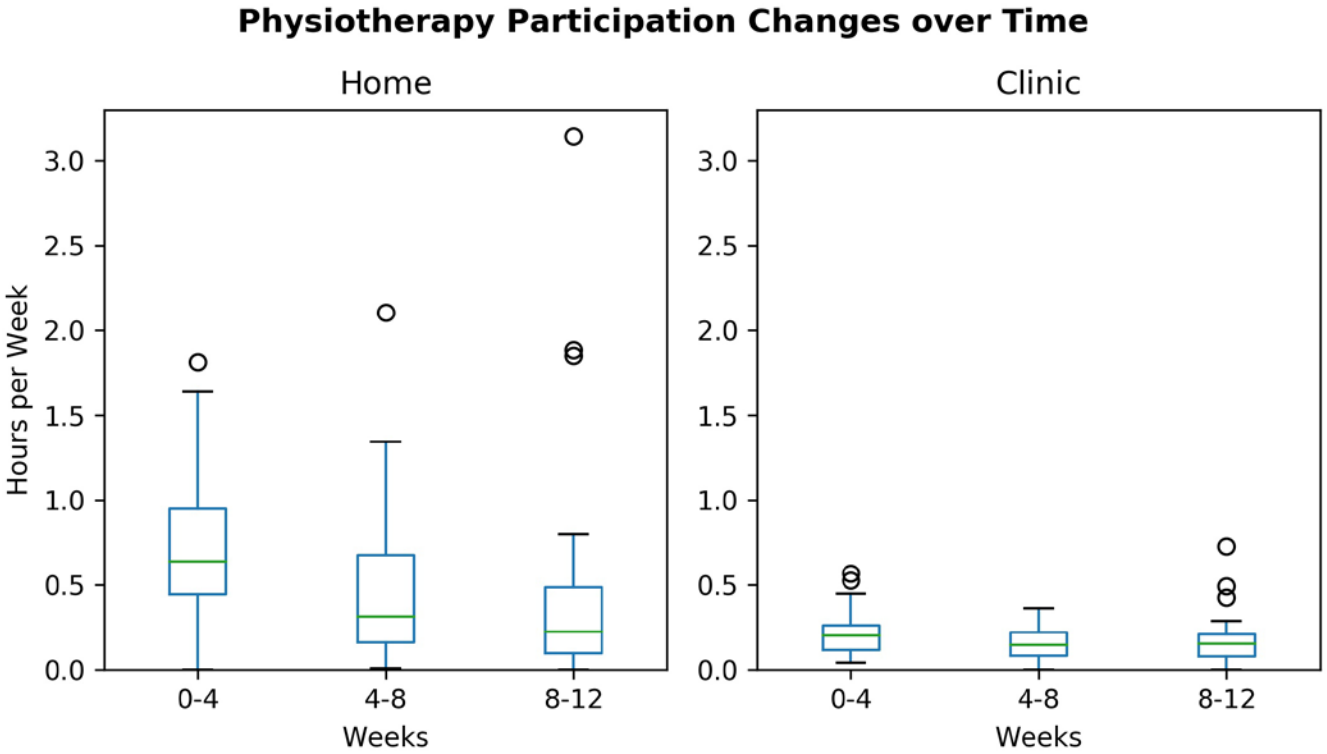

Figure 3: Changes in physiotherapy participation: Home physiotherapy participation decreases significantly over time and clinic participation remains approximately constant.

DELAYED ADMINISTRATION OF HIGH DOSE HUMAN IMMUNOGLOBULIN G REDUCES NEUROINFLAMMATION AND IMPROVES FUNCTIONAL RECOVERY AFTER TRAUMATIC CERVICAL SPINAL CORD INJURY

Jonathon Chon Teng Chio[1,2,3], Jian Wang[1], Vithushan Surendran[1], Lijun Li[1], Mohammad-Masoud Zavvarian[1], Kataryzna Pieczonka[1], Michael G. Fehlings[1,2,3]

[1]Division of Experimental and Translational Neuroscience, Krembil Research Institute, University Health Network, Toronto, Ontario, Canada

[2]Institute of Medical Science, University of Toronto, Toronto, Ontario, Canada

[3]University of Toronto, Toronto, Ontario, Canada

Introduction: The spinal cord is normally protected by the vertebrae, a series of interlocking bones that form the spinal column. However, following a spinal cord injury (**SCI**), the physical trauma causes contusive and compressive injuries to the cord. The initial physical injury triggers multiple secondary injury cascades that exacerbate the initial damage[1,2]. A major component of the cascade is neuroinflammation, which is defined as the infiltration of immune cells past the compromised blood-spinal cord barrier (**BSCB**) and encompasses the effector functions of these cells[3]. Neuroinflammation contributes to the motor and sensory dysfunction observed in SCI patients and pre-clinical SCI models[4]. Currently, the primary treatments for SCI involve surgically decompressing the spinal cord [5] as well as administering the immunosuppressant, methylprednisolone sodium succinate (**MPSS**), within 8 hours post-SCI in humans[6]. But, the application of MPSS presents clinical challenges, as i) the immune response is both beneficial and harmful after SCI[3], and ii) patients already have a weakened immune response post-injury[7], thus further immune suppression will increase the likelihood of infection[8]. Impetus exists to develop new clinically-relevant therapies that modulate (rather than suppress) the immune response and remain efficacious when administered at delayed time points after 8 hours.

Human immunoglobulin G (**hIgG**) is an immunomodulatory therapy approved by the Food and Drug Administration for immunodeficiency and autoimmune conditions[9–11]. The immunoglobulin G molecule consists of F_c and $F_{(ab)2}$ fragments[9]. Both fragments mediate the immunomodulatory effects of IgG, but the mechanism of action (e.g. F_c and $F_{(ab)}$ fragments) is disease-dependent[9,12]. We have published that hIgG (2g/kg) is the ideal dose for SCI therapy[13]. But, to promote translation of hIgG therapy to the clinic, it is important to establish the effective time window for hIgG (2g/kg) administration and to examine how hIgG (2g/kg) mitigates the neuroinflammatory response post-SCI. Given these gaps in knowledge, we utilized a well-characterized clip compression-contusion model of SCI[14] to identify the optimal time window of hIgG (2g/kg) administration post-injury and examined its short- and long-term effects on SCI pathophysiology. This work builds on our prior publications[13,15] by demonstrating that delayed hIgG (2g/kg) administration yields both short and long-term benefits post-SCI. hIgG results in a stronger BSCB and causes change in blood and spleen leukocyte populations.

Methods: Female Adult Wistar rats were used in this study. Females were used due to the relative ease in manual bladder expression post-injury; resulting in a lower rate of urinary tract infections and mortality[16]. Rats were randomly divided into sham (laminectomy only) or SCI groups. SCI was induced by using a modified aneurysm clip to deliver 35 grams of force at the cervical 7/thoracic 1 (C7/T1) level of the spinal cord to compress the cord for 1 minute. At 15 minutes, 1 hour and 4 hours post-SCI in rat, which is approximately equivalent to 1 hour, 4 hours and 16 hours in man[4], a single bolus of hIgG (2g/kg) or volume matched control buffer (Takeda, Japan) was administered through the tail vein. Injured and sham rats were sacrificed at 24 hours or 8 weeks in order to assess how delayed hIgG administration alters short and long-term SCI pathophysiology, respectively. Animals sacrificed at 24 hours were used for molecular readouts (Western Blot, myeloperoxidase (**MPO**) assay and flow cytometry) designed to assess changes in the acute inflammatory response. For animals sacrificed at 8 weeks post-SCI, they were tested weekly to gage recovery of function in the forelimb, hindlimb and body/trunk and sensation using

grip strength, Basso Beattie and Bresnahan scale, inclined plane, somatosensory evoked potential (**SSEP**) and tail flick respectively. Assessment of spinal cord tissue preservation after SCI will complement motor and sensory readouts. Procedures and analyses were performed by examiners blinded to treatment groups. Data are reported as mean ± standard error of mean (**SEM**) and statistical analyses were performed using Prism 6.0 Software. Differences were considered significant if $p<0.05$ after applying post-hoc tests.

Main Result 1: Delayed hIgG (2g/kg) administration improves BSCB post-SCI - In the normal physiological state, the infiltration of immune cells into the spinal cord and central nervous system is prevented by the BSCB[17,18]. Permeability of the BSCB is mediated in part by the expression of tight junction (**TJ**) proteins (zonula occludens (**ZO**)-1, occludin) and inflammatory enzymes that can degrade the TJ proteins[19]. Importantly, the downregulation of these proteins is associated with excessive immune cell infiltration into the spinal cord after SCI[13,18]. We have shown that hIgG (2g/kg) administered at 15 minutes post-SCI increases the expression of TJ proteins and reduces expression of matrix metalloproteinases (**MMP**)[13]; a class of inflammatory enzymes secreted by immune cells under inflammatory conditions to degrade TJ proteins[20,21]. With Western Blot (Fig. 1A), we show a protective effect of delayed hIgG (2g/kg) administration up to 4 hours post-SCI. There is a significant increase in TJ protein (ZO-1, occludin) expression in the injured spinal cord after hIgG (2g/kg) treatment, which correlates with a decrease in active MMP-9 expression (Figures 1B, C, D). Lower BSCB permeability is indicated by lower levels of albumin in the spinal cord after delayed hIgG (2g/kg) administration (Figure 1E), as albumin (a large, biologically inert protein) enters into the CNS after BSCB damage.[22]. Improved BSCB integrity after hIgG (2g/kg) treatment aligns with published results[13].

Main Result *2:* hIgG (2g/kg) significantly reduces neutrophil infiltration in the cord, while increasing neutrophil counts in the spleen - The presence of a stronger BSCB after hIgG (2g/kg) administration prompted us to look at potential changes in immune cell infiltration into the spinal cord. Neutrophils play critical roles in early SCI pathophysiology by secreting inflammatory chemokines/cytokines to propagate downstream neuroinflammation[3,23,24]. Myeloperoxidase (**MPO**) is an enzyme found predominantly in neutrophils and its activity is an excellent correlate with the number of neutrophils in the tissue[25,26]. We have previously shown that hIgG (2g/kg) reduces MPO activity in the spinal cord, and thus indicates lower amounts of neutrophils in the spinal cord[13]. In these sets of experiments, we elaborate upon these results by establishing that delayed administration of hIgG (2g/kg) achieves similar effects (Figure 2A). hIgG (2g/kg) can be administered up to 4 hours post-SCI and effectively reduces neutrophil infiltration in the spinal cord.

A reduction in the number of neutrophils in the spinal cord led to investigating if similar changes are occurring in the systemic circulation. Neutrophils are derived from myeloid precursors in the bone marrow[27,28]. In a pro-inflammatory state, such as SCI, neutrophils mobilize from bone marrow, enter into the blood stream, follow chemoattractant gradients and migrate to the injured tissue[28,29]. With flow cytometry, we identified that delayed hIgG (2g/kg) administration (4 hours post-SCI) significantly decreased the number of neutrophils in the blood at 24 hours post-injury (Figures 2B, C). A reduction in neutrophils in the systemic circulation can indicate that the neutrophils are either dying (through various cellular mechanisms) or being trafficked to other organs. To determine if delayed administration of hIgG (2g/kg) influenced the migration of neutrophils, we used flow cytometry to assess neutrophil populations in various organs of hIgG (2g/kg) treated animals after SCI. We observed a greater number of neutrophils in the spleen of these animals along with an increase in splenic weight (Figures 2D, E, F). The spleen is a potent immune organ for mediating the inflammatory response after SCI[30,31]; serving as both a reservoir for immune cells deployed after SCI and a sink for mobilized immune cells[32–34].

Main Result 3: hIgG (2g/kg) significantly enhances tissue preservation and function after SCI - We previously reported that hIgG administered at 15 minutes post-SCI yielded long-term histological and behavioral recovery after SCI[13,15]. However, it was unknown if delayed

administration will yield similar results. To analyze the long-term effects of delayed hIgG (2g/kg) administration on tissue preservation and behavioral recovery, the identical surgical procedure and treatment paradigm were performed and animals were sacrificed at 8 weeks post-SCI. Prior to sacrifice, rats in both groups were subjected to weekly behavioral assessments and evaluated on multiple aspects of motor function; trunk stability/ strength (using inclined plane assessment), forelimb function (based on grip strength readouts) and hindlimb function (employing the Basso Beattie and Bresnahan scale). Starting at 3 weeks post-SCI, behavioral improvements were observed in animals treated with hIgG (2g/kg) up to 4 hours post-SCI (Figures 3A, B, C). To complement the motor assessments, sensory function was evaluated using somatosensory evoked potentials (**SSEP**) and tail-flick assessments. As seen in (Figures 3E, F), delayed administration of hIgG (2g/kg) up to 4 hours post-SCI resulted in greater electrical activity in the brain that results from tactile stimulation at the tibialis anterior. However, these SSEPs do not suggest hypo/hyperalgesia, as there were no differences in pain sensation across all groups (Figure 3D). The observed improvements in motor and sensory function prompted the evaluation of tissue preservation. In (Figures 3G, H), delayed hIgG (2g/kg) administration led to greater volumes of white and gray matter and a concurrent decrease in cavity and lesion tissue volumes. Correlations between tissue preservation and function recovery align with previous findings[13,15,35].

Discussion: We show that delayed administration of hIgG (2g/kg) up to 4 hours post-SCI in rat (equivalent to 16 hours in man) dampens the acute neuroinflammatory response, yields improved motor and sensory function, and enhances tissue preservation. This is accomplished by strengthening the BSCB, reducing neutrophil infiltration and potentially diverting neutrophils to the spleen. Therefore, in promoting the clinical translation of hIgG as an immunomodulatory therapy for SCI, these data suggest that delayed hIgG (2g/kg) administration is beneficial.

An intact BSCB is essential for maintaining homeostasis in the central nervous system; preventing the entry of large molecules and peripheral immune cells into the brain and spinal cord[36]. Even though a compromised BSCB is primarily harmful in regards of neuroinflammation after injury in the central nervous system (**CNS**), it is important to note that a porous BSCB can be advantageous by allowing pharmacological molecules (such as those with high molecular weight and polar structure; which would normally be excluded from CNS) to mediate its effects. The dual properties of a porous BSCB is similar to the neuroinflammatory response after CNS injury, which is both beneficial and harmful[3]. The immune cells are needed to remove debris and secrete factors to enhance repair and growth. However, should the immune cells persist for too long, they can mediate additional damage. This may explain why the reduction of neutrophil infiltration, as shown by our lab and others, has mainly resulted in improved recovery after injury[13,36–39]. However, reduction of neutrophils has also led to worse recovery after SCI[40].

Furthermore, spinal cord decompression within the initial hours after SCI represents the primary treatment for cervical SCI and improves outcomes[5,41]. But, it fails to attenuate the secondary injury response, which is primarily responsible for mediating most of the tissue damage that accounts for sensory and motor dysfunctions. While MPSS improves function when given up to 8 hours post-SCI[42], aforementioned side effects of MPSS presents clinical challenges[8,43]. Thus, impetus exists to explore therapeutic time window of immunomodulatory drugs.

Conclusion and next steps: We show that hIgG (2g/kg) can be administered at acute stages post-SCI and sustain long-term benefits. To inform design of Phase 1 clinical trials regarding the use of hIgG (2g/kg) as a therapy for SCI, future studies will determine the time window when hIgG (2g/kg) administration becomes ineffective. Furthermore, to promote clinical translation, the mechanism of action can be identified by cleaving hIgG into F_c and $F_{(ab)2}$ fragments. By intravenously administering these fragments into the rat after SCI and using aforementioned readouts, outcomes resulting from administering F_c or $F_{(ab)2}$ fragments will be compared to those after hIgG administration and determine which part of hIgG molecule mediates immunomodulatory effects.

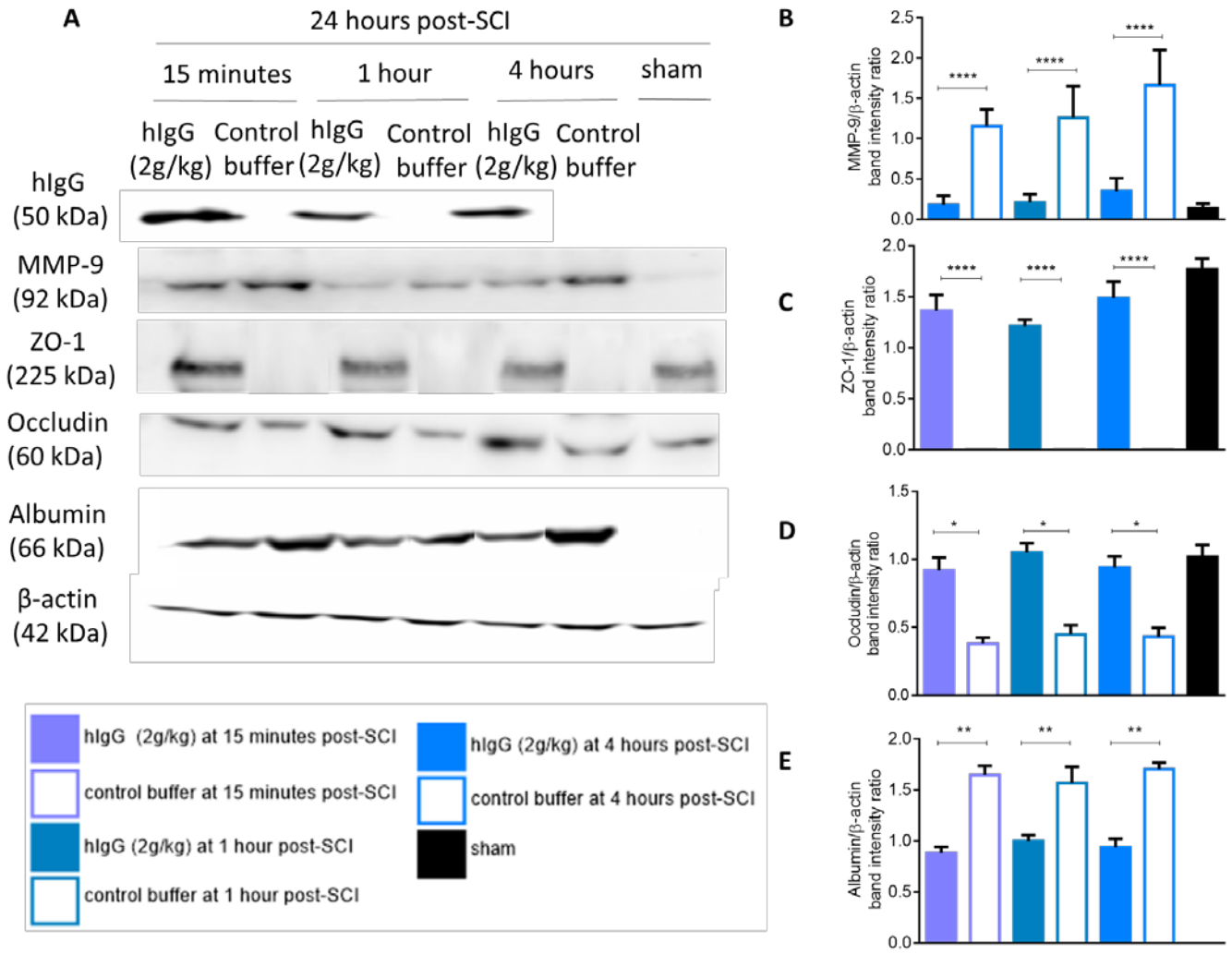

Figure 1: Delayed administration of hIgG (2g/kg) enhances blood-spinal cord-barrier integrity at 24 hours post-SCI. (**A**) At 24 hours post-injury, protein levels of active MMP-9, ZO-1, occludin and albumin were determined by Western Blot. Presence of hIgG in the spinal cords was detected by Western blot as well. β-actin served as the loading control. Representative Western Blots of all proteins are shown. Densitometric analysis of the signal ratios between MMP-9: β-actin (**B**), ZO-1: β-actin (**C**), occludin: β-actin (**D**) and albumin: β-actin (**E**) showed that hIgG (2g/kg) led to significant changes on expression of these proteins when administered at all 3 time points. hIgG (2g/kg) decreases the levels of MMP-9 and albumin, while increasing levels of ZO-1 and occludin. One-way analysis of variance (**ANOVA**), Tukey post-hoc (*p<0.05, **p<0.01, ***p<0.001, ****p<0.0001). Data presented as mean ± standard error of mean (SEM) values.

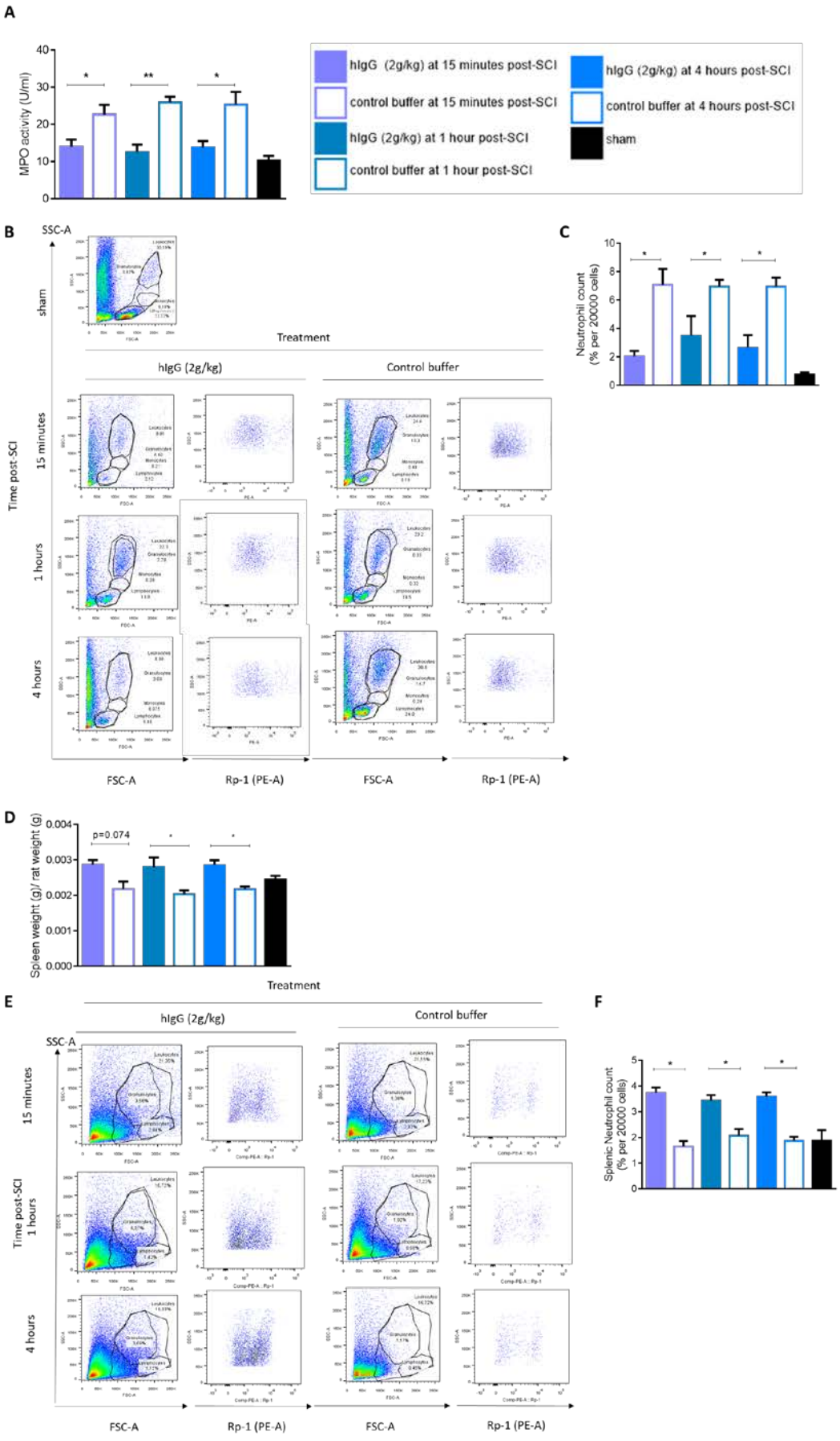
A
MPO activity (U/ml)
hIgG (2g/kg) at 15 minutes post-SCI
control buffer at 15 minutes post-SCI
hIgG (2g/kg) at 1 hour post-SCI
control buffer at 1 hour post-SCI
hIgG (2g/kg) at 4 hours post-SCI
control buffer at 4 hours post-SCI
sham
B
SSC-A
Treatment
hIgG (2g/kg)
Control buffer
Time post-SCI
15 minutes
1 hours
4 hours
FSC-A
Rp-1 (PE-A)
C
Neutrophil count (% per 20000 cells)
D
Spleen weight (g)/ rat weight (g)
p=0.074
Treatment
E
F
Splenic Neutrophil count (% per 20000 cells)

Figure 2: At 24 hours post-SCI, delayed administration of hIgG (2g/kg) decreases the amount of infiltrating neutrophils in the injured spinal cord and reduces the number of circulating neutrophils. hIgG (2g/kg) therapy increased splenic weight and enhances the number of neutrophils within the spleen at 24 hours post-SCI. (**A**) The MPO Assay was used as an indirect measure of neutrophil infiltration. Relative to control buffer at all 3 time points, hIgG (2g/kg) significantly decreased MPO activity at 24 hours post-SCI. (**B**) With flow cytometry, at 24 hours post-SCI, hIgG (2g/kg) administration significantly decreases the percentage of circulating leukocytes and neutrophils in the blood. This decrease was observed when hIgG (2g/kg) was administered at all 3 time points post-injury. Representative flow plots are shown. (**C**) Quantification of neutrophils in the blood at 24 hours post-SCI and in different treatment groups. (**D**) Quantification of splenic weight indicates that hIgG (2g/kg) increases weight of the spleens, but the administration of volume-matched control buffer did not have this effect. (**E**) With flow cytometry, at 24 hours post-SCI, hIgG (2g/kg) administration significantly increases the splenic neutrophil populations. Representative flow plots are shown. (**F**) Quantification of the neutrophils in the spleen at 24 hours post-SCI. One-way ANOVA, Tukey post-hoc (*$p<0.05$, **$p<0.01$, ***$p<0.001$, ****$p<0.0001$). Data presented as mean ± SEM values.

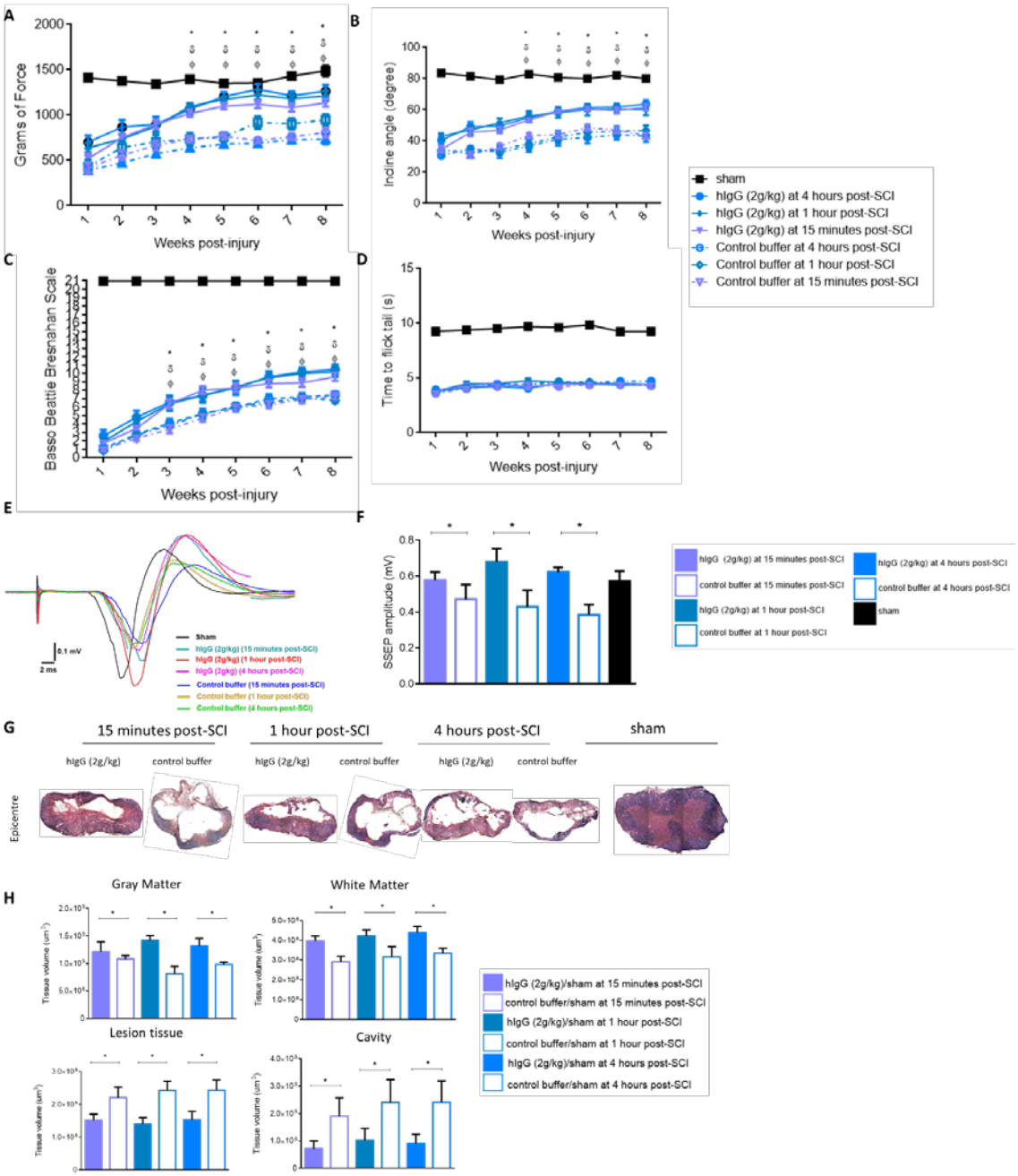

Figure 3: Delayed administration of hIgG (2g/kg) improves motor and sensory abilities of animals and enhances tissue preservation at 8-weeks post-SCI. (**A**) Delayed hIgG (2g/kg) administration improved forelimb function of injured rats as assessed by the grip strength, (**B**) whereas animals also demonstrate greater trunk stability and function as evaluated by the inclined plane assessment. (**C**) With the Basso, Beattie and Bresnahan Scale, animals treated with hIgG (2g/kg) demonstrate better hindlimb function. (**D**) hIgG (2g/kg) fails to alter sensitivity of animal to thermal pain as assessed by tail flick analysis. (**E**) Representative somatosensory evoked potentials of animals treated with hIgG (2g/kg) and control buffer at all 3 time points post-SCI. (**F**) Quantification of amplitudes of SSEPs in animals of all treatment groups and greater SSEP amplitude was observed after treatment with hIgG (2g/kg). (**G**) Delayed administration of hIgG (2g/kg) improves tissue preservation in the rat spinal cords at 8 weeks post-SCI. Representation sections of rat spinal cords (epicenter) stained with Luxol Fast Blue/Hematoxylin and Eosin. (**H**) Quantification of the white matter, gray matter, lesion tissue and cavity volumes in the spinal cords demonstrate significant increases in white and gray matter volumes and lower cavity and lesion tissue volumes. For (**A**), (**B**), (**C**), two-way ANOVA, Tukey post-hoc (*p<0.05, **p<0.01, ***p<0.001, ****p<0.0001). Data presented as mean ± standard errors of mean (SEM) values. For (**F**) and (**H**), one-way ANOVA, Tukey post-hoc (*p<0.05, **p<0.01, ***p<0.001, ****p<0.0001). Data presented as mean ± SEM value.

References

1. LaPlaca MC, Simon CM, Prado GR, Cullen DK. CNS injury biomechanics and experimental models. *Prog Brain Res*. 2007;161:13-26. doi:10.1016/s0079-6123(06)61002-9
2. Choo AM, Liu J, Lam CK, Dvorak M, Tetzlaff W, Oxland TR. Contusion, dislocation, and distraction: primary hemorrhage and membrane permeability in distinct mechanisms of spinal cord injury. *J Neurosurg Spine*. 2007;6(3):255-266. doi:10.3171/spi.2007.6.3.255
3. Donnelly DJ, Popovich PG. Inflammation and its role in neuroprotection, axonal regeneration and functional recovery after spinal cord injury. *Exp Neurol*. 2008;209(2):378-388. doi:10.1016/j.expneurol.2007.06.009
4. Fleming JC, Norenberg MD, Ramsay DA, et al. The cellular inflammatory response in human spinal cords after injury. *Brain*. 2006;129(Pt 12):3249-3269. doi:10.1093/brain/awl296
5. Fehlings MG, Vaccaro A, Wilson JR, et al. Early versus delayed decompression for traumatic cervical spinal cord injury: results of the Surgical Timing in Acute Spinal Cord Injury Study (STASCIS). *PLoS One*. 2012;7(2):e32037. doi:10.1371/journal.pone.0032037
6. Fehlings MG, Wilson JR, Tetreault LA, et al. A Clinical Practice Guideline for the Management of Patients With Acute Spinal Cord Injury: Recommendations on the Use of Methylprednisolone Sodium Succinate. *Glob Spine J*. 2017;7(3 Suppl):203s-211s. doi:10.1177/2192568217703085
7. Riegger T, Conrad S, Schluesener HJ, et al. Immune depression syndrome following human spinal cord injury (SCI): a pilot study. *Neuroscience*. 2009;158(3):1194-1199. doi:10.1016/j.neuroscience.2008.08.021
8. Wilson JR, Vaccaro AR, Fehlings MG. w. *Contemp Spine Surg*. 2014;15(10):1-8. doi:10.1097/01.css.0000454919.91757.34
9. Nimmerjahn F, Ravetch J V. Anti-inflammatory actions of intravenous immunoglobulin. *Annu Rev Immunol*. 2008;26:513-533. doi:10.1146/annurev.immunol.26.021607.090232
10. Samuelsson A, Towers TL, Ravetch J V. Anti-inflammatory activity of IVIG mediated through the inhibitory Fc receptor. *Science (80-)*. 2001;291(5503):484-486. doi:10.1126/science.291.5503.484
11. Tzekou A, Fehlings MG. Treatment of spinal cord injury with intravenous immunoglobulin G: preliminary evidence and future perspectives. *J Clin Immunol*. 2014;34 Suppl 1:S132-8. doi:10.1007/s10875-014-0021-8
12. Zuercher AW, Spirig R, Baz Morelli A, Kasermann F. IVIG in autoimmune disease - Potential next generation biologics. *Autoimmun Rev*. 2016;15(8):781-785. doi:10.1016/j.autrev.2016.03.018
13. Chio JCT, Wang J, Badner A, Hong J, Surendran V, Fehlings MG. The effects of human immunoglobulin G on enhancing tissue protection and neurobehavioral recovery after traumatic cervical spinal cord injury are mediated through the neurovascular unit. *J Neuroinflammation*. 2019;16(1):141. doi:10.1186/s12974-019-1518-0
14. Rivlin AS, Tator CH. Objective clinical assessment of motor function after experimental spinal cord injury in the rat. *J Neurosurg*. 1977;47(4):577-581. doi:10.3171/jns.1977.47.4.0577
15. Nguyen DH, Cho N, Satkunendrarajah K, Austin JW, Wang J, Fehlings MG. Immunoglobulin G (IgG) attenuates neuroinflammation and improves neurobehavioral recovery after cervical spinal cord injury. *J Neuroinflammation*. 2012;9:224. doi:10.1186/1742-2094-9-224
16. Onifer SM, Rabchevsky AG, Scheff SW. Rat models of traumatic spinal cord injury to assess motor recovery. *Ilar j*. 2007;48(4):385-395.
17. Mastorakos P, McGavern D. The anatomy and immunology of vasculature in the central nervous system. *Sci Immunol*. 2019;4(37). doi:10.1126/sciimmunol.aav0492

18. Figley SA, Khosravi R, Legasto JM, Tseng YF, Fehlings MG. Characterization of vascular disruption and blood-spinal cord barrier permeability following traumatic spinal cord injury. *J Neurotrauma*. 2014;31(6):541-552. doi:10.1089/neu.2013.3034
19. Nakagawa S, Deli MA, Kawaguchi H, et al. A new blood-brain barrier model using primary rat brain endothelial cells, pericytes and astrocytes. *Neurochem Int*. 2009;54(3-4):253-263. doi:10.1016/j.neuint.2008.12.002
20. Noble LJ, Donovan F, Igarashi T, Goussev S, Werb Z. Matrix metalloproteinases limit functional recovery after spinal cord injury by modulation of early vascular events. *J Neurosci*. 2002;22(17):7526-7535. http://www.jneurosci.org/content/22/17/7526.full.pdf.
21. Vandooren J, Van den Steen PE, Opdenakker G. Biochemistry and molecular biology of gelatinase B or matrix metalloproteinase-9 (MMP-9): the next decade. *Crit Rev Biochem Mol Biol*. 2013;48(3):222-272. doi:10.3109/10409238.2013.770819
22. Pan W, Kastin AJ. Increase in TNFalpha transport after SCI is specific for time, region, and type of lesion. *Exp Neurol*. 2001;170(2):357-363. doi:10.1006/exnr.2001.7702
23. Taoka Y, Okajima K, Uchiba M, et al. Role of neutrophils in spinal cord injury in the rat. *Neuroscience*. 1997;79(4):1177-1182.
24. Neirinckx V, Coste C, Franzen R, Gothot A, Rogister B, Wislet S. Neutrophil contribution to spinal cord injury and repair. *J Neuroinflammation*. 2014;11:150. doi:10.1186/s12974-014-0150-2
25. Bao F, Brown A, Dekaban GA, Omana V, Weaver LC. CD11d integrin blockade reduces the systemic inflammatory response syndrome after spinal cord injury. *Exp Neurol*. 2011;231(2):272-283. doi:10.1016/j.expneurol.2011.07.001
26. Kooijman E, Nijboer CH, van Velthoven CT, et al. Long-term functional consequences and ongoing cerebral inflammation after subarachnoid hemorrhage in the rat. *PLoS One*. 2014;9(6):e90584. doi:10.1371/journal.pone.0090584
27. Mantovani A. The yin-yang of tumor-associated neutrophils. *Cancer Cell*. 2009;16(3):173-174. doi:10.1016/j.ccr.2009.08.014
28. Kolaczkowska E, Kubes P. Neutrophil recruitment and function in health and inflammation. *Nat Rev Immunol*. 2013;13(3):159-175. doi:10.1038/nri3399
29. Langereis JD. Neutrophil integrin affinity regulation in adhesion, migration, and bacterial clearance. *Cell Adh Migr*. 2013;7(6):476-481. doi:10.4161/cam.27293
30. Maldonado-Bouchard S, Peters K, Woller SA, et al. Inflammation is increased with anxiety- and depression-like signs in a rat model of spinal cord injury. *Brain Behav Immun*. 2015. doi:10.1016/j.bbi.2015.08.009
31. DePaul MA, Palmer M, Lang BT, et al. Intravenous multipotent adult progenitor cell treatment decreases inflammation leading to functional recovery following spinal cord injury. *Sci Rep*. 2015;5:16795. doi:10.1038/srep16795
32. Carpenter RS, Kigerl KA, Marbourg JM, et al. Traumatic spinal cord injury in mice with human immune systems. *Exp Neurol*. 2015;271:432-444. doi:10.1016/j.expneurol.2015.07.011
33. Liu ZH, Yip PK, Adams L. A Single Bolus of Docosahexaenoic Acid Promotes Neuroplastic Changes in the Innervation of Spinal Cord Interneurons and Motor Neurons and Improves Functional Recovery after Spinal Cord Injury. 2015;35(37):12733-12752. doi:10.1523/jneurosci.0605-15.2015
34. Bendall LJ, Bradstock KF. G-CSF: From granulopoietic stimulant to bone marrow stem cell mobilizing agent. *Cytokine Growth Factor Rev*. 2014;25(4):355-367. doi:10.1016/j.cytogfr.2014.07.011
35. Brennan FH, Kurniawan ND, Vukovic J, et al. IVIg attenuates complement and improves spinal cord injury outcomes in mice. *Ann Clin Transl Neurol*. 2016:n/a-n/a. doi:10.1002/acn3.318
36. Ditor DS, Bao F, Chen Y, Dekaban GA, Weaver LC. A therapeutic time window for anti-CD 11d monoclonal antibody treatment yielding reduced secondary tissue damage and

enhanced behavioral recovery following severe spinal cord injury. *J Neurosurg Spine*. 2006;5(4):343-352. doi:10.3171/spi.2006.5.4.343

37. Bao F, Chen Y, Dekaban GA, Weaver LC. Early anti-inflammatory treatment reduces lipid peroxidation and protein nitration after spinal cord injury in rats. *J Neurochem*. 2004;88(6):1335-1344. http://onlinelibrary.wiley.com/store/10.1046/j.1471-4159.2003.02240.x/asset/j.1471-4159.2003.02240.x.pdf?v=1&t=i3kp9h5j&s=aa60263cc04338713e8aaffb6e2087d0cbe66f4c.
38. Bao F, Omana V, Brown A, Weaver LC. The systemic inflammatory response after spinal cord injury in the rat is decreased by alpha4beta1 integrin blockade. *J Neurotrauma*. 2012;29(8):1626-1637. doi:10.1089/neu.2011.2190
39. Gris D, Marsh DR, Oatway MA, et al. Transient blockade of the CD11d/CD18 integrin reduces secondary damage after spinal cord injury, improving sensory, autonomic, and motor function. *J Neurosci*. 2004;24(16):4043-4051. doi:10.1523/jneurosci.5343-03.2004
40. Stirling DP, Liu S, Kubes P, Yong VW. Depletion of Ly6G/Gr-1 leukocytes after spinal cord injury in mice alters wound healing and worsens neurological outcome. *J Neurosci*. 2009;29(3):753-764. doi:10.1523/jneurosci.4918-08.2009
41. Furlan JC, Noonan V, Cadotte DW, Fehlings MG. Timing of decompressive surgery of spinal cord after traumatic spinal cord injury: an evidence-based examination of pre-clinical and clinical studies. *J Neurotrauma*. 2011;28(8):1371-1399. doi:10.1089/neu.2009.1147
42. Fehlings MG, Wilson JR, Harrop JS, et al. Efficacy and Safety of Methylprednisolone Sodium Succinate in Acute Spinal Cord Injury: A Systematic Review. *Glob Spine J*. 2017;7(3 Suppl):116s-137s. doi:10.1177/2192568217706366
43. Riegger T, Conrad S, Liu K, Schluesener HJ, Adibzahdeh M, Schwab JM. Spinal cord injury-induced immune depression syndrome (SCI-IDS). *Eur J Neurosci*. 2007;25(6):1743-1747. doi:10.1111/j.1460-9568.2007.05447.x

*Translational Research

DEEP BRAIN STIMULATION OF THE NUCLEUS ACCUMBENS IN THE TREATMENT OF SEVERE ALCOHOL USE DISORDER: TARGETING THE BRAIN'S REWARD SYSTEM TO TREAT ADDICTION

Benjamin Davidson (SSTP), Peter Giacobbe, Clement Hamani, Nir Lipsman
Harquail Center for Neuromodulation, Sunnybrook Heath Sciences Centre, and University of Toronto

BACKGROUND

Alcohol use disorder (AUD) is the most common, costly, and lethal substance abuse disorder worldwide, with prevalence continuing to rise.[1,2] Five percent of all deaths worldwide are attributable to alcohol consumption; this rate climbs to 25% in the 20-39 age group.[3] AUD affects >10% of the general population, accounts for 3.3 billion dollars of healthcare expenditures annually in Canada, and shortens the lifespan by at least 20 years.[4-6] There is a shortage of effective treatments, with over 75% relapsing within 3 years.[7,8]

Novel therapies for AUD, and addictions in general, are desperately needed. Such therapies should be informed by a growing knowledge of the neurocircuitry underlying addiction. Although the etiology of AUD involves complex genetic and psychosocial factors, the cravings, compulsivity, and relapse aspects of AUD have been mapped to dysfunctional reward circuitry in the brain, centered around the nucleus accumbens (NAc). The NAc, a pivotal node in the mesolimbic reward and motivational systems, receives inappropriate dopamine release in response to alcohol and alcohol-associated cues, but becomes increasingly insensitive to natural rewards and motivations, plunging the addicted brain into a negative feedback cycle of trying to escape persistent dysphoria.

Deep brain stimulation (DBS), a standard neurosurgical treatment used in movement disorders, has been performed over 200,000 times worldwide.[9] This safe, targeted, neuromodulation procedure, also offers the ability to intervene in aberrant neurocircuit dysfunction seen in AUD and other addictions. It has been theorized that DBS to the NAc could disrupt the pathologic peaks and troughs in reward-related dopamine release, thought to drive the cravings, compulsivity, and relapse which characterize AUD. In rodents, DBS of the NAc has been shown to mitigate compulsive alcohol use,[10,11] therefore sparking considerable interest in human applications.[12,13] Here we present the preliminary results from a novel, phase-1 trial of DBS for AUD in humans, which was recently featured as the cover story in Macleans Magazine. (https://www.macleans.ca/society/health/frank-plummers-brain-science/)

HYPOTHESIS

Deep brain stimulation of the NAc disrupts aberrant reward circuitry helping mitigate alcohol consumption, cravings, compulsivity, and relapse in AUD.

PURPOSE: Conduct a phase-1 trial of deep brain stimulation (DBS) of the nucleus accumbens in AUD. Use task-based functional magnetic resonance imaging (fMRI) to interrogate the changes in the brain's reward network in response to treatment.

METHODS:

6 patients with severe, refractory AUD were enrolled in a registered, Health Canada-Approved phase-1 clinical trial, involving DBS of the NAc (NCT03660124) (See **Table 1** for baseline demographic information). The primary outcome of interest was safety, however, an extensive battery of validated tests were used to asses psychosocial, neurocognitive, general, and AUD-specific functioning at baseline, and at regular follow-up intervals until 12-months

postoperatively. Secondary outcome measures included alcohol consumption (Timeline Followback Alcohol Use Questionnaire(TLFB)[14] – a validated tool for tracking alcohol use), cravings and compulsivity (measured using the Alcohol Cravings Questionnaire - ACQ), mood (Hamilton Depression Rating Scale, HAMD[15]), anxiety, and markers of liver dysfunction.

Task-based fMRI was used to investigate changes in neural responsiveness and connectivity within the NAc, and the rest of the brain. Patients underwent a previously validated fMRI task[16,17], which involves subjects viewing neutral, and alcohol-related images. The exact validated image set was generously shared by the original authors in ref [16]). Scanning took place preoperatively, and 6 months postoperatively. Due to concerns surrounding the safe MRI scanning of a DBS device[18,19], we performed a series of phantom safety experiments prior to scanning humans (for a published account of our phantom tests see refs [20,21]).

RESULTS:
In this world-first trial, DBS was found to be safe in patients with advanced, treatment refractory AUD. DBS did not result in hemorrhages, infarcts, or neurologic deficits. Subject #3 (partial-responder), developed an unusual cellulitis around their implanted pulse generator at 10 months, requiring device explantation. There were no other serious adverse events.

Overall, 2/6 patients were considered to be clinical responders, with both patients seeing dramatic improvements in quality of life and drinking behaviour. 3/6 patients were partial responders, displaying reduced cravings and increased control of alcohol consumption. The non-responder reported reduced pleasure/enjoyment from ETOH consumption, and despite maintaining 6-months of abstinence, relapsed to pre-DBS levels of drinking shortly before the 12-month follow-up.

In 5/6 patients, there was a reduction in alcohol consumption (reduction of 8.5 standard drinks/day, p=0.03) and alcohol-related compulsivity (ACQ-Factor 1 pre=5.0, last follow-up=2.7,p=0.05). All patients reported diminished cravings (ACQ-total preop=58, last follow-up=45, p=0.09). There was also a trend towards improved anxiety and depression (reduction in BAI = 50% (p=0.17), reduction in HAMD = 18.5% (p=0.18)).

DBS had significant and sustained effects on the brain's reward circuitry. On fMRI analysis, comparing preoperative versus 6-months, DBS was found to reduce activation in the left nucleus accumbens in response to visual alcohol cues ($p_{uncorrected}<0.05$) (**Figure 2**).

CONCLUSION
DBS for severe refractory AUD is a promising therapy. It resulted in a significant reduction in alcohol consumption, likely mediated through a marked reduction in cravings and compulsivity. A possible mechanism underlying this change is a reduction in nucleus accumbens, demonstrated on real-time fMRI. These results suggest that direct-to-circuit neuromodulation of the brain's reward pathways may be a promising approach to addressing addiction, among the most challenging public health issues.

Table 1. Baseline Demographics

Subject	Age/Sex	Alcohol consumption	ETOH-Related Comorbidities
1	66/M	6-8 drinks of scotch/day (on transplanted liver)	Liver transplant Delirium Tremens
2	56/M	Binge consumption of ~12 SD's of vodka/day	Delirium Tremens Transaminitis
3	44/F	20 SD's/day vodka	Nil
4	47/F	18 SD's/day vodka	Nil
5	51/M	9-12 SD's of vodka/day, over 4-5 hrs.	Delirium Tremens Thrombocytopenia Tremors
6	20/M	Binge consumption of up to 20 SD's of vodka every 2-3 days	Transaminitis Gastritis

SD's: Standard Drinks

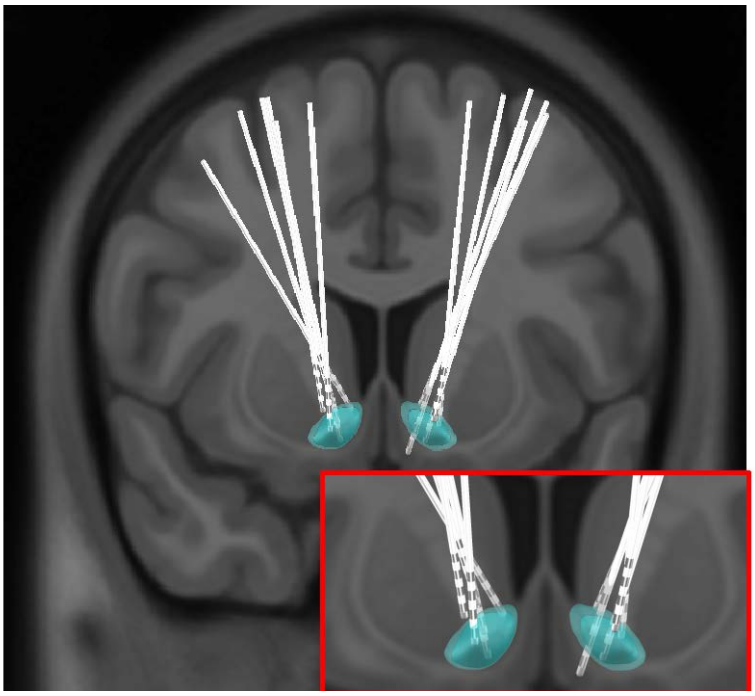

Figure 1. Reconstructed imaged of NAc DBS electrodes from 6 patients, normalized to MNI152 space.

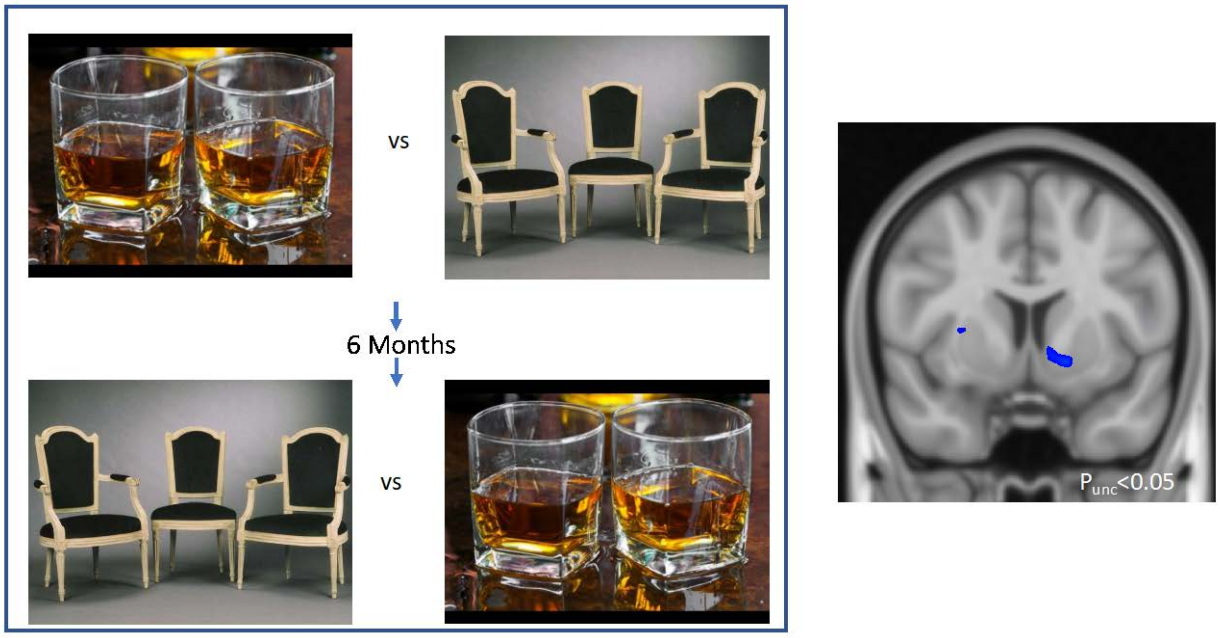

Figure 2. *Left:* Illustration of the fMRI task, which involved subjects viewing images of alcoholic beverages and neutral images, which was repeated 6-months postoperatively. *Right:* Reduced BOLD activation seen in the left nucleus accumbens (larger blue cluster) region while viewing alcohol images at 6 months compared to preoperatively ($p_{uncorrected}$ <0.05).

*Translational Research

References

1. Rehm J, Gnam W, Popova S, et al. The costs of alcohol, illegal drugs, and tobacco in Canada, 2002. J Stud Alcohol Drugs 2007;68:886-95.
2. Schuckit MA. Remarkable Increases in Alcohol Use Disorders. JAMA Psychiatry 2017;74:869-70.
3. WHO global status report on alcohol 2004. Geneva: World Health Organization; 2004.
4. Poznyak V, Rekve D. Global Status Report on Alcohol and Health 2014: World Health Organization; 2014.
5. Grant BF, Goldstein RB, Saha TD, et al. Epidemiology of DSM-5 Alcohol Use Disorder: Results From the National Epidemiologic Survey on Alcohol and Related Conditions III. JAMA Psychiatry 2015;72:757-66.
6. George TP. Alcohol use and misuse. CMAJ 2007;176:621-2.
7. Schwarzinger M, Thiebaut SP, Baillot S, Mallet V, Rehm J. Alcohol use disorders and associated chronic disease - a national retrospective cohort study from France. BMC Public Health 2017;18:43.
8. Westman J, Wahlbeck K, Laursen TM, et al. Mortality and life expectancy of people with alcohol use disorder in Denmark, Finland and Sweden. Acta Psychiatr Scand 2015;131:297-306.
9. Lozano AM, Lipsman N, Bergman H, et al. Deep brain stimulation: current challenges and future directions. Nat Rev Neurol 2019;15:148-60.
10. Knapp CM, Tozier L, Pak A, Ciraulo DA, Kornetsky C. Deep brain stimulation of the nucleus accumbens reduces ethanol consumption in rats. Pharmacol Biochem Behav 2009;92:474-9.
11. Henderson MB, Green AI, Bradford PS, Chau DT, Roberts DW, Leiter JC. Deep brain stimulation of the nucleus accumbens reduces alcohol intake in alcohol-preferring rats. Neurosurg Focus 2010;29:E12.
12. Salib AN, Ho AL, Sussman ES, Pendharkar AV, Halpern CH. Neuromodulatory Treatments for Alcohol Use Disorder: A Review. Brain Sci 2018;8.
13. Ho AL, Salib AN, Pendharkar AV, Sussman ES, Giardino WJ, Halpern CH. The nucleus accumbens and alcoholism: a target for deep brain stimulation. Neurosurg Focus 2018;45:E12.
14. wennberg P. The timeline follow back technique: psychometric properties of a 28-day timeline for measuring alcohol consumption. German J Psychiatry 1998;2:62-8.
15. Hamilton M. Rating depressive patients. J Clin Psychiatry 1980;41:21-4.
16. Vollstadt-Klein S, Wichert S, Rabinstein J, et al. Initial, habitual and compulsive alcohol use is characterized by a shift of cue processing from ventral to dorsal striatum. Addiction 2010;105:1741-9.
17. Strosche A, Zhang X, Kirsch M, et al. Investigation of brain functional connectivity to assess cognitive control over cue-processing in Alcohol Use Disorder. Addict Biol 2020:e12863.
18. Boutet A, Rashid T, Hancu I, et al. Functional MRI Safety and Artifacts during Deep Brain Stimulation: Experience in 102 Patients. Radiology 2019:190546.
19. Boutet A, Hancu I, Saha U, et al. 3-Tesla MRI of deep brain stimulation patients: safety assessment of coils and pulse sequences. J Neurosurg 2019:1-9.
20. Yang B, Tam F, Davidson B, et al. Technical Note: An anthropomorphic phantom with implanted neurostimulator for investigation of MRI safety. Med Phys 2020.
21. Davidson B, Tam F, Yang B, et al. Three-Tesla Magnetic Resonance Imaging of Patients With Deep Brain Stimulators: Results From a Phantom Study and a Pilot Study in Patients. Neurosurgery 2020.

STEREOTACTIC BODY RADIOTHERAPY VERSUS SURGERY IN OLDER ADULTS WITH NON-SMALL CELL LUNG CANCER – A POPULATION-BASED, MATCHED ANALYSIS OF LONG-TERM DEPENDENCY OUTCOMES

Dhruvin H. Hirpara[1], Biniam Kidane[2,3,4], Alexandre Louie[5], Victoria Zuk[6,7], Gail Darling[8], Mathieu Rousseau[9], Tyler Chesney[10], Natalie Coburn[6,7,11], Julie Hallet[6,7,11]

Affiliations:

[1]Department of Surgery, University of Toronto, Toronto, Ontario, Canada;
[2]Section of Thoracic Surgery, Department of Surgery, University of Manitoba, Winnipeg, Manitoba, Canada;
[3]Department of Community Health Sciences, University of Manitoba, Winnipeg, Manitoba, Canada;
[4]Research Institute in Oncology and Hematology, Cancer Care Manitoba, Winnipeg, Manitoba, Canada;
[5]Division of Radiation Oncology, Odette Cancer Centre – Sunnybrook Health Sciences Centre, Toronto, Ontario, Canada;
[6]Clinical Evaluative Sciences, Sunnybrook Research Institute, Toronto, Ontario, Canada;
[7]ICES, Toronto, Ontario, Canada;
[8]Division of Thoracic Surgery, Department of Surgery, University Health Network, Toronto, Ontario, Canada;
[9]Department of Thoracic Surgery, University of Montréal, Montréal, Québec, Canada
[10]Department of Surgery, St. Michael's Hospital, Toronto, Ontario, Canada;
[11]Division of Surgical Oncology, Odette Cancer Centre – Sunnybrook Health Sciences Centre, Toronto, Ontario, Canada.

Principal Investigator/Supervisor:
Julie Hallet, MD MSc FRCSC
2075 Bayview avenue, Toronto, Ontario, Canada, M4N 3M5
T: 416-480-4774; F: 416-480-6002; E: julie.hallet@sunnybrook.ca

Disclosures: JH has received speaking honoraria from Ipsen Biopharmaceuticals Canada and Advanced Accelerator Applications. NC receives salary support from Ontario Health (Cancer Care Ontario) as the Clinical Lead for Patient Reported Outcomes and Symptoms Management.

Introduction
Stereotactic body radiotherapy (SBRT) is a less invasive treatment compared to surgery for stage I non-small cell lung cancer (NSCLC), particularly in potentially vulnerable older adults. Our current understanding of the comparative effectiveness of these modalities is guided by several non-randomized studies of varying quality.[1-11] While overall survival is thought to favour surgery over SBRT, lung-cancer specific survival has been shown to be similar across modalities.[1-3] Given comparable oncologic outcomes, quality of life (QOL) and survivorship is of increasing importance, especially for potentially vulnerable older adults. This study aimed to examine functional and long-term healthcare dependency outcomes of SBRT to surgery for older adults with stage I NSCLC.

Methods
We conducted a population-based analysis of adults ≥70 years old with stage I NSCLC treated with surgery or SBRT from January 2010 to December 2017, by linking administrative datasets housed at ICES. This study was approved by the Sunnybrook Health Sciences Centre Research Ethics Board. It was conducted and reported following the RECORD (REporting of studies Conducted using Observational Routinely-collected Data) statement.[18] SBRT patients were matched 1:1 using a propensity score including age, comorbidity burden, chronic obstructive pulmonary disease, socioeconomic status, and a hard-match on frailty. Post-treatment homecare utilization per 100 eligible patients, probability of being alive and at home, and 1-year days at home, were compared using Andersen-Gill, piecewise Cox, and negative binomial regression models, respectively. E-value methods assessed the potential for residual confounding. Statistical significance was set at p≤0.05. All analyses were conducted using SAS Enterprise Guide 7.1 (SAS Institute, Cary, NC, USA).

Results
A total of 3,699 patients with ES-NSCLC were selected for the final analysis. This included 2,570 patients undergoing surgery and 1,129 patients undergoing SBRT. The majority of patients in the surgery group were treated with video-assisted thoracic surgery (VATS; 72%) lobectomy (71%). Of those treated with sublobar resection, 16% underwent segmentectomy and 13% underwent a wedge resection. Median follow-up was 38 months (IQR 20-61 months). A total of 1,016 patients were matched in each group. The matched cohorts were well-balanced with respect to age, sex, frailty, comorbidity burden, COPD, rurality and material deprivation (Standardized Mean Difference <10%; Table 1).

A greater proportion of patients undergoing surgery required homecare in the immediate post-operative period. This number decreased within six months of surgery with a consistently greater proportion of SBRT patients requiring homecare in the six months to five years following treatment, compared to the surgical cohort (Figure 1). This difference persisted, albeit only for three years post-treatment, in a stratified analysis adjusting for patient frailty. Overall, a greater proportion of frail patients required post-treatment homecare in both the surgical and SBRT cohorts. Using the Andersen-Gill regression, SBRT was associated with a higher overall risk of post-treatment homecare utilization (HR 1.75, 95%CI 1.37, 2.23) than surgery. The E-value for homecare utilization was 2.31, indicating that residual confounding could explain the observed association if there exists an unmeasured covariate having a relative risk association at least as large as 2.31 with both SBRT and homecare use. It is important to contextualize this with hazard ratios for some of the well-known risk factors for homecare use such as high comorbidity burden (HR 1.46, 95%CI 1.20, 1.77), and COPD (HR 1.56, 95%CI 1.23, 1.99).

SBRT was associated with a greater likelihood of being alive and at home in the first three months after treatment. Surgery, however, was associated with higher probability of being alive

and at home beyond this period, at 3-6 months (HR1.98, 95%CI 1.12, 3.48), 6-12 months (HR 1.87, 95%CI 1.33, 2.64), 2-3 years (HR 2.31, 95%CI 1.64, 3.24), and 4-5 years (HR 1.79, 95%CI 1.11, 2.91) in comparison to SBRT, on piecewise Cox regression (Figure 2). The E-value for being alive and at home was 2.38. We note the hazard Ratios for other well-known risk factors for this outcome such as advanced age (HR1.56, 95%CI 1.29, 1.89), high comorbidity burden (HR 1.19, 95%CI 1.07, 1.33), and COPD (HR 1.56, 95%CI 1.34, 1.81).

SBRT patients also had statistically fewer days at home (median 352 days, IQR 346-355 days) than those with surgery (median 358 days, IQR 351-360 days; $p<0.01$) in the year following treatment (Rate Ratio 1.01, 95%CI 1.01, 1.02).

Discussion

This population-based analysis provides a unique description of long-term functional and dependency outcomes of older adults treated with SBRT and surgery for stage I NSCLC. Our propensity score-matched analysis suggests that while SBRT is less invasive, it is associated with higher long-term home care utilization, as well as lower probability of being alive and at home and fewer 1-year days at home, than surgery in adults over the age of 70. The findings persisted in adjusted analyses accounting for age, comorbidity burden, and presence of COPD, as well as in stratified analyses for frail and non-frail patients. E-values indicated it was unlikely that the observed estimates could be explained away by unmeasured confounders.

The need for care services for older adults with lung cancer is expected to increase in part due to an ageing population coupled with the advent of screening in high-risk patients and associated improvements in long-term survival.[19] Determining which treatment (i.e. surgery or SBRT) is optimal for a patient with early-stage NSCLC requires careful consideration of disease, treatment, and patient-specific factors. These include oncologic outcomes like propensity for local control and overall survival, juxtaposed with the patient's fitness for surgery, risk of treatment toxicity and QOL. Nugent et al. (2020) recently provided important longitudinal data on 127 patients, evaluating changes in self-reported QOL, before, during and after (up to 12 months) treatment with surgery or SBRT for stage I NSCLC.[15] In this prospective, multi-site study, surgical resection was associated with a steeper decline, particularly in global and physical QOL, during and 4-6 weeks after treatment compared to SBRT. This decline, however, was short-lived and recovered within a year for most patients. Conversely, patients that received SBRT had relatively stable global and physical QOL scores at each timepoint, though up to 30% had clinically significant worse scores than baseline at 12-months.[15] The existing body of literature on this topic, however, does not account for functional outcomes and dependency, which remain important aspects of health-related QOL.[12-17] Understanding the impact of treatment on functional outcomes is pivotal in improving patient preparedness by establishing realistic expectations and tailored care pathways to optimize the patient experience. This is especially crucial in older adults in whom increased functional dependency can hinder QOL, which in turn, is prognostic of clinical outcomes.[20]

In our analysis, monthly homecare utilization was observed to peak in the immediate post-operative period. This was followed by a steep decline in the number of surgical patients requiring homecare services in the six months following surgery, with a consistently greater proportion of SBRT patients requiring homecare in the six months to five years following treatment. This finding in functional outcomes and dependency after surgery mirrors a similar phenomenon described in patient-reported symptom burden: that of the early deterioration, which improves and stabilizes in the 6-12 months following surgery.[16,22] The proportion of SBRT patients requiring homecare, albeit higher than the surgical cohort over time, remained relatively

constant throughout the follow up period. This corresponds to our current understanding of the relatively small changes reported in health-related QOL after SBRT in the NSCLC literature.[12,15] Surgical patients were also more likely to be alive and at home after 3 months and beyond, as well as spend more days at home in the year following surgery. The abovementioned differences, albeit smaller in magnitude, persisted after stratifying for patient frailty. It is important to note that including age, comorbidity burden, frailty and COPD status in the matching algorithm, does not preclude baseline discrepancy between the groups. This is evidenced by higher pre-treatment homecare use in the SBRT group (23% vs. 12%) with a standardized mean difference of 29% in the matched cohort. This raises the possibility of unmeasured or unknown confounders that may not have been accounted for by the frailty and comorbidity indices utilized in this study. Although, our E-value calculations suggest that any such variable would only have a substantial effect on the outcomes of interest by having a relative risk exceeding 2.31 (for homecare utilization) or 2.38 (for being alive and at home). This is in comparison to the magnitude of association of other well-known risk factors with the primary outcomes of this study such as advanced age (HR 1.56-1.83), and COPD status (HR 1.56), amongst others.

Our findings may also be contextualized by assessing the global burden of a lung cancer diagnosis and treatment, including short-term side effects and late repercussions. Severe physical (i.e., fatigue, dyspnea) and psychological symptoms can persist for up to one year after a lung cancer diagnosis, regardless of stage.[21] Those at risk of experiencing a high burden of severe symptoms, including patients with a high comorbidity burden, would benefit from targeted symptom management and psychosocial support aimed at improving health-related QOL, which may in turn enhance functional outcomes.

The results of this study should be interpreted in the context of the following key limitations. Despite a robust matching process, unmeasured confounders such as clinician judgement and patient preference, can persist and influence the outcomes. Selection criteria for patients who underwent either modality is not available, hence the possibility of uncontrolled confounding or selection bias remains. Our findings are also affected by limited case ascertainment due to coding changes and lack of granularity with respect to several important variables like pulmonary function tests, performance status, and tumor location. We also attempted to improve comparability between cohorts by excluding patients undergoing more extensive resections such as pneumonectomy.

Conclusion

This is one of the largest population-based analyses of long-term dependency outcomes after SBRT and surgery in older adults with stage I NSCLC. Our findings address an important gap in the NSCLC literature by describing the association of SBRT and surgery with important patient-centered outcomes such as homecare utilization and institution-free days at home. These findings merit prospective validation in a randomized fashion to better examine the complex interplay of disease, treatment and patient factors on long-term functional and dependency outcomes. In the meantime, the information gleaned from our study can be used to better empower patients, and to guide counselling and shared-decision making with older adults diagnosed with early-stage NSCLC.

References

1. Chen H, Laba JM, Boldt RG, et al. Stereotactic Ablative Radiation Therapy Versus Surgery in Early Lung Cancer: A Meta-analysis of Propensity Score Studies. Int J Radiat Oncol Biol Phys. 2018 May 1;101(1):186-194. doi: 10.1016/j.ijrobp.2018.01.064.
2. Chi A, Fang W, Sun Y, et al. Comparison of Long-term Survival of Patients With Early-Stage Non-Small Cell Lung Cancer After Surgery vs Stereotactic Body Radiotherapy. JAMA Netw Open. 2019 Nov 1;2(11): e1915724.
3. Razi SS, Kodia K, Alnajar A, et al. Lobectomy Versus Stereotactic Body Radiotherapy In Healthy Octogenarians With Stage I Lung Cancer. Ann Thorac Surg. 2020 Sep 3:S0003-4975(20)31448-X. doi: 10.1016/j.athoracsur.2020.06.097.
4. Crabtree TD, Denlinger CE, Meyers BF, et al. Stereotactic body radiation therapy versus surgical resection for stage I non-small cell lung cancer. J Thorac Cardiovasc Surg 2010;140: 377-386.
5. Shirvani SM, Jiang J, Chang JY, et al. Comparative effectiveness of 5 treatment strategies for early-stage non-small cell lung cancer in the elderly. Int J Radiat Oncol Biol Phys 2012;84: 1060-1070.
6. Matsuo Y, Chen F, Hamaji M, et al. Comparison of long-term survival outcomes between stereotactic body radiotherapy and sublobar resection for stage I non-small-cell lung cancer in patients at high risk for lobectomy: A propensity score matching analysis. Eur J Cancer 2014;50: 2932-2938.
7. Shirvani SM, Jiang J, Chang JY, et al. Lobectomy, sublobar resection, and stereotactic ablative radiotherapy for early-stage non-small cell lung cancers in the elderly. JAMA Surg 2014;149: 1244-1253.
8. Ezer N, Veluswamy RR, Mhango G, et al. Outcomes after stereotactic body radiotherapy versus limited resection in older patients with early-stage lung cancer. J Thorac Oncol 2015;10: 1201-1206.
9. Hamaji M, Chen F, Matsuo Y, et al. Video-assisted thoracoscopic lobectomy versus stereotactic radiotherapy for stage I lung cancer. Ann Thorac Surg 2015;99: 1122-1129.
10. Paul S, Lee PC, Mao J, et al. Long-term survival with stereotactic ablative radiotherapy (SABR) versus thoracoscopic sublobar lung resection in elderly people: National population-based study with propensity matched comparative analysis. BMJ 2016;354: i3570.
11. Puri V, Crabtree TD, Kymes S, et al. A comparison of surgical intervention and stereotactic body radiation therapy for stage I lung cancer in high-risk patients: A decision analysis. J Thorac Cardiovasc Surg 2012;143: 428-436.
12. Chen H, Louie AV, Boldt RG, et al. Quality of Life After Stereotactic Ablative Radiotherapy for Early-Stage Lung Cancer: A Systematic Review. Clin Lung Cancer. 2016 Sep;17(5):e141-e149. doi: 10.1016/j.cllc.2015.12.009.
13. Wolff HB, Alberts L, Kastelijn EA, et al. Differences in Longitudinal Health Utility between Stereotactic Body Radiation Therapy and Surgery in Stage I Non-Small Cell Lung Cancer. J Thorac Oncol. 2018 May;13(5):689-698. doi: 10.1016/j.jtho.2018.01.021.
14. Schwartz RM, Alpert N, Rosenzweig K, et al. Changes in quality of life after surgery or radiotherapy in early-stage lung cancer. J Thorac Dis. 2019;11(1):154-161. doi:10.21037/jtd.2018.12.30
15. Nugent SM, Golden SE, Hooker ER, et al. Longitudinal Health-related Quality of Life among Individuals Considering Treatment for Stage I Non-Small-Cell Lung Cancer. Ann Am Thorac Soc. 2020 Aug;17(8):988-997. doi: 10.1513/AnnalsATS.202001-029OC.
16. Hirpara DH, Kidane B. Early Worsening of Quality of Life after Treatment of Stage I Lung Cancer. Ann Am Thorac Soc. 2020;17(8):935-936. doi:10.1513/AnnalsATS.202005-523ED

17. Louie AV, van Werkhoven E, Chen H, et al. Patient reported outcomes following stereotactic ablative radiotherapy or surgery for stage IA non-small-cell lung cancer: results from the ROSEL multicenter randomized trial. Radiother Oncol 2015;117: 44–8.
18. Benchimol EI, Smeeth L, Guttmann A, et al; RECORD Working Committee. The REporting of studies Conducted using Observational Routinely-collected health Data (RECORD) statement. PLoS Med. 2015 Oct 6;12(10):e1001885. doi: 10.1371/journal.pmed.1001885.
19. Luo YH, Luo L, Wampfler JA, et al. 5-year overall survival in patients with lung cancer eligible or ineligible for screening according to US Preventive Services Task Force criteria: a prospective, observational cohort study. Lancet Oncol. 2019 Aug;20(8):1098-1108. doi: 10.1016/S1470-2045(19)30329-8.
20. Montazeri A. Quality of life data as prognostic indicators of survival in cancer patients: an overview of the literature from 1982 to 2008. Health Qual Life Outcomes. 2009 Dec 23;7:102. doi: 10.1186/1477-7525-7-102.
21. Hirpara DH, Gupta V, Davis LE, et al. Severe symptoms persist for Up to one year after diagnosis of stage I-III lung cancer: An analysis of province-wide patient reported outcomes. Lung Cancer. 2020 Apr;142:80-89. doi: 10.1016/j.lungcan.2020.02.014.
22. Khullar OV, Rajaei MH, Force SD, et al. Pilot Study to Integrate Patient Reported Outcomes After Lung Cancer Operations Into The Society of Thoracic Surgeons Database. Ann Thorac Surg. 2017 Jul;104(1): 245-253.

Table 1. Demographics and clinical characteristics of included patients stratified by treatment group, in the entire and matched cohorts.

Characteristic		Entire cohort			Matched cohort		
		Surgery (n= 2,570)	**SBRT (n=1,129)**	**Standardized difference (%)***	**Surgery (n=1,016)**	**SBRT (n=1,016)**	**Standardized difference (%)***
Age (years old) – median (IQR)		75 (72-79)	79 (75-83)	0.64	78 (74-82)	79 (74-83)	7%
Female		1,204 (46.8%)	541 (47.9%)	2%	482 (47.4%)	485 (47.7%)	1%
Frailty		198 (7.7%)	179 (15.9%)	25%	482 (47.4%)	485 (47.7%)	1%
High comorbidity burden (ACG ≥10)		1,366 (53.2%)	588 (52.1%)	0.02	131 (12.9%)	131 (12.9%)	0%
Chronic obstructive pulmonary disease		189 (7.4%)	207 (18.3%)	33%	547 (53.8%)	564 (55.5%)	3%
Rural residence		332 (12.9%)	131 (11.6%)	4%	127 (12.5%)	122 (12.0%)	2%
Material deprivation quintile	1st (least deprived)	490 (19.0%)	1674 (15.4%)	11%	176 (17.3%)	156 (15.4%)	5%
	2nd	466 (18.1%)	213 (18.9%)	2%	165 (16.2%)	193 (19.0%)	7%
	3rd	542 (21.1%)	242 (21.4%)	1%	216 (21.3%)	223 (21.9%)	2%
	4th	552 (21.5%)	237 (21.0%)	1%	223 (21.9%)	208 (20.5%)	4%
	5th (most deprived)	520 (20.2%)	263 (23.3%)	7%	236 (23.2%)	236 (23.2%)	0%
Pre-treatment homecare		245 (9.5%)	276 (24.4%)	41%	122 (12.0%)	232 (22.8%)	29%

%Values are n (%) unless otherwise specified
*standardized difference <10% represents a negligible difference
IQR: inter-quartile range; ACG : aggregated clinical groups

Figures

Figure 1. Monthly homecare utilization per 100 patients eligible by treatment type in the entire (A) and matched cohort (B).

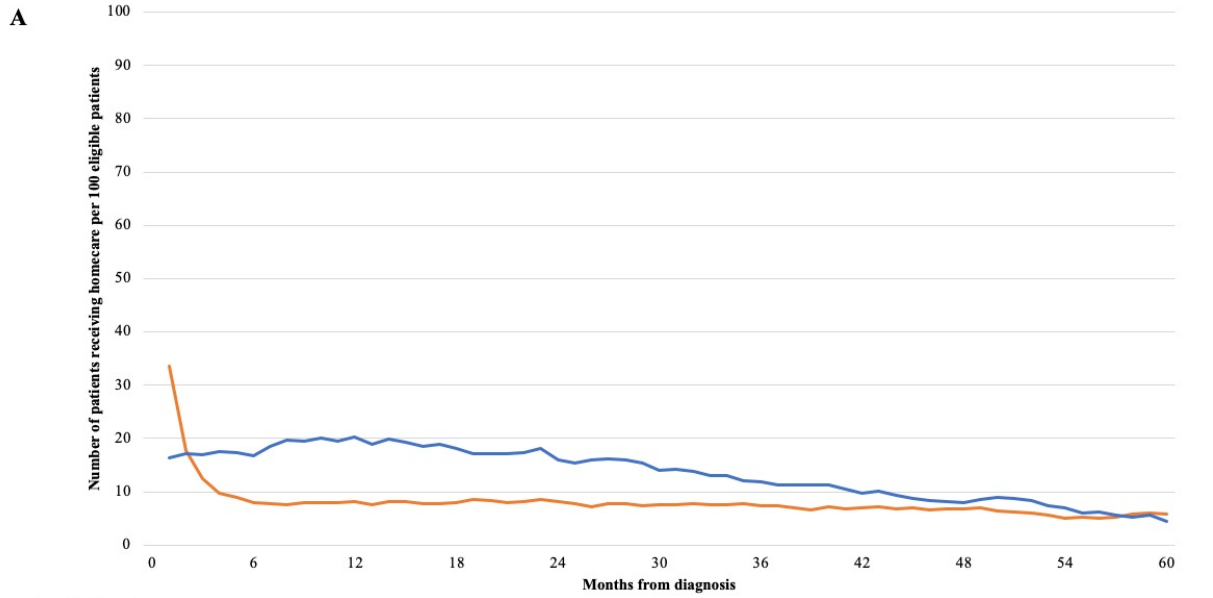

Number of eligible patients

Surgery	2570	2453	2360	2258	2156	2068	1996	1909	1849	1786	1743
SBRT	1129	1073	969	850	771	711	661	627	598	572	557

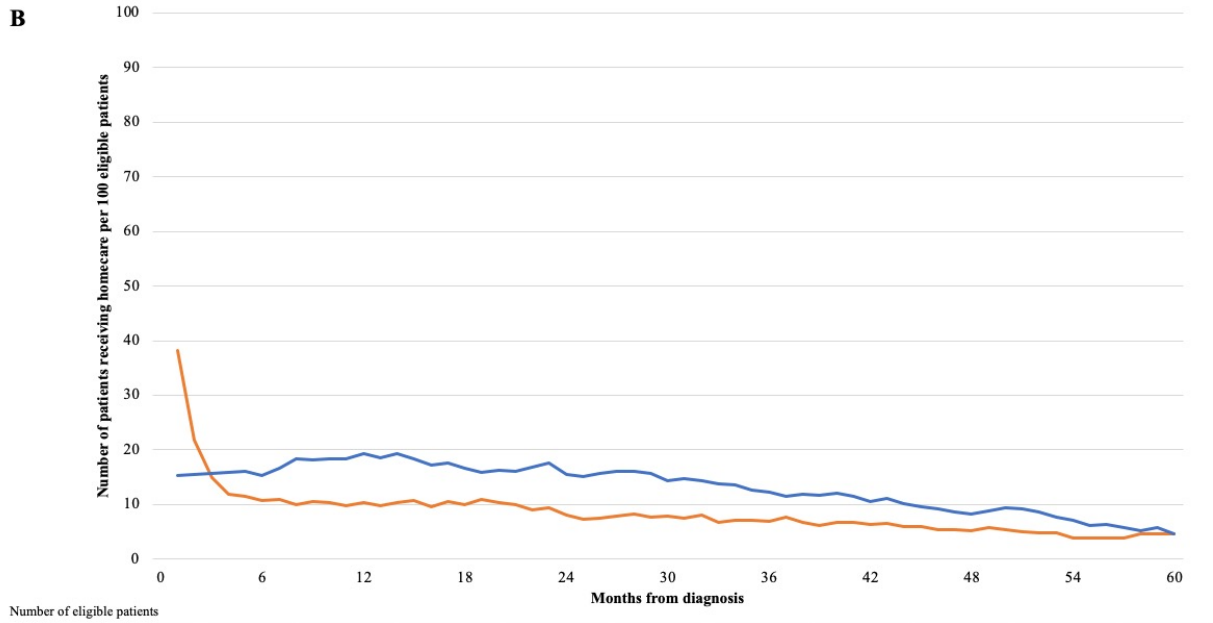

Number of eligible patients

Surgery	1016	958	916	869	826	790	767	732	709	687	673
SBRT	1016	965	877	771	704	649	602	569	540	514	500

Figure 2. Probability of being alive and at home by treatment type in the entire (A) and matched cohort (B)

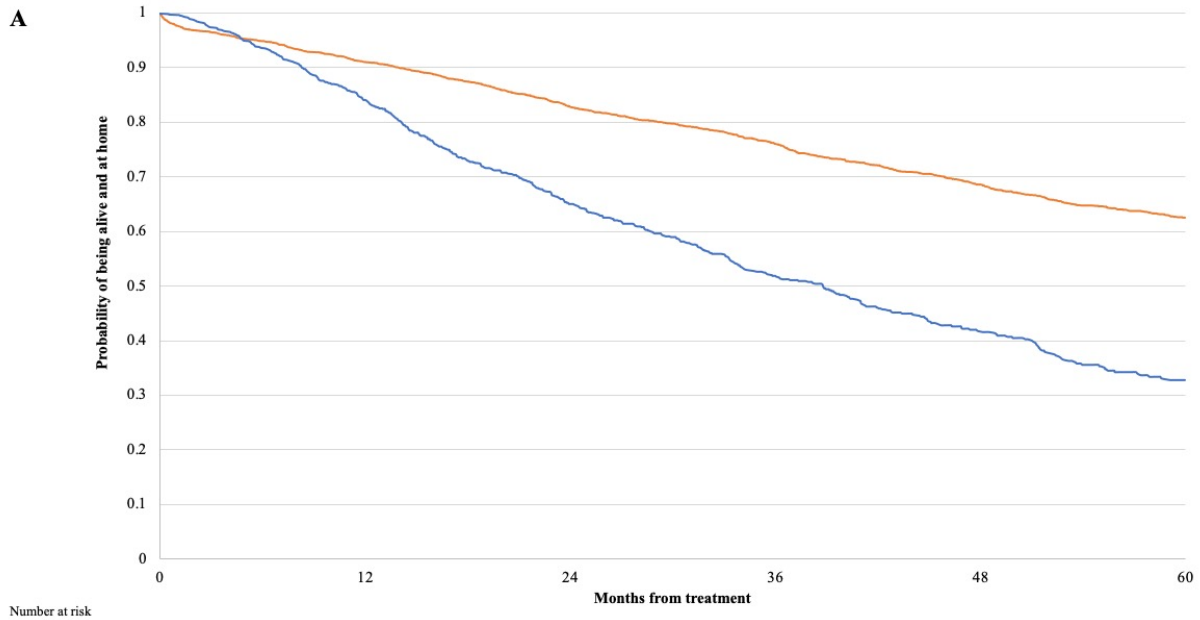

Number at risk

Surgery	1129	921	561	334	197	101
SBRT	2570	2301	1882	1476	1097	788

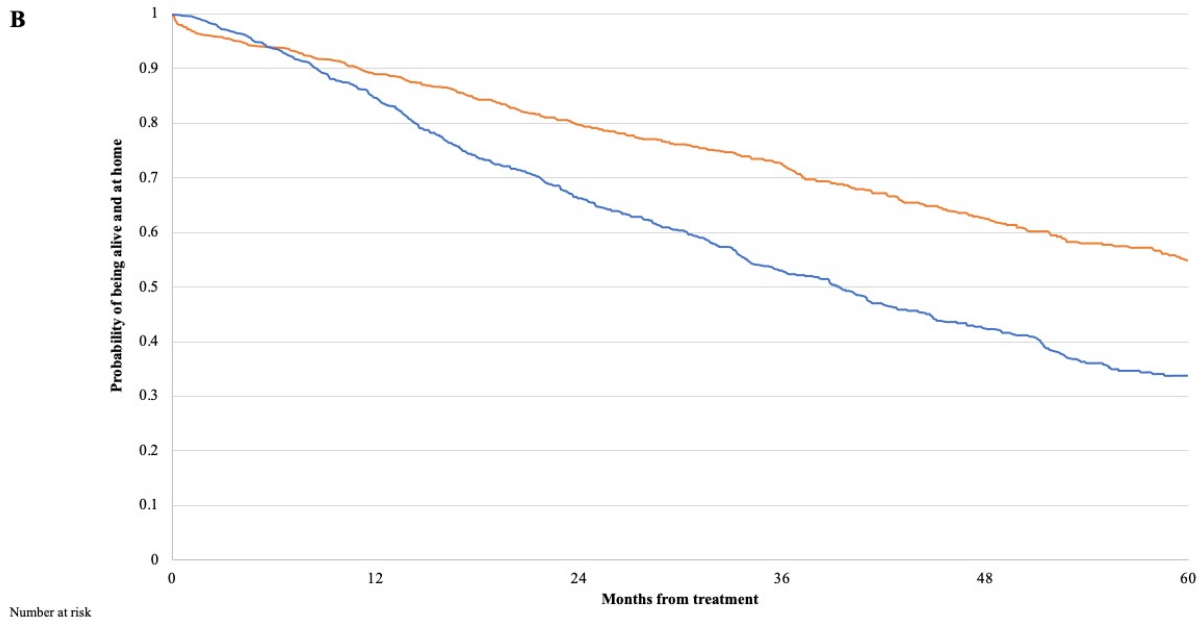

Number at risk

Surgery	1016	837	528	319	192	100
SBRT	1016	877	654	446	282	185

We are pleased to submit our study entitled “Stereotactic Body Radiotherapy versus Surgery in Older Adults with Non-Small Cell Lung Cancer – a population-based, matched analysis of long-term dependency outcomes” for the oral presentation competition at the 47th Gallie Day.

This study aimed to examine functional and long-term healthcare dependency outcomes of SBRT to surgery for older adults with stage I NSCLC. While less invasive, SBRT was associated with inferior long-term dependence outcomes than surgery for older adults with stage I NSCLC, with higher homecare utilization and lower probability of being alive and at home. These are important patient-centred endpoints for counselling and shared-decision making for older adults with early-stage lung cancer.

This study was conducted primarily at the Sunnybrook Research Institute between June-December 2020. The work was supported by ICES, which is funded by an annual grant from the Ontario Ministry of Health and Long-Term Care (MOHLTC). We confirm that all authors have contributed to critical portions of the study including conception and design, data acquisition, data analysis, drafting of the manuscript and revisions, and have approved this version to be submitted. The manuscript, including related data, figures and tables is not yet published.

Thank you for your consideration.

Sincerely,

Dhruvin H. Hirpara, MD (PGY-IV, General Surgery)
Julie Hallet, MD MSc FRCSC (Supervisor/Principal Investigator)

USING EXPLAINABLE ARTIFICIAL INTELLIGENCE TO DEVELOP AN INTERPRETABLE MACHINE LEARNING MODEL TO PREDICT RISK OF SIDE-SPECIFIC EXTRAPROSTATIC EXTENSION IN MEN WITH PROSTATE CANCER

Jethro CC Kwong[1,2], Adree Khondker[3], Christopher Tran[3], Emily Evans[3], Amna Ali[4], Munir Jamal[1], Thomas Short[1], Frank Papanikolaou[1], John R. Srigley[5], Andrew H. Feifer[1,4]

[1]Division of Urology, Department of Surgery, University of Toronto, Toronto, ON, Canada
[2]Temerty Centre for AI Research and Education in Medicine, University of Toronto, Toronto, Canada
[3]Temerty Faculty of Medicine, University of Toronto, Toronto, ON, Canada
[4]Institute for Better Health, Trillium Health Partners, Mississauga, ON, Canada
[5]Department of Laboratory Medicine and Pathobiology, University of Toronto, Toronto, ON, Canada

Hypothesis and Purpose: Extra-prostatic extension (EPE) is a well-established prognostic factor in prostate cancer[1]. Accurate prediction and identification of EPE helps inform surgical planning for nerve-sparing at radical prostatectomy (RP). Current validated nomograms are limited to assessing overall risk of EPE and are powered by factors such as total Gleason score, serum prostate-specific antigen (PSA), and clinical stage[2,3]. We hypothesize that use of machine learning (ML) methods to integrate additional parameters readily available in prostate biopsy reports may provide more robust and personalized side-specific EPE (ssEPE) predictions, allowing for a more tailored surgical strategy. However, the advantages of ML-based analysis have been plagued by poor interpretability[4]. To improve on this, several approaches have been developed under the umbrella of "explainable artificial intelligence" (XAI). Previously used in intra-operative hypoxemia prediction[5], we set out to employ these novel XAI techniques to develop an intuitive web application to provide accurate, interpretable, and personalized predictions for ssEPE.

Methods: A retrospective sample of 900 prostatic lobes (450 patients) from RP specimens at Credit Valley Hospital, Mississauga, between 2010 and 2020, was used as the training cohort. Features (ie: variables) included patient demographics, clinical, sonographic, and site-specific data from transrectal ultrasound-guided prostate biopsy. The primary label (ie: outcome) of interest was the presence of EPE in the ipsilateral lobe of the prostatectomy specimen. All pathology was reviewed by a dedicated uro-pathologist. A separate logistic regression model by Sayyid *et al.*[6], which has the highest performance out of current predictive models for ssEPE, was used as the baseline model for comparison.

Dimensionality reduction was performed by removing highly correlated features (Pearson correlation > 0.8) and using a modified Boruta algorithm[7]. This method involves fitting all features to a random forest model and determining feature importance by comparing the relevance of each feature to that of random noise. Given that our dataset contains both categorical and numerical features, SHAP (Shapley Additive exPlanations)[8] was specifically selected in lieu of impurity-based measures to reduce bias towards high cardinality features.

Using the final set of the most important and independent features, a ten-fold stratified cross-validation method was performed to train a gradient-boosted model, optimize hyperparameters, and for internal validation. In stratified cross-validation, the training cohort was randomly partitioned into ten equal folds, with each fold containing the same percentage of positive ssEPE cases. Nine folds were used for model training and hyperparameter tuning while the remaining fold made up the validation cohort. This process was repeated ten times such that each fold served as the validation cohort once. Model performance was determined based on the average performance across all ten validation cohorts to improve generalizability of the models. All models

were further externally validated using a testing cohort of 122 lobes (61 patients) from RP specimens at Mississauga Hospital, Mississauga, between 2016 and 2020.

Discriminative capability was quantified by area under receiver-operating-characteristic (AUROC) and precision-recall curve (AUPRC). Clinical utility was determined by decision curve analysis, in which the net benefit is plotted against various threshold probabilities for three different treatment strategies: treat all, treat none, and treat only those predicted to have ssEPE by the model. SHAP was used to interpret the ML model's predictions.

Results: The incidence of ssEPE in the training and testing cohorts were 30.7 and 41.8%, respectively. Our ML model outperformed the baseline model with a mean AUROC of 0.81 vs 0.75 ($p<0.01$) and mean AUPRC of 0.69 vs 0.60, respectively (**Figure 1**). Similarly, our ML model performed favourably on the external testing cohort with an AUROC of 0.81 vs 0.76 ($p=0.03$) and AUPRC of 0.78 vs 0.72. On decision curve analysis, our ML model achieved a higher net benefit than the baseline model for threshold probabilities between 0.15 to 0.65 (**Figure 2**). This translates to a reduction in avoidable non-nerve-sparing radical prostatectomies by 10 vs 4 per 100 patients at a threshold value of 0.2. A web application incorporating our ML model was developed in which de-identified patient data can be inputted to generate an individualized ssEPE prostate map with annotated explanations to highlight which features had the greatest impact on model predictions (**Figure 3**, www.ssepe.ml).

Conclusions: We have developed a user-friendly application that enables physicians without prior ML experience to assess ssEPE risk and understand the factors driving these predictions to aid surgical planning and patient counselling. Further assessment of the applicability of this model is warranted.

References

1. Jeong BC, Chalfin HJ, Lee SB, et al. The relationship between the extent of extraprostatic extension and survival following radical prostatectomy. *Eur Urol*. 2015;67(2):342-346. doi:10.1016/j.eururo.2014.06.015
2. Steuber T, Graefen M, Haese A, et al. Validation of a nomogram for prediction of side specific extracapsular extension at radical prostatectomy. *J Urol*. 2006;175(3):939-944. doi:10.1016/S0022-5347(05)00342-3
3. Prostate Cancer Nomograms: Dynamic Prostate Cancer Nomogram: Coefficients | Memorial Sloan Kettering Cancer Center. https://www.mskcc.org/nomograms/prostate/pre_op/coefficients. Accessed March 24, 2020.
4. Chen J, Remulla D, Nguyen JH, et al. Current status of artificial intelligence applications in urology and their potential to influence clinical practice. *BJU Int*. 2019;124(4):567-577. doi:10.1111/bju.14852
5. Lundberg SM, Nair B, Vavilala MS, et al. Explainable machine-learning predictions for the prevention of hypoxaemia during surgery. *Nat Biomed Eng*. 2018;2(10):749-760. doi:10.1038/s41551-018-0304-0
6. Sayyid R, Perlis N, Ahmad A, et al. Development and external validation of a biopsy-derived nomogram to predict risk of ipsilateral extraprostatic extension. *BJU Int*. 2017;120(1):76-82. doi:10.1111/bju.13733
7. Kursa MB, Rudnicki WR. Feature selection with the boruta package. *J Stat Softw*. 2010;36(11):1-13. doi:10.18637/jss.v036.i11
8. Lundberg SM, Allen PG, Lee S-I. *A Unified Approach to Interpreting Model Predictions*.; 2017.

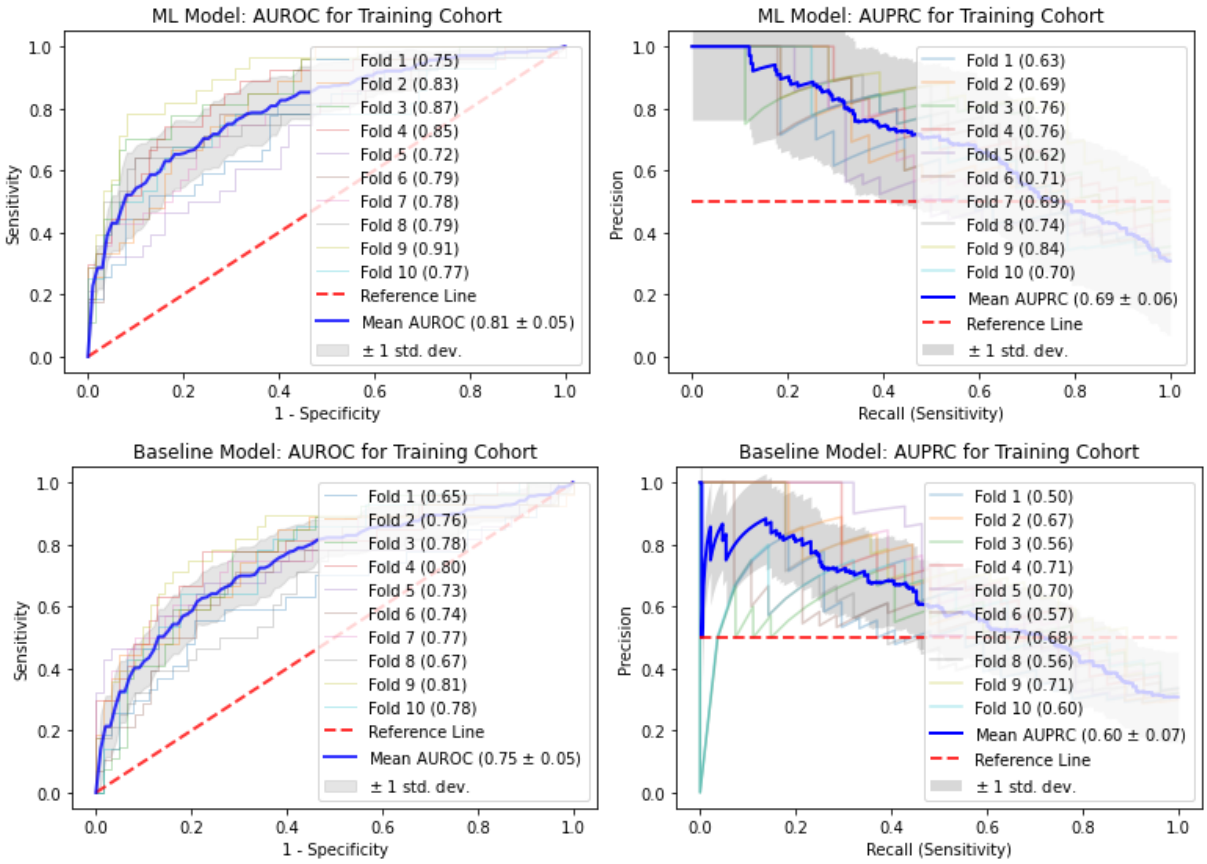

Figure 1. Discriminative ability of the ML and baseline models by AUROC and AUPRC analysis using stratified cross-validation of the training cohort.

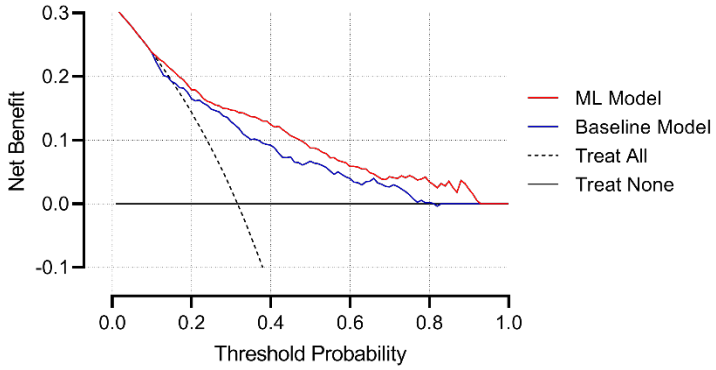

Threshold Probability	Reduction in avoidable treatment per 100 patients	
	ML Model	Baseline Model
0.2	10	4
0.3	26	22
0.4	36	32
0.5	42	40
0.6	47	46

Figure 2. Decision curves of the ML and baseline models. The clinical utility profiles for both predictive models across various threshold probabilities is shown on the right. Reduction in avoidable non-nerve-sparing radical prostatectomies using each predictive model is based on comparison with the “Treat All” strategy.

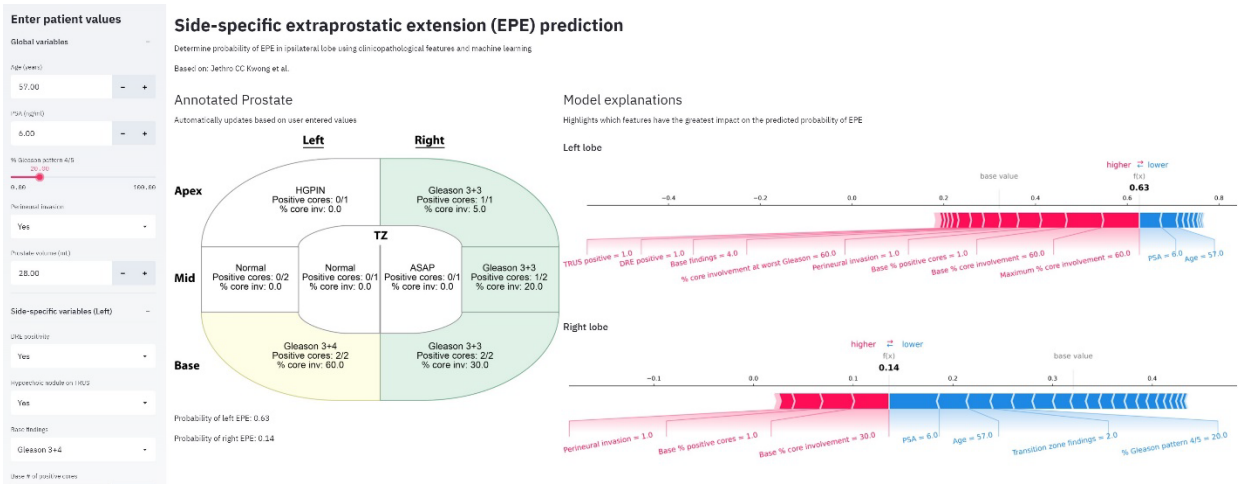

Figure 3. Web application incorporating the ML model. De-identified user-inputted data is entered to generate an annotated prostate diagram showing the location and severity of prostate cancer. A predicted probability of ssEPE is calculated for the left and right prostatic lobe to help tailor surgical planning (ie: nerve-sparing). Accompanying model explanations highlight which features had the greatest impact on model predictions.

POLO-LIKE KINASE 4 (PLK4) PROMOTES PERITONEAL METASTASIS THROUGH ACTIVATION OF THE RAC1 GUANINE NUCLEOTIDE EXCHANGE FACTOR PREX2

Deanna Ng[1,2], Karineh Kazazian[1,2,3], Olga Brashavitskaya[1], Kiera Lee[1], Aiman Ali[4], Karina Pacholczyk[1], Shelly Luu (SSTP)[1,2,3], Michelle Lee[1], Monica Hasegan[1], Savtaj Brar[3], Marco Magalhaes[4], Carol J. Swallow[1,2,3]

[1]Lunenfeld-Tanenbaum Research Institute, Sinai Health System, Toronto, Ontario
[2]Institute of Medical Science, University of Toronto
[3]Department of Surgery, University of Toronto
[3]Faculty of Dentistry, University of Toronto

Introduction: Gastric adenocarcinoma (GCa) is the 3rd leading cause of cancer death worldwide [1, 2]. In Canada, over half of patients present with distant metastatic disease, and are incurable [1, 3, 4]. Following curative intent resection of GCa, 40% of patients recur within 2 years, and die at a median of 6 months thereafter [1, 5, 6]. Transperitoneal dissemination of GCa, resulting in peritoneal metastasis, portends a particularly poor prognosis [7, 8]. It often causes intractable symptoms and is resistant to conventional systemic treatment [7, 9, 10]. Our laboratory is investigating the underlying mechanisms of peritoneal metastasis in GCa, to aid in the development of new therapies that might lead to improved survival and quality of life in patients at high risk of peritoneal dissemination.

High expression of Polo-like kinase 4 (Plk4) has been identified as a molecular predictor of aggressive behavior in patients with breast, pancreas and colorectal cancers [11-13]. Work from our laboratory has shown that Plk4 promotes cancer cell motility and invasion, driving aggressive local and metastatic progression in breast cancer xenografts [14-16]. These cellular behaviours depend on increased actin polymerization at the leading cell edge, stimulated by Plk4 [15]. Furthermore, the specific endogenous Plk4 kinase inhibitor FAM46C has the opposite effect on cancer cell motility and invasion, suppressing cancer progression in murine models [14]. We seek to understand the signalling pathways that translate increased Plk4 expression into rearrangement of the actin cytoskeleton.

The family of small Rho GTPases, which includes RhoA, Rac1 and Cdc42, is of interest as potential mediators of Plk4-driven migration and invasion [16]. Rho GTPase regulation is effected by over 80 known activating guanine exchange factors (GEFs) and 60 inactivating GTPase activating proteins (GAPs), which enable cells to reorganize their cytoskeleton in response to intra- and extracellular cues [17]. GEFs facilitate the exchange of GTP for GDP on Rac1 [18], resulting in activation of downstream effectors, promoting motility and invasion. Here we demonstrate that Plk4 facilitates peritoneal metastasis in GCa by enhancing cell migration, invasion and adhesion to the peritoneum, through the Rac1 activating GEF PREX2.

Methods and results: **Increased Plk4 activity in GCa promotes cancer cell migration, invasion, clearance of the mesothelium and peritoneal adhesion (Fig. 1).** We assessed Plk4 kinase activity in human gastric cancer by measuring mRNA expression of Plk4 relative to its endogenous inhibitor FAM46C [14, 19] in 94 patients who underwent curative resection and consented to tumour banking at Mount Sinai Hospital, Toronto. Plk4 activity was five-fold higher in tumour compared to adjacent normal mucosa derived from the same patient (Fig. 1A). To explore the potential role of Plk4 as a driver of aggressive behaviour in gastric cancer cells, we tested the effect of Plk4 depletion on motility and invasion in gastric cancer cell lines AGS and Hs746T. To deplete Plk4, lentiviral shRNA transduction was chosen as a system to achieve stable Plk4 knockdown. Using Plk4 shRNA constructs and lentiviral infection followed by puromycin selection, stable cell lines were generated with Plk4 knockdown to 30-50% of control, as confirmed by real time RT-PCR (Fig. 1B). Real-time scratch wound healing migration assays were

performed on confluent cells, with images obtained q1h. Depletion of Plk4 markedly suppressed scratch wound healing by AGS gastric cells at 16h and 24h (Fig. 1B). Plk4 knockdown also impaired 3D invasion by Hs746T cells through a Matrigel-Collagen I matrix over the course of 4 days (Fig. 1C). A mesothelial cell clearance assay was developed to model the interaction between GCa cells and the mesothelial cell layer of the peritoneum. Gastric cancer cells engineered to express mCherry (red) were cultured as spheroids which were then seeded onto a layer of mesothelial cells engineered to express GFP (green). Mesothelial clearance was measured by median FITC intensity, where a lower FITC intensity reflected more clearance of GFP-mesothelial cells. Depletion of Plk4 to approximately 20-30% of control markedly suppressed mesothelial clearance by Hs746T cells (Fig. 1D). A human peritoneal explant model was developed to recapitulate the microenvironment of GCa peritoneal metastasis. After obtaining REB approval and patient consent, fresh peritoneal tissue samples were taken from patients undergoing abdominal surgery. The specimens were suspended with the mesothelial side down above a monolayer of red fluorescent stained AGS cells, without direct contact. Over the ensuing 3 days, en face images of the peritoneal surface were captured by confocal microscopy and tissue cross-sections taken for H&E staining q24h. Adhesion of AGS cells to the mesothelial surface of the ex vivo peritoneum was assessed by scoring the number of red fluorescent cells on the background of green matrix autofluorescence (Fig. 1E). Knockdown of Plk4 markedly suppressed adhesion of AGS cells over the course of 3 days (Fig. 1E), during which time the peritoneum remained viable, with similar findings on analysis of H&E sections (not shown). The velocity of movement of AGS cells within the peritoneal tissue was decreased by Plk4 knockdown (not shown).

Plk4 interacts physically and functionally with the Rac1 guanine nucleotide exchange factor (GEF) PREX2 (Fig. 2). The small RhoGTPase Rac1, which mediates directional migration in many cell types, binds to PAK-PBD in its activated form. Knockdown of Plk4 in HeLa cells resulted in a reduction in active Rac1 relative to total Rac1 (Fig. 2A), in keeping with signaling for increased motility through regulation of Rac1 activity. In an unbiased screen searching for known Rac1 GEFs and GAPs that possess a Plk4 consensus phosphorylation motif, we identified 8 GEFs. Amongst these, PREX2 (phosphatidylinositol 3,4,5-trisphosphate (PIP3)-dependent Rac exchanger 2) possessed 2 Plk4 phosphorylation motifs (residues 406-472, located between two DEP domains; and residues 1346-1352, within the IP4P domain (Fig. 2B). While the N-terminal DH-PH module of PREX2 is most responsible for Rac1 binding and GEF activity [20], the DEP (Dishevelled, Egl-10, and Pleckstrin) domains, with known sites of phosphorylation, also interact with the components of the mTOR pathway and thereby regulate cell migration [21]. The C-terminal inositol polyphosphate 4-phosphatase (IP4P) domain, with many known phosphorylation sites, has been shown to bind PTEN with high affinity and is required for PTEN inhibition of PREX2 [22]. Further evidence that PREX2 was a good candidate as a mediator of Plk4 Rac1 activation came from a screen of Rac1 GEFs for localization to the cell edge, similar to that of Plk4. HeLa cells were transiently transfected with a GFP (or V5 for PREX2)-tagged GEF together with FLAG-Plk4 and their localization was determined by immunofluorescence. Of the GEFs examined, only PREX2 localized to cell edges/protrusions together with Plk4 (Fig. 2B). PREX2 was tested for physical interaction with Plk4 by co-immunoprecipitation (co-IP). HEK293T cells were transiently transfected with full length FLAG-Plk4 and full length GFP-PREX2. PREX2 reciprocally co-immunoprecipitated with Plk4 (Fig. 2C). To determine whether PREX2 was indeed a *bona fide* substrate for Plk4, an *in vitro* kinase assay was performed. This showed dose-dependent phosphorylation of wild-type (WT) PREX2 in the presence of wild-type Plk4; kinase dead K41M Plk4 served as a control (Fig. 2D). Plk4 showed strong autophosphorylation, as expected [23]. We hypothesize that Plk4 activates Rac1 through phosphorylation of PREX2 (Fig. 2E). To assess the functional effect of PREX2 on GCa cell migration, we performed real-time scratch wound healing assays. Lentiviral-mediated knockdown of PREX2 in AGS cells to approximately 35%-40% of control was achieved (Fig. 2F). As with Plk4 depletion, knockdown of

PREX2 suppressed scratch wound healing at 16h and 24h (Fig. 2F), demonstrating its potential for mediation of Plk4-driven AGS cell migration.

Plk4 drives aggressive behaviour in GCa via phosphorylation of PREX2 (Fig. 3). To determine whether Plk4 acts through PREX2 to promote cell migration, the role of PREX2 in wound healing by U2OS cells stably overexpressing YFP-Plk4 was examined. As expected, tetracycline induction of Plk4 expression (tet +) resulted in enhanced migration (Fig. 3A). PREX2 depletion by means of siRNA (pool of 4) suppressed migration compared with siLuciferase control (tet -). Importantly, forced expression of Plk4 (tet +) failed to stimulate wound healing in PREX2-depleted cells. (Fig. 3A). PREX2 mutants lacking Plk4 consensus phosphorylation motifs were generated by site directed mutagenesis and confirmed with Sanger sequencing. Three PREX2 mutants were generated: T468A alone, S1349A alone, and a double mutant T468A/S1349A (Fig. 3B). An *in vitro* kinase assay showed that in addition to phosphorylating wild-type (WT) PREX2, wild-type (WT) FLAG-Plk4 phosphorylates both single mutants (i.e. PREX2-T468A and PREX2-S1349A), but not the double mutant (Fig. 3B), demonstrating that Plk4 is capable of phosphorylating PREX2 at each of the two sites. To determine which site was required for stimulation of GCa cell migration, the ability of the PREX2 mutants to rescue impaired scratch wound assay healing in Plk4 depleted AGS cells was tested. While PREX2 WT and PREX2-S1349A rescued, PREX2-T468A and PREX2-T468A/S1349A did not (Fig. 3C), demonstrating that the functional phosphorylation site was at T468. Similar dependency on T468 phosphorylation was revealed in adhesion assays using human peritoneal tissue (Fig. 3D). Of note, analysis of patient data derived from the TCGA annotated GCa database showed that a high expression of PREX2 in tumour tissue is associated with a worse overall survival following resection of GCa (Fig. 3F).

Discussion: Peritoneal dissemination of gastric cancer is a complex and dynamic process comprising multiple steps: 1) detachment of cancer cells from the primary tumour at the serosal surface, 2) migration across the peritoneal cavity, 3) attachment of free tumour cells to the peritoneal mesothelial cells, 4) invasion into the submesothelial space and 5) invasion into subperitoneal tissues [24, 25]. This differs significantly from other forms of metastasis (lymphatic, hematogenous), where cancer cells first migrate through interstitial matrix, then between endothelial cells, and into the turbulent flow within a vessel, finishing with active extravasation, growth and angiogenesis [26, 27]. Here we have used a unique human peritoneal explant model to recapitulate the specific complexities of peritoneal metastasis.

In these experiments, we have shown that Plk4 promotes GCa cell migration, invasion and mesothelial clearance *in vitro*, and adhesion to peritoneal tissue *ex vivo*. We further show that these aggressive cell behaviours are dependent on phosphorylation by Plk4 of the Rac1 GEF PREX2. While Plk4 can phosphorylate PREX2 within both the DEP (468aa) and IP4P (1349aa) domains, only the former appears functional in mediating Plk4's promotion of GCa cell migration and invasion. Since the DEP domain interacts with components of the mTOR pathway, this finding suggests a potential feedback look that serves to further enhance Rac1 activation[21].

The usefulness of Plk4 inhibition as a therapeutic strategy in advanced cancer is currently under investigation. The highly selective Plk4 inhibitor centrinone is not available in an orally active form [28]. The only orally available potent Plk4 inhibitor to be tested *in vivo*, CFI-400945, suppressed the growth of murine xenografts [29], but long-term Plk4 inhibition may impair immune function and lead to second malignancies through haploinsufficient dysregulation of cytokinesis [12]. Here, we have identified a distinct Plk4-driven PREX2-mediated pathway that facilitates peritoneal spread of GCa, and may be generalizable to other epithelial malignancies that are prone to peritoneal metastasis, such as ovarian, appendiceal, and gallbladder cancers [30-32]. Therapies that target the Plk4-PREX2 interaction could be useful in preventing and/or treating peritoneal dissemination that shortens quantity and degrades quality of life in patients suffering with these cancers.

References

1. Machlowska, J., et al., *Gastric Cancer: Epidemiology, Risk Factors, Classification, Genomic Characteristics and Treatment Strategies.* Int J Mol Sci, 2020. **21**(11).
2. Rawla, P. and A. Barsouk, *Epidemiology of gastric cancer: global trends, risk factors and prevention.* Prz Gastroenterol, 2019. **14**(1): p. 26-38.
3. Yang, D., et al., *Survival of metastatic gastric cancer: Significance of age, sex and race/ethnicity.* J Gastrointest Oncol, 2011. **2**(2): p. 77-84.
4. Koemans, W.J., et al., *Synchronous peritoneal metastases of gastric cancer origin: incidence, treatment and survival of a nationwide Dutch cohort.* Gastric Cancer, 2021. **25**(10): p. 021-01160.
5. Nakagawa, M., et al., *Patterns, timing and risk factors of recurrence of gastric cancer after laparoscopic gastrectomy: reliable results following long-term follow-up.* Eur J Surg Oncol, 2014. **40**(10): p. 1376-82.
6. Spolverato, G., et al., *Rates and patterns of recurrence after curative intent resection for gastric cancer: a United States multi-institutional analysis.* J Am Coll Surg, 2014. **219**(4): p. 664-75.
7. Kitayama, J., et al., *Treatment of patients with peritoneal metastases from gastric cancer.* Ann Gastroenterol Surg, 2018. **2**(2): p. 116-123.
8. Yarema, R., et al., *Gastric cancer with peritoneal metastases: Efficiency of standard treatment methods.* World J Gastrointest Oncol, 2020. **12**(5): p. 569-581.
9. Wang, Z., et al., *Issues on peritoneal metastasis of gastric cancer: an update.* World J Surg Oncol, 2019. **17**(1): p. 019-1761.
10. Kim, D.W., et al., *Multicenter Retrospective Analysis of Intraperitoneal Paclitaxel and Systemic Chemotherapy for Advanced Gastric Cancer with Peritoneal Metastasis.* J Gastric Cancer, 2020. **20**(1): p. 50-59.
11. Rosario, C.O., et al., *Plk4 is required for cytokinesis and maintenance of chromosomal stability.* Proc Natl Acad Sci U S A, 2010. **107**(15): p. 6888-93.
12. Ko, M.A., et al., *Plk4 haploinsufficiency causes mitotic infidelity and carcinogenesis.* Nat Genet, 2005. **37**(8): p. 883-8.
13. Macmillan, J.C., et al., *Comparative expression of the mitotic regulators SAK and PLK in colorectal cancer.* Ann Surg Oncol, 2001. **8**(9): p. 729-40.
14. Kazazian, K., et al., *FAM46C/TENT5C functions as a tumor suppressor through inhibition of Plk4 activity.* Commun Biol, 2020. **3**(1): p. 020-01161.
15. Kazazian, K., et al., *Plk4 Promotes Cancer Invasion and Metastasis through Arp2/3 Complex Regulation of the Actin Cytoskeleton.* Cancer Res, 2017. **77**(2): p. 434-447.
16. Rosario, C.O., et al., *A novel role for Plk4 in regulating cell spreading and motility.* Oncogene, 2015. **34**(26): p. 3441-51.
17. Cook, D.R., K.L. Rossman, and C.J. Der, *Rho guanine nucleotide exchange factors: regulators of Rho GTPase activity in development and disease.* Oncogene, 2014. **33**(31): p. 4021-35.
18. Li, Z., et al., *Role of guanine nucleotide exchange factor P-Rex-2b in sphingosine 1-phosphate-induced Rac1 activation and cell migration in endothelial cells.* Prostaglandins Other Lipid Mediat, 2005. **76**(1-4): p. 95-104.
19. Luu S, K.K., Conner J, Swett-Cosentino J, Pacholczyk K, Brar S, Govindarajan A, Swallow C, *Expression of the Plk4 inhibitor FAM46C predicts better survival following resection of gastric adenocarcinoma. .* Can J Surg (4 Suppl 2), August 2019 — Abstracts, 2019.

20. Lissanu Deribe, Y., et al., *Truncating PREX2 mutations activate its GEF activity and alter gene expression regulation in NRAS-mutant melanoma.* Proc Natl Acad Sci U S A, 2016. **113**(9): p. 16.
21. Pandiella, A. and J.C. Montero, *Molecular pathways: P-Rex in cancer.* Clin Cancer Res, 2013. **19**(17): p. 4564-9.
22. Mense, S.M., et al., *PTEN inhibits PREX2-catalyzed activation of RAC1 to restrain tumor cell invasion.* Sci Signal, 2015. **8**(370): p. 2005840.
23. Sillibourne, J.E., et al., *Autophosphorylation of polo-like kinase 4 and its role in centriole duplication.* Mol Biol Cell, 2010. **21**(4): p. 547-61.
24. Kanda, M. and Y. Kodera, *Molecular mechanisms of peritoneal dissemination in gastric cancer.* World J Gastroenterol, 2016. **22**(30): p. 6829-40.
25. Karunasena, E., et al., *Genomics of Peritoneal Malignancies.* Surg Oncol Clin N Am, 2018. **27**(3): p. 463-475.
26. Mikuła-Pietrasik, J., et al., *The peritoneal "soil" for a cancerous "seed": a comprehensive review of the pathogenesis of intraperitoneal cancer metastases.* Cell Mol Life Sci, 2018. **75**(3): p. 509-525.
27. Gao, Y., et al., *Metastasis Organotropism: Redefining the Congenial Soil.* Dev Cell, 2019. **49**(3): p. 375-391.
28. Wong, Y.L., et al., *Cell biology. Reversible centriole depletion with an inhibitor of Polo-like kinase 4.* Science, 2015. **348**(6239): p. 1155-60.
29. Mason, J.M., et al., *Functional characterization of CFI-400945, a Polo-like kinase 4 inhibitor, as a potential anticancer agent.* Cancer Cell, 2014. **26**(2): p. 163-76.
30. Jacobson, R., et al., *Peritoneal Metastases in Colorectal Cancer.* Ann Surg Oncol, 2018. **25**(8): p. 2145-2151.
31. Maplanka, C., *Gallbladder cancer, treatment failure and relapses: the peritoneum in gallbladder cancer.* J Gastrointest Cancer, 2014. **45**(3): p. 245-55.
32. Kuijpers, A.M., et al., *Treatment of ovarian metastases of colorectal and appendiceal carcinoma in the era of cytoreductive surgery and hyperthermic intraperitoneal chemotherapy.* Eur J Surg Oncol, 2014. **40**(8): p. 937-42.

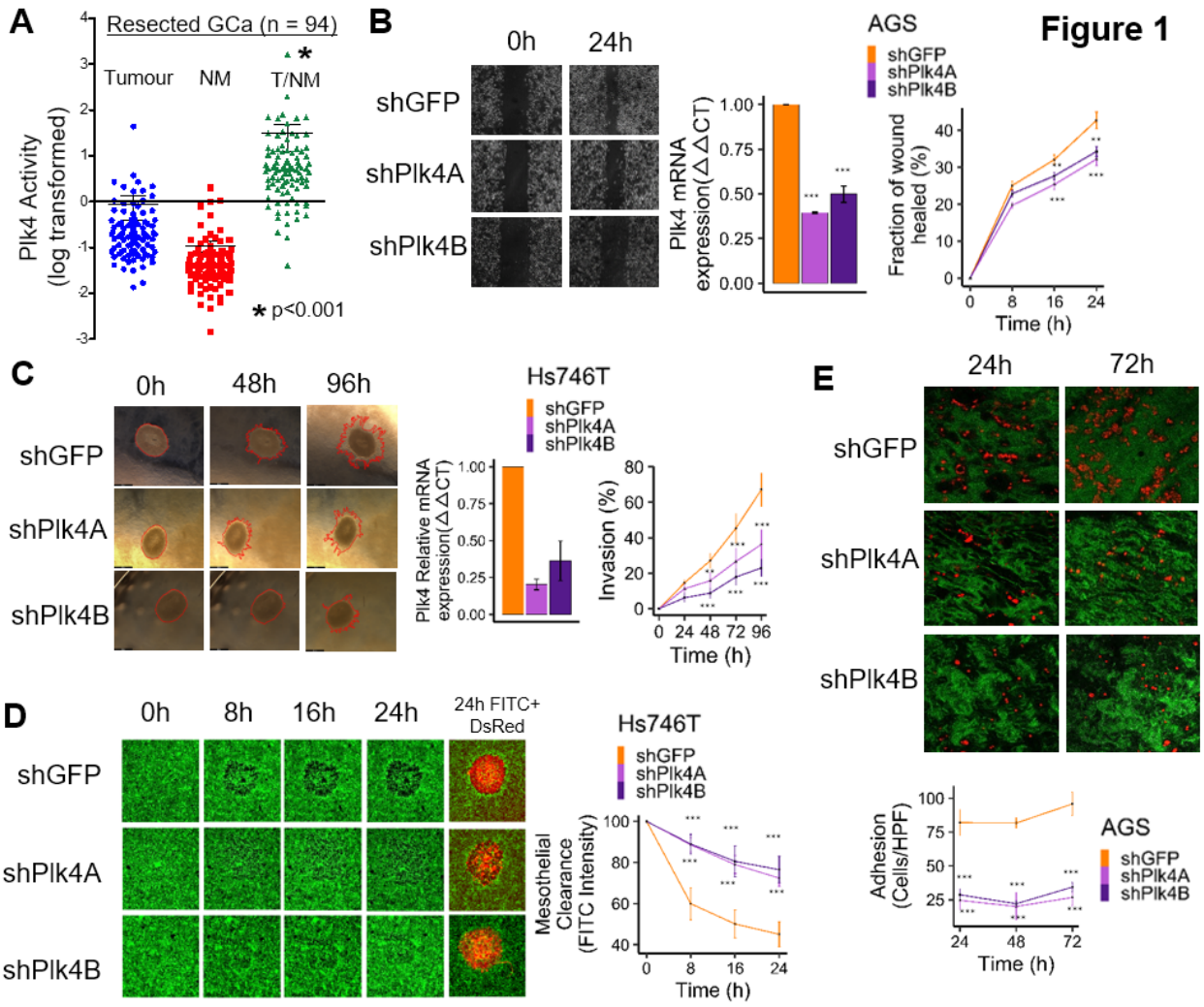

Figure 1. Increased Plk4 activity in gastric cancer (GCa) promotes cancer cell migration, invasion, clearance of mesothelial cells and peritoneal adhesion. A Plk4 activity is increased five-fold in tumour (T) vs. paired normal mucosa (NM) in resected GCa. mRNA expression of Plk4/endogenous inhibitor FAM46C, normalized to GAPDH, in 94 consecutive resected GCa specimens, Mount Sinai, Toronto. **B** Plk4 enhances directional migration by AGS GCa cells. ***Left*** Time-lapse phase-contrast images from scratch-wound assays performed on shPlk4A and shPlk4B vs shGFP (control) cell lines. ***Right*** Quantification demonstrates impaired directional migration upon Plk4 knockdown. **C** Plk4 enhances invasion by Hs746T GCa cells. ***Left*** Time-lapse images from 3D invasion in a Collagen I/Matrigel matrix performed on shPlk4A and shPlk4B vs shGFP (control) cell lines. ***Right*** Quantification demonstrates impaired invasion upon Plk4 knockdown. **D** Plk4 enhances clearance of mesothelial cells by Hs746T GCa cells. ***Left*** Time-lapse images of shPlk4A and shPlk4B vs shGFP (control) cell line spheroids seeded onto a mesothelial cell layer. ***Right*** Quantification demonstrates impaired mesothelial clearance with Plk4 knockdown. **E** Plk4 enhances adhesion to *ex-vivo* human peritoneal tissue by AGS GCa cells. ***Top*** Time-lapse images of human peritoneum exposed to shPlk4A and shPlk4B vs shGFP cells, without direct contact. ***Bottom*** Quantification demonstrates reduced adhesion with Plk4 knockdown. All data are mean ± SEM, n=3 independent experiments.*p<0.05, **p<0.005, ***p<0.001vs control

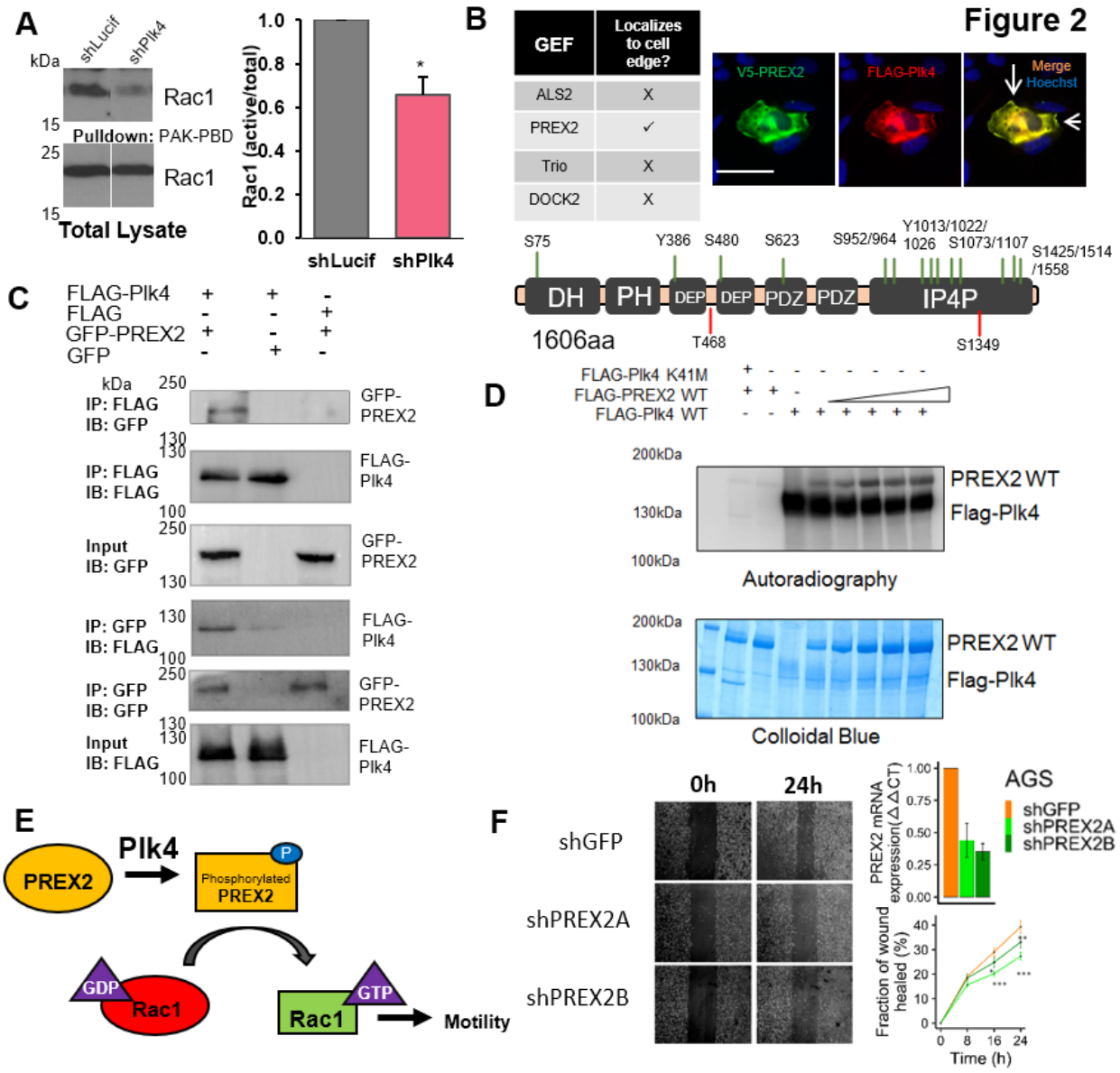

Figure 2. Plk4 interacts physically and functionally with the Rac 1 GEF PREX2. **A** Plk4 knockdown reduces level of active Rac1. Representative blot (***left)*** and quantification (***right***) showing less active Rac1 (pulled down by PAK-PBD) vs. total Rac1 in shPlk4 vs. shLucif (control) HeLa cells. **B** Rac1 GEF PREX2 has 2 putative Plk4 phosphorylation sites and localizes with Plk4. ***Top left*** Rac1 GEFs with Plk4 phosphorylation consensus motifs screened for localization with Plk4.***Top right*** IF imaging shows PREX2 and Plk4 localizing to cell edge. ***Bottom*** Known phosphosphorylation sites (green) and putative Plk4 phosphorylation sites (red) within PREX2 domain structure. **C** PREX2 physically interacts with Plk4. Immunoblots from reciprocal co-IP showing GFP-PREX2 and FLAG-Plk4 interaction. **D** Wild-type (WT) but not kinase-dead (K41M) FLAG-Plk4 phosphorylates PREX2 in an *in vitro* kinase assay. **E** Cartoon depicting putative activation of Rac1 by Plk4 through phosphorylation of PREX2. **F** PREX2 enhances directional migration by AGS GCa cells. ***Left*** Time-lapse phase contrast images from scratch-wound assays. ***Right*** Quantification shows impaired directional migration with PREX2 knockdown. Data are means ±SEM, n=3 experiments, *p<0.05, **p<0.005, ***p<0.001

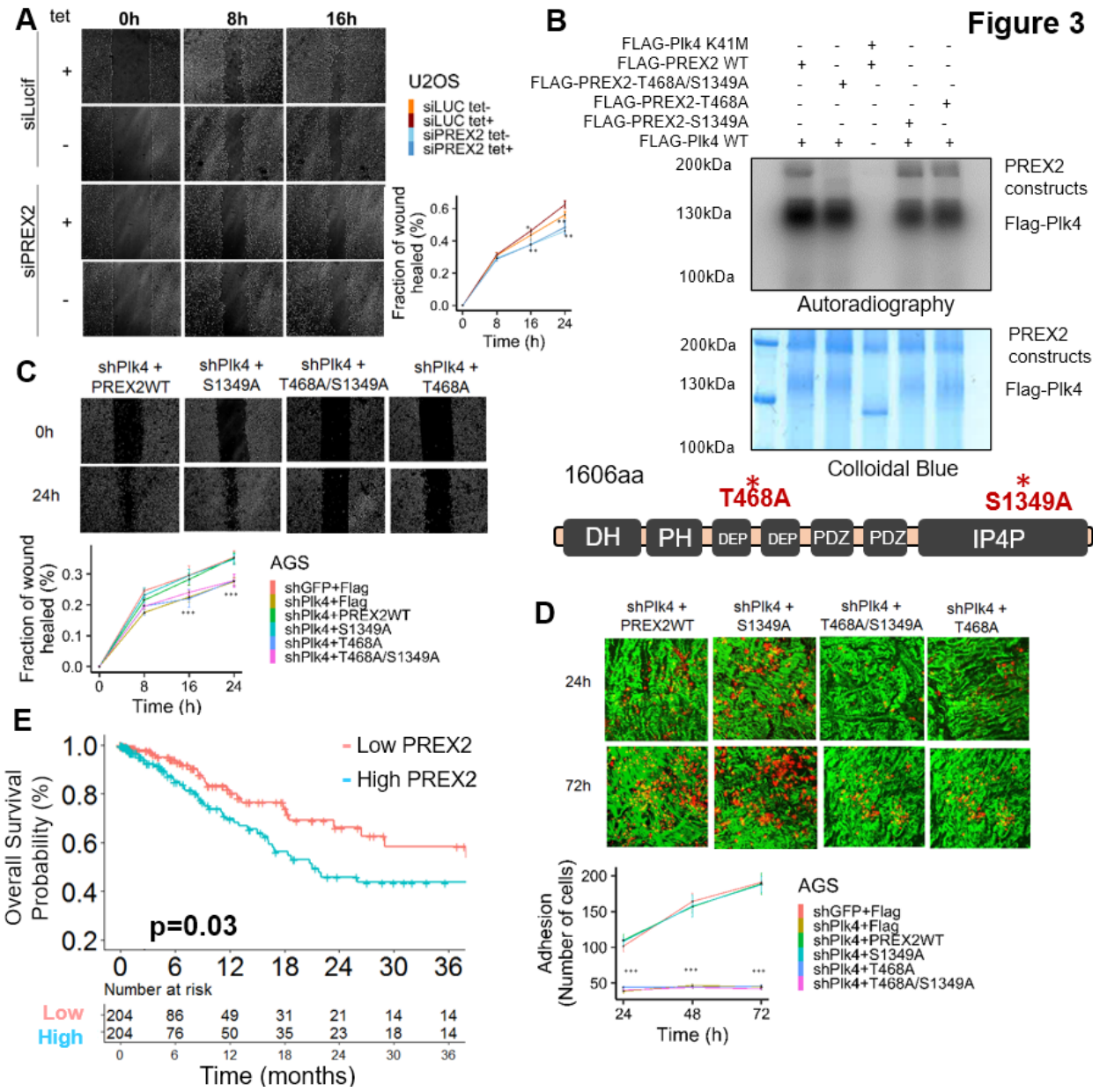

Figure 3. Plk4 drives aggressive behaviour in GCa via phosphorylation of PREX2. A PREX2 mediates upregulation of cell motility by Plk4. In a 2D migration assay, depletion of PREX2 prevents the enhanced wound healing induced by forced expression of Plk4 (tet +, 0.01ug/ml). siPREX2=pool of 4. **B** Mutations generated at two Plk4 consensus phosphorylation sites in PREX2 (***bottom***). Wild-type (WT) FLAG-Plk4 phosphorylates PREX2 WT, PREX2-T468A and PREX2-S1349A, but not double mutant T468A/S1349A in an *in vitro* kinase assay (***top***) showing that Plk4 can phosphorylate PREX2 at both sites. **C,D** Impaired wound healing (**C**) and adhesion to explanted peritoneum (**D**) induced by Plk4 knockdown in AGS GCa cells is rescued by PREX2 -WT and -S1349A, but not by PREX2-T468A or -T468A/S1349A, demonstrating that the functional phosphorylation site is at T468. **E** Kaplan-Meier survival curves showing that high PREX2 expression is associated with a worse prognosis in patients with GCa (TCGA database). Data are means ±SEM, n=3 experiments, *p<0.05, **p<0.005, ***p<0.001

Ex Vivo Treatment of Cytomegalovirus in Human Donor Lungs Using A Novel Chemokine-Based Immunotoxin

Rafaela VP Ribeiro[1], Terrance Ku[2], Aizhou Wang[1], Layla Pires[1], Victor H Ferreira[2], Vinicius Michaelsen[1], Aadil Ali[1], Marcos Galasso[1], Sajad Moshkelgosha[1], Anajara Gazzalle[1], Mingyao Liu[1], Lianne G. Singer[2], Deepali Kumar[2], Shaf Keshavjee[1], John Sinclair[3], Thomas Kledal[4], Atul Humar[2], Marcelo Cypel[1,2]

[1]Latner Thoracic Surgery Laboratories, Toronto General Research Institute, University Health Network, Toronto, Ontario, Canada

[2]Ajmera Transplant Centre, University Health Network, Toronto, Ontario, Canada.

[3]Department of Medicine, Addenbrooke's Hospital, University of Cambridge.

[4]Synklino ApS, Ole Måløes vej X, 2200 Copenhagen N. Denmark.

INTRODUCTION

Human cytomegalovirus (CMV) is an ubiquitous virus with a mean seroprevalence amongst world's population of 83% and, specifically for blood and organ donors, its prevalence is as high as 86% (1). CMV is the most common and single most important viral infection in solid organ transplant recipients. It has devastating impacts on patient outcomes after transplantation (2), including tissue invasive viral disease (3), and acute and chronic graft dysfunction (4). The risk of the development of CMV disease and CMV-related mortality after lung transplantation is highly dependent on the CMV status of both the donor and recipient. Seronegative recipients who receive lungs from seropositive donors (D+/R- status) are at highest risk for CMV complications (5). Despite this, current clinical practice does not attempt to avoid this donor to recipient CMV mismatch since greater than 50% of donors are CMV+, and there is a severe shortage of donor organs.

The main obstacle to CMV treatment is that the virus is primarily in a latent state at the time of organ transplantation. The available antivirals are not effective in reducing the burden of virus within the graft since these drugs only target the virus in its lytic phase. Some cell types support latent infection, including CD34+ myeloid progenitor cells and CD14+ monocytes, and these cells express a number of latency-associated viral proteins, some of which are located on cell membranes (6). Specifically, CMV latently infected cells express the viral protein US28, a G-coupled transmembrane receptor expressed on the surface of latently and lytically infected cells, which functions as a chemokine receptor (7) and can activate or repress pathways linked to proliferation depending on cell type (6,8). A novel chemokine-based immunotoxin called F49A-FTP (9), developed using the technology of fusion toxin proteins (FTP), targets and kills latently infected cells with CMV. F49A-FTP is based on a CX3CL1 chemokine variant, F49A that is engineered to be selective towards US28 over the endogenous CX3CR1 receptor, conjugated to the *Pseudomonas aeruginosa* exotoxin A. It was engineered to have ultra-high affinity and specificity for US28, which has a high binding affinity for CX3CL1. Once F49A-FTP binds to US28, it is internalized with the receptor, the pseudomonas exotoxin is cleaved off from the chemokine moiety and subsequently induces apoptosis (10). In previous studies, F49A-FTP has been shown to 1) kill latently infected monocytes and CD34+ progenitor cells, 2) reduce CMV viral burden in naturally, latently infected CD14+ monocytes, 3) reduce the frequency of virus reactivation *in vitro*, and 4) reduce viral replication in humanized mice infected with human CMV (9,10).

Normothermic ex-vivo lung perfusion (EVLP) is a well-established method of donor lung preservation and treatment, which allows donor lungs to be assessed and treated under protective physiological conditions (11,12). Previous studies have shown that EVLP can be used as a platform to decrease donor lung inflammation and treat donor bacterial pneumonia (13–15). More recently, we have demonstrated the use of this platform to treat hepatitis C virus and Epstein-Barr virus (16–18). We thus hypothesized that F49A-FTP could form the basis of a novel approach to greatly reduce the clinical threat of CMV-positive lung allografts in the transplant setting, by providing therapy with the novel fusion toxin protein during EVLP to mitigate or eliminate CMV reactivation after transplantation.

RESULTS

Reactivation of latent cytomegalovirus from primary human lung tissue: In order to demonstrate that F49A-FTP treatment of the donor lung during EVLP could eliminate latent CMV and prevent viral reactivation, it was critical to first investigate whether CMV could be reactivated from seropositive human lung tissue biopsies. To do this, biopsies from human donor lungs rejected for transplantation from three CMV seropositive donors (CMV+) underwent cell sorting to specifically select monocytes, which are known cellular reservoirs of latent CMV. These cells were cultured with an immunosuppressive media to stimulate differentiation and maturation to mature dendritic cells (mDCs), which is essential for reactivation of latent viral genomes (19).

After magnetic cell isolation, we were able to achieve a cell population that consisted of 97.9% ± 0.5% (mean±SD) (**Fig 1a**) CD14+ cells, demonstrating effective isolation of cells of interest to proceed with the reactivation protocol. **Fig 1b** shows that sorted cells, incubated with differentiation media, clearly differentiated into mDCS, which did not occur for control cells, incubated with control media. Finally, we co-cultured these CD14+ monocyte-derived mDCs with human foreskin fibroblasts (HFFs), a cell type fully permissive for CMV productive infection, and quantified infectious foci in the fibroblasts by immunofluorescent staining for CMV IE-1/2 as a measure of reactivation of infectious virus (**Fig 1c**). The average number of reactivation events measured with CMV IE-1/2 staining was 30% ± 15% (mean±SD) of the total number of cells in each assay. We concluded that this newly developed cell culture model using CD14+ cells isolated from CMV+ donor lungs was able to consistently quantify CMV reactivation events which was a critical step to evaluate the effect of our treatment during EVLP.

F49A-FTP delivery through EVLP significantly reduces CMV reactivation: To evaluate the therapeutic effect of F49A-FTP delivered ex-vivo to human donor lungs, we studied 12 CMV+ donor lungs rejected for transplantation. Donors were tested using ELISA for CMV IgG titer and only included in the study if seropositive, confirming latent CMV infection. Donor lungs were retrieved as normal clinical practice, assessed and randomly allocated to either 6h of EVLP alone (control group, n=6) or EVLP with 1 mg/L F49A-FTP delivered through the pulmonary artery after reaching first hour of perfusion (F49A-FTP group, n=6). Tissue biopsies were sampled from similar locations at baseline (pre-EVLP) and at the end of perfusion (post-EVLP) for subsequent CMV reactivation studies, as described above, to assess efficacy of the compound. Treatment with F49A-FTP markedly reduced viral reactivation (**Fig 2a-b**). Untreated control EVLP lungs demonstrated a median increase from baseline of 32% [-16% to +112.5%] in viral reactivation, whereas F49A-FTP EVLP treated lungs demonstrated a significant median reduction of 76% [-15% to -99.9%], p = 0.0087. One donor lung from the control group did not have evidence of viral reactivation from either pre- and post-EVLP tissue samples, leading us to conclude this donor may have been CMV seronegative (e.g. false positive serology due to blood products) and, therefore, was excluded from the analysis.

The majority of the treated donor lungs demonstrated more than 75% reduction in viral reactivation and two donors demonstrated more than 95% reduction; however, we did notice slight variability in efficacy. We quantified the concentration of F49A-FTP in perfusate samples and correlated with efficacy of F49A-FTP for each donor lung to elucidate if this variability was due to different drug uptake for each lung. To determine F49A-FTP levels in perfusate we used a bioassay that detects CX3CL1, since the immunotoxin is based on the soluble extracellular domain of this US28 binding ligand. As this assay can detect endogenous production of CX3CL1, we normalized the data relative to the first hour (before adding F49A-FTP). The average concentration of CX3CL1 was 119,978 ± 80,061 (mean±SD) pg/mL in the treated lungs vs. 8,140.4 ± 12,181.5 (mean±SD) pg/mL for controls, p=0.004 (**Fig 2c**) indicating tissue uptake of the drug. Interestingly, we observed a correlation between the uptake of CX3CL1 and efficacy of our immunotoxin: the lungs that presented higher levels of reduction in viral reactivation were the ones with lower levels of F49A-FTP in perfusate, indicating improved drug uptake (r^2=0.75, p=0.02) (**Fig 2d**).

Several factors could be involved in this difference in drug uptake, including pH and drug distribution through dependent and non-dependent regions of the lungs due to uneven perfusion during EVLP. Different pH levels can impact drug endocytosis and we indeed found a correlation between low pH and efficacy of the immunotoxin (r^2=0.85, $p<0.01$). To evaluate the role of disparities in regional drug delivery, we performed one proof-of-concept CMV+ EVLP with F49A-FTP treatment and collected biopsies from the different regions of the lung after 4h of perfusion. When compared to controls set as 100% of reactivation, viral reactivation was indeed different for each region of the lung: the upper non-dependent regions of the lung presented 31.2% ± 14.2% (mean±SD), while the lower dependent regions presented only 14.5% ± 5.2 (mean±SD).

F49A-FTP delivery through EVLP does not result in off-target effects: US28 has 38% homology to the human chemokine receptor CX3CR1 (20), which is expressed on cells from the myeloid lineage, and could, therefore, be targeted non-specifically by F49A-FTP. This could lead to possible adverse effects on the lung graft due to the potentially high number of cells that could undergo F94A-FTP-associated programmed cell death (apoptosis). To evaluate off-target effects, the degree of cell death/apoptosis in CD34+ cells and CD14+ monocytes were assessed through flow cytometry from lung tissue biopsies from pre- and post-EVLP. To account for the inter-donor heterogeneity in our samples, we used post-to-pre EVLP cell ratios to analyze the proportional change of each measurement from baseline.

Number of live and apoptotic CD14+ monocytes and CD34+ cells showed no significant differences (**Fig 3a-b**). Since only the minority of CD14+ and CD34+ cells in the lungs are expected to be latently infected with CMV, this result suggests that no major non-specific binding occurs, which is consistent with previous findings of a 200-fold higher affinity of F49A-FTP towards US28 relative to CX3CR1 (10).

F49A-FTP delivery through EVLP does not induce acute lung injury: We also evaluated if F49A-FTP treatment had any adverse impact on lung functional parameters. In order to assess this, lung function was assessed hourly during EVLP as per clinical protocol (11). Functional parameters such as graft oxygenation, static and dynamic compliance, peak and plateau airway pressure as well as pulmonary artery pressure were evaluated. We did not observe any difference in lung physiological parameters between control and F49A-FTP treated lungs during 6h of perfusion, suggesting that F49A-FTP does not induce acute deleterious effects on human lungs during EVLP (**Fig 3 c-h**).

To further investigate safety of the novel therapy in human lungs, a broad panel of inflammatory cytokines associated with lung injury (21) including TNF-alpha, IFN-gamma, IL-6, IL-8, IL1-β, IL-2, M-CSF and GM-CSF were assessed in perfusate at 1h, 3h and 6h and in lung tissue before and after EVLP with or without F49A-FTP. No significant differences were observed in any of the cytokines assessed within the panel.

CONCLUSIONS AND FUTURE DIRECTIONS

This study demonstrates that the delivery of F49A-FTP can target and kill latent CMV infection in human donor lungs during ex-vivo lung perfusion. Most importantly, this treatment significantly reduces subsequent reactivation of the virus. Furthermore, we did not find any evidence of lung injury associated with the treatment.

We believe that before moving to a clinical study the treatment delivery needs to be further optimized, with a dose-escalation study and modifications in the EVLP parameters to enhance drug distribution within lung tissue. These studies are planned for the near future.

Latent CMV in donor organs plays a major role in disease development after lung transplantation. The proposed novel approach would potentially significantly improve the outcomes after lung transplantation by preventing one of the most serious complications after this procedure.

FIGURES

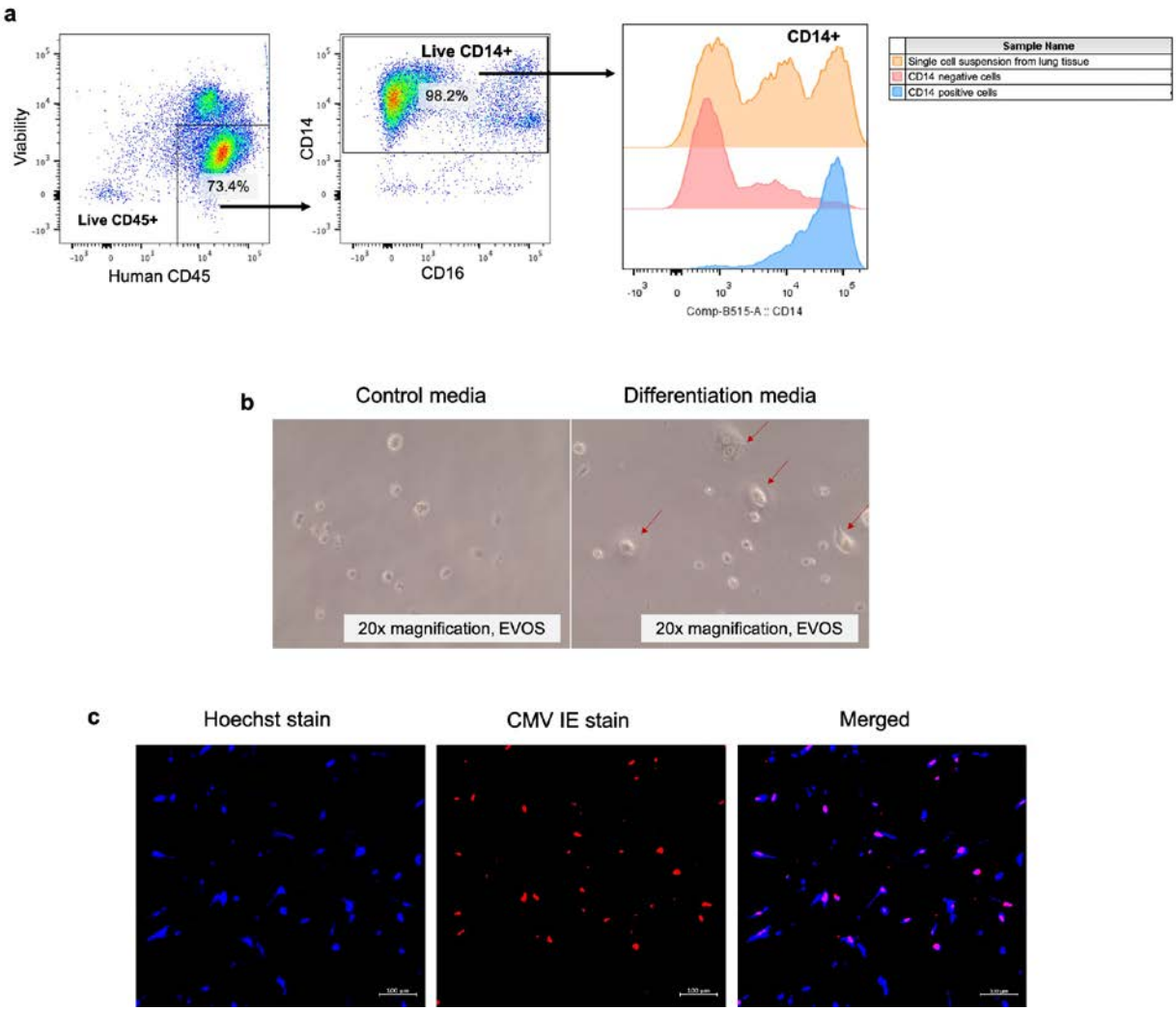

Figure 1. Reactivation of CMV in primary human lung tissue
Three CMV seropositive human lung tissue biopsies underwent cell sorting using CD14+ magnetic microbeads. **(a)** Single cell suspension from whole lung tissue before sorting and immediately after separation were stained for CD45+, CD14+, CD16+ and viability antibodies and checked with flow cytometry. The proportion of viable CD14+ cells was taken from total live CD45+ cells. In our experiments, proper sorting was achieved where 97.9% ± 0.5% of cells consisted of CD14+ cells. **(b)** Positive CD14+ cells were then cultured in differentiation media for 7 days to induce differentiation into mDCS. Whilst no differentiation was visualized when CD14+ cells were cultured for with control media (left panel), cells cultured in media with HC resulted in larger cells with elongated cytoplasmatic projections and irregular nuclei (red arrows). **(c)** After a further 21 days of co-culture with HFFs, reactivation of infectious virus was quantified with IF for CMV IE. Positive reactivation was considered when there was nuclei co-localization of both Hoechst (left panel) and CMV stains (middle panel). Data within samples was normalized by dividing total number of IE by total number of cells.

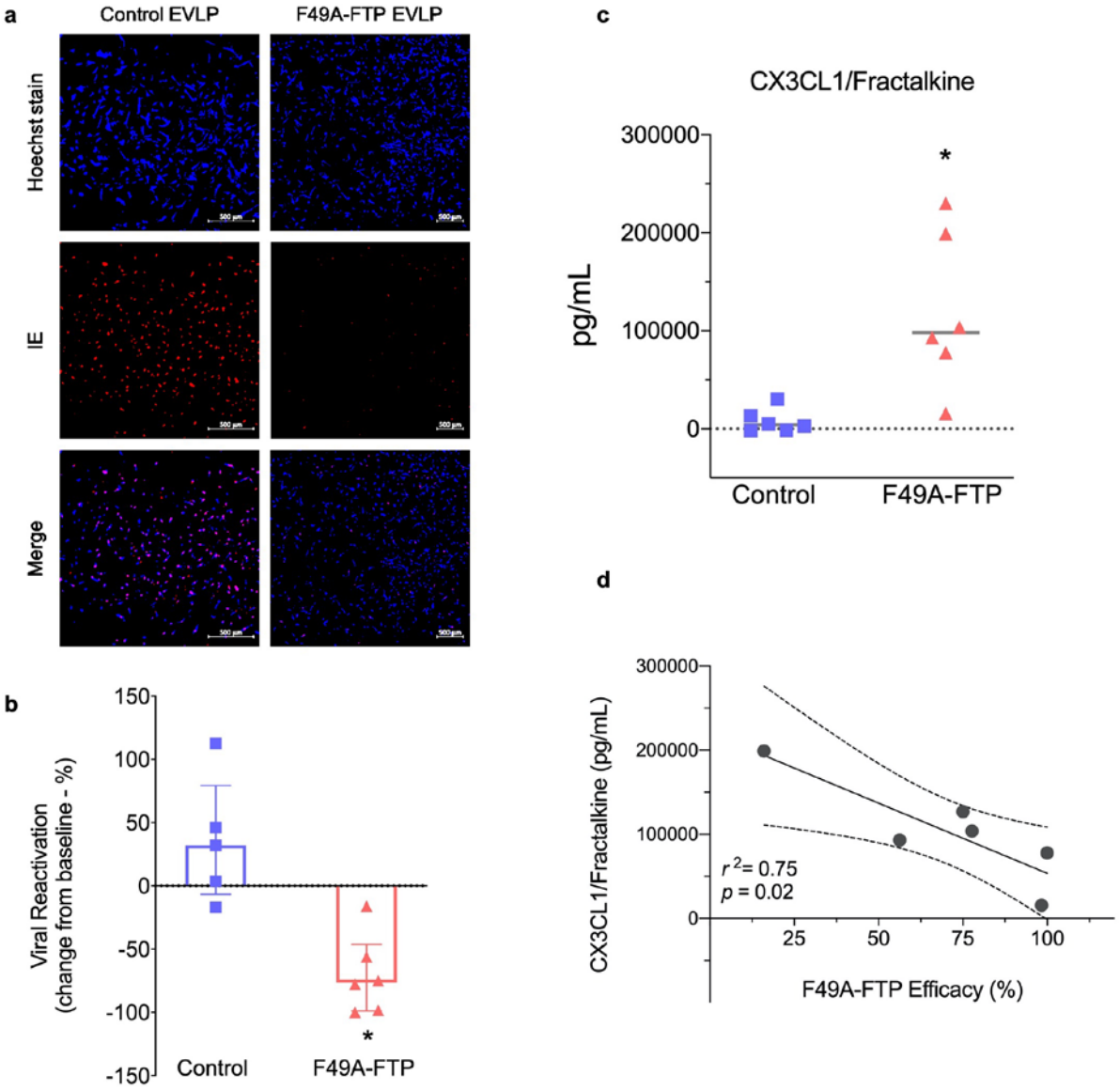

Figure 2. F49A-FTP delivered during ex-vivo lung perfusion reduces CMV reactivation events in human lungs

Fresh tissue samples from pre- and post-EVLP from both study groups underwent the CMV reactivation studies to assess F49A-FTP efficacy. **(a)** The IF analysis shows a marked reduction in viral reactivation in the F49A-FTP treated group (right panel) when compared to control lungs (left panel). **(b)** Quantitative analysis of IF demonstrates a median reduction from baseline of 76% in the treated group compared to a median increase of 32% in the control group (Mann-Whitney test; results expressed as median and IQR ranges, and each donor is represented with individual symbols). To further explore distribution of the immunotoxin in our treated lungs, concentration of F49A-FTP was measured by detecting fractalkine in the perfusate samples. **(c)** The concentration of fractalkine was much higher in the treated lungs compared to controls, indicating the presence of our immunotoxin in the perfusate solution. (Mann-Whitney test; bars represent median concentration, and each donor is represented with individual symbols). **(d)** A simple linear regression analysis shows a correlation between uptake of fractalkine and efficacy of F49A-FTP, where the lungs that showed the most reduction in viral reactivation were the ones with lower levels of F49A-FTP in perfusate. (Solid line represents the slope of and dashed lines are the 95% confidence intervals).

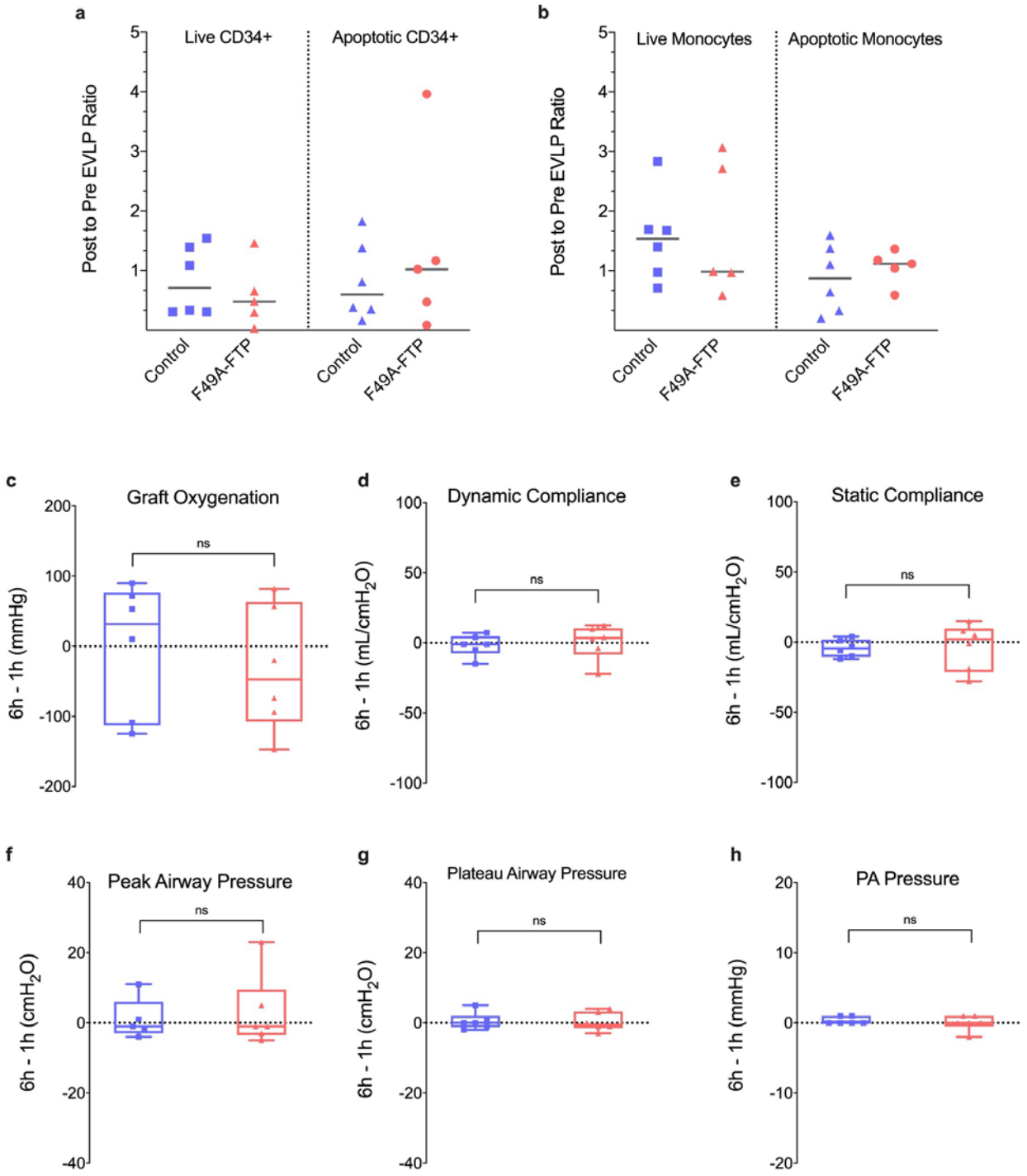

Figure 3. Safety of F49A-FTP delivery during ex-vivo lung perfusion
The possibility of an off-target effect of F49A-FTP with consequent adverse effects on the lung graft due to the potentially high number of cells that could undergo programmed apoptosis was evaluated with flow cytometry by quantification of live and apoptotic CD14+ monocytes and CD34+ cells in lung tissue samples. **(a-b)** Post-to-pre EVLP ratios were calculated to account for donor variability and normalize data within donors. No differences were noted in live or apoptotic cells between control and treated groups. (Mann-Whitney test; bars represent median ratio and each donor's ratio is represented with individual symbols). **(c-h)** Results of physiologic evaluation from the beginning to the end of EVLP (6h-1h) shows no difference between groups. (Mann-Whitney test; middle bar represents median with lower and upper limits and each donor represented with individual symbols).

REFERENCES

1. Zuhair M, Smit GSA, Wallis G, Jabbar F, Smith C, Devleesschauwer B, et al. Estimation of the worldwide seroprevalence of cytomegalovirus: A systematic review and meta-analysis. Rev Med Virol. 2019 May;29(3):e2034.

2. Valapour M, Lehr CJ, Skeans MA, Smith JM, Uccellini K, Lehman R, et al. OPTN/SRTR 2017 Annual Data Report: Lung. Am J Transplant. 2019 Feb;19:404–84.

3. Snyder LD, Finlen-Copeland CA, Turbyfill WJ, Howell D, Willner DA, Palmer SM. Cytomegalovirus Pneumonitis Is a Risk for Bronchiolitis Obliterans Syndrome in Lung Transplantation. Am J Respir Crit Care Med. 2010 Jun 15;181(12):1391–6.

4. Paraskeva M, Bailey M, Levvey BJ, Griffiths AP, Kotsimbos TC, Williams TP, et al. Cytomegalovirus Replication Within the Lung Allograft Is Associated With Bronchiolitis Obliterans Syndrome: CMV in the Allograft Is Associated With BOS. American Journal of Transplantation. 2011 Oct;11(10):2190–6.

5. Mitsani D, Nguyen MH, Kwak EJ, Silveira FP, Vadnerkar A, Pilewski J, et al. Cytomegalovirus disease among donor-positive/recipient-negative lung transplant recipients in the era of valganciclovir prophylaxis. The Journal of Heart and Lung Transplantation. 2010 Sep;29(9):1014–20.

6. McSharry B, Avdic S, Slobedman B. Human Cytomegalovirus Encoded Homologs of Cytokines, Chemokines and their Receptors: Roles in Immunomodulation. Viruses. 2012 Oct 25;4(11):2448–70.

7. Kledal TN, Rosenkilde MM, Schwartz TW. Selective recognition of the membrane-bound CX $_3$ C chemokine, fractalkine, by the human cytomegalovirus-encoded broad-spectrum receptor US28. FEBS Letters. 1998 Dec 18;441(2):209–14.

8. Krishna BA, Poole EL, Jackson SE, Smit MJ, Wills MR, Sinclair JH. Latency-Associated Expression of Human Cytomegalovirus US28 Attenuates Cell Signaling Pathways To Maintain Latent Infection. Imperiale MJ, editor. mBio. 2017 Dec 29;8(6):mBio.01754-17, e01754-17.

9. Krishna BA, Spiess K, Poole EL, Lau B, Voigt S, Kledal TN, et al. Targeting the latent cytomegalovirus reservoir with an antiviral fusion toxin protein. Nature Communications. 2017 Feb 2;8:14321.

10. Spiess K, Jeppesen MG, Malmgaard-Clausen M, Krzywkowski K, Dulal K, Cheng T, et al. Rationally designed chemokine-based toxin targeting the viral G protein-coupled receptor US28 potently inhibits cytomegalovirus infection in vivo. Proc Natl Acad Sci U S A. 2015 Jul 7;112(27):8427–32.

11. Cypel M, Yeung JC, Liu M, Anraku M, Chen F, Karolak W, et al. Normothermic ex vivo lung perfusion in clinical lung transplantation. N Engl J Med. 2011 Apr 14;364(15):1431–40.

12. Yeung JC, Krueger T, Yasufuku K, de Perrot M, Pierre AF, Waddell TK, et al. Outcomes after transplantation of lungs preserved for more than 12 h: a retrospective study. The Lancet Respiratory Medicine. 2017 Feb;5(2):119–24.

13. Cypel M, Liu M, Rubacha M, Yeung JC, Hirayama S, Anraku M, et al. Functional repair of human donor lungs by IL-10 gene therapy. Sci Transl Med. 2009 Oct 28;1(4):4ra9.

14. Hashimoto K, Kim H, Oishi H, Chen M, Iskender I, Sakamoto J, et al. Annexin V homodimer protects against ischemia reperfusion–induced acute lung injury in lung transplantation. The Journal of Thoracic and Cardiovascular Surgery. 2016 Mar;151(3):861–9.

15. Nakajima D, Cypel M, Bonato R, Machuca TN, Iskender I, Hashimoto K, et al. Ex Vivo Perfusion Treatment of Infection in Human Donor Lungs. Am J Transplant. 2016 Apr;16(4):1229–37.

16. Galasso M, Feld JJ, Watanabe Y, Pipkin M, Summers C, Ali A, et al. Inactivating hepatitis C virus in donor lungs using light therapies during normothermic ex vivo lung perfusion. Nature Communications [Internet]. 2019 Dec [cited 2019 May 6];10(1). Available from: http://www.nature.com/articles/s41467-018-08261-z

17. Cypel M, Feld JJ, Galasso M, Pinto Ribeiro RV, Marks N, Kuczynski M, et al. Prevention of viral transmission during lung transplantation with hepatitis C-viraemic donors: an open-label, single-centre, pilot trial. The Lancet Respiratory Medicine. 2019 Oct;S2213260019302681.

18. Ku TJY, Ribeiro RVP, Ferreira VH, Galasso M, Keshavjee S, Kumar D, et al. Ex-vivo delivery of monoclonal antibody (Rituximab) to treat human donor lungs prior to transplantation. EBioMedicine. 2020 Oct;60:102994.

19. Collins-McMillen D, Buehler J, Peppenelli M, Goodrum F. Molecular Determinants and the Regulation of Human Cytomegalovirus Latency and Reactivation. Viruses. 2018 Aug 20;10(8):444.

20. Krishna B, Miller W, O'Connor C. US28: HCMV's Swiss Army Knife. Viruses. 2018 Aug 20;10(8):445.

21. Cross LJM, Matthay MA. Biomarkers in Acute Lung Injury: Insights into the Pathogenesis of Acute Lung Injury. Critical Care Clinics. 2011 Apr;27(2):355–77.

THE CLINICAL PREDICTORS OF COLD SENSITIVITY AND THE IMPACT OF CARPAL TUNNEL RELEASE IN PATIENTS WITH CARPAL TUNNEL SYNDROME

Moaath Saggaf (SSTP)[1,2], Aaron M Drucker[3], Christine B Novak[1], Larry R Robinson[3], Dimitri J Anastakis[1,2,4]

[1]Division of Plastic and Reconstructive Surgery, Department of Surgery, University of Toronto, [2]Institute of Medical Science, University of Toronto; [3]Institute of Health Policy, Management and Evaluation and Department of Medicine, University of Toronto; [4]Krembil Research Institute, Toronto Western Hospital, University Health Network, Toronto, Ontario, Canada

Background/Purpose:

Carpal tunnel syndrome (CTS) is the most common nerve compression syndrome affecting approximately 4% of adults in the United States (1). CTS is the most expensive upper extremity musculoskeletal disorder with an annual estimated $2 billion cost in the United States (2). CTS is prevalent and causes a significant burden to both the patients and the healthcare system.

Cold sensitivity is defined as an abnormal response to cold temperatures resulting in pain, numbness, weakness, stiffness or colour changes (3). It is a known to occur following peripheral nerve injuries (4-6). In our scoping review, the prevalence of cold sensitivity in upper extremity nerve compression syndrome ranged from 20% to 69%, yet it is understudied (7). Cold sensitivity is associated with significant disability (4) and lower health-related quality of life (8). There is limited literature on the predictors of cold sensitivity in patients with CTS, and the relationship between the severity of CTS and cold sensitivity is not well-defined. Understanding the relationship between CTS and cold sensitivity may provide a better understanding of the biological plausibility model of developing cold sensitivity in upper extremity nerve compression syndromes, especially with the identification of a positive linear relationship.

Although cold sensitivity is moderately prevalent in CTS patients, the impact of a carpal tunnel release (CTR) on cold sensitivity is not known (7). In traumatic peripheral nerve injuries, cold sensitivity is a long-term sequela (9). Previous studies reviewing the effect of surgery on cold sensitivity are limited by selecting a proper control group and the consistent utilization of validated instruments limiting generalizable conclusions (7). Knowing the effect CTR and nighttime splinting on cold sensitivity may provide evidence for an earlier surgical intervention in high-risk patients to decrease the severity of cold sensitivity.

Study Aims:

The primary aim of the study was to assess the effect of a CTR on cold sensitivity. The secondary aim of the study was to assess the relationship between the severity of cold sensitivity and severity of CTS. We hypothesised that a CTR will decrease the severity of cold sensitivity as measured by patient-reported outcomes, and patients with more severe CTS will have a higher degree of cold sensitivity.

Methods:

Using a prospective cohort study design, adult patients with CTS were screened for cold sensitivity and invited to participate in the study. We excluded patients with traumatic peripheral nerve injuries, previous upper extremity surgeries, insulin-dependent diabetes mellitus or polyneuropathy. We measured CTS severity with the validated Boston Carpal Tunnel Questionnaire (BCTQ) Symptom Severity Scale (10) and measured cold sensitivity with the Cold Intolerance Symptom Severity (CISS) questionnaire (3). CISS is a self-administered validated questionnaire measuring cold sensitivity, and it has demonstrated good internal consistency and acceptable test-retest reliability (3, 11).

Patients were treated with either nighttime splinting or surgery. A surgical release was performed using an open CTR approach. Patients were fitted with a splint and were instructed to wear it every night for three months. Before and 3 months after the intervention, we assessed CTS severity using BCTQ and cold sensitivity using the CISS scale. The questionnaires were self-administered and physician-administered by phone. Following Research Ethics Board approval, patients were enrolled from Toronto Western Hospital and Sunnybrook Health Sciences Centre.

The association between the BCTQ and CISS scores was assessed with the Pearson correlation coefficient. We used multiple linear regression to assess associations between clinical factors and cold sensitivity severity. In the first model, we used baseline CISS scores as the dependent variable, with age, sex, smoking, comorbidities and BCTQ scores as covariates. In the second model, we added cold-induced pain, numbness and weakness as covariates. We used likelihood ratio tests to compare both models. We validated both models using a bootstrapping method with 500 repeats. We verified the normality and homoscedasticity assumptions. No evidence of collinearity was seen in both models using variance inflation factors.

To determine the impact of treatment, we assessed the treatment response between surgery and splinting with an independent t-test. We used multiple linear regression to model post-treatment CISS scores as the outcome, with age, sex, treatment group baseline CISS scores and baseline BCTQ scores as covariates. After verifying the model met all the statistical assumptions, we validated it using a bootstrapping method with 500 repeats. All the models were selected based on priori hypotheses and using a knowledge-based approach. In a secondary analysis, we used paired t-tests to estimate the within-subjects treatment effect for each cohort.

Results:

A total of 90 patients were included in the study: mean age 56 years (SD=12.9); 62 (69%) female participants. The mean BCTQ score was 3 (SD=0.9), and the mean CISS score was 43 (SD=20.0). The most frequent symptom was cold-induced numbness (n=57, 63%) followed by cold-induced pain and tingling (n= 51, 57%).

There were 49 patients who completed the study: surgery (n=23); splinting (n=26). The mean follow-up duration was 3 months. The mean age was 56 years (SD=12.5), and 36 participants were females (73.5%). The mean baseline CISS scores were 43 (SD=22.2) for the surgical cohort and 43 (SD=19.1) for the splinting cohort, respectively. Table 1 summarizes the baseline characteristics for the study participants.

There was a positive correlation between CTS severity and cold sensitivity severity (r_p=0.61, 95% CI: 0.47-0.73, p<0.0001). In the regression analysis, increasing BCTQ scores were associated with increasing CISS scores (Beta=13.9, 95% CI: 9.7 to 18.1, p<0.0001). Age, sex, smoking status and medical comorbidities were not significantly associated with cold sensitivity. The R^2 and the adjusted R^2 from the validated model were 39% and 36%, respectively. In the second model, the presence of cold-induced numbness predicted the highest increase in cold sensitivity (Beta=9.5, 95% CI: 2.8 to 16.2, p=0.006). After validating the model, the R^2 and the adjusted R^2 were 50% and 45%, respectively. Analysis of variance from both models reached statistical significance (p<0.0001). The likelihood ratio test indicated that the model with additional cold-induced symptoms performed better in predicting CISS scores (p<0.0001). Table 2 describes the treatment effect for the prediction model.

Compared to splinting, open CTR improved CISS scores by a mean change of 27.8 points (95% CI 17.79 to 37.83, p<0.0001). After adjusting for age, sex, CTS severity and baseline CISS scores, surgical patients improved by 28.0 (95% CI 17.60 to 38.42, p<0.0001) more points on the CISS compared to the splinting cohort. Table 3 details the adjusted analysis for estimating the treatment effect. In a secondary analysis for within-subjects difference, the surgical cohort improved by 25.9 points in their CISS score (95% CI: 16.1 to 35.7, p<0.0001) while the splinting

cohort had no statistically significant difference in CISS scores (mean=-1.3, 95% CI: -9.6 to 7.0, p=0.75).

Discussion:

This study found more improvement in cold sensitivity with CTR compared with nighttime splinting. We also identified clinical associations with worse cold sensitivity, with CTS severity being among the most important association.

Cold sensitivity is associated with significant disability and lower health status [12]. We previously reported a moderate prevalence of cold sensitivity in CTS [7]. In our scoping review, only a few studies reviewed the impact of treatment on cold sensitivity [7]. Most studies had methodological limitations, including the lack of a control group and using various measurement tools before and after surgery [7]. Our study compared CTR to nighttime splinting, and we identified a significant improvement at the three-month follow-up visit.

Previous studies have found associations between cold sensitivity and CTS, but most used only unadjusted comparisons or correlation analyses [3, 9, 12-14]. There is limited literature on the relationship between CTS severity and cold sensitivity. We identified a positive linear relationship between patient-reported CTS severity and cold sensitivity. This relationship may be explained by a compression injury to the A-Delta and C fibers within the median nerve as a precipitating factor for the development of cold sensitivity [15]. Our study provides evidence to support the conceptual framework for developing cold sensitivity.

There are several strengths to this study. We provided evidence to support surgical intervention in CTS patients with cold sensitivity using a priori hypothesis while accounting for known confounders. We also described the positive relationship between CTS severity and cold sensitivity. We were able to identify cold-induced symptoms that predicted worse CISS scores.

Our study was limited by lack of randomization to account for confounding by indication and unmeasured confounders. In our design, we were able to account for potential confounders by restriction. We also accounted for additional confounders in our regression analyses. However, it is possible to have unmeasured confounders in our study. There is also a risk for interviewer bias when administering the questionnaires remotely. We minimized the potential for bias by using standardized scripts and trained interviewers. This study was also limited by not accounting for the duration of nighttime splinting before study enrollment. Most patients had a poor recall due to inconsistent use of the splint before seeking treatment. We did not objectively measure compliance with nighttime splinting, but most patients received counseling before the initiation of nighttime splinting, and they indicated compliance on their 3-month assessment visit. Finally, although the treatment effect was sizable in our study, the minimal clinically important difference (MCID) for CISS scores is not reported in the literature. Nevertheless, we were able to estimate an effect size beyond the minimally detectable change (MDC) in CISS (MDC_{95}=12 points) [16], which can be attributed to measurement errors. Thus, our estimate is likely relevant to CTS patients using distribution-based approaches. Future studies should determine MCID for CISS to better assist patients in their decision-making.

Conclusion:

Increased CTS severity was associated with worse cold sensitivity. CTR was associated with improved cold sensitivity at 3-months following surgery compared with nighttime splinting. Future studies with larger sample sizes and randomized designs are needed to determine the relative efficacy of surgery for cold sensitivity and the MCID for the CISS.

Table 1: Baseline Characteristics of the Study Participants

Baseline Characteristics of All Study Participants			
	Overall n= 90 (%) +/- SD	**Surgical Arm n= 51 (%) +/-SD**	**Splinting Arm n= 39 (%) +/- SD**
Age (Years)	55.9 +/- 12.9	57.6 +/- 12.1	53.4 +/- 13.2
Sex = Female	58 (70%)	34 (67%)	28 (72%)
Comorbidities	32 (36%)	22 (43%)	10 (26%)
Smoking	9 (10%)	4 (8%)	5 (13%)
Handedness	Right: 80 (89%) Left: 7 (8%) Ambidextrous: 3 (3%)	Right: 46 (90%) Left: 4 (8%) Ambidextrous: 1 (2%)	Right: 34 (87%) Left: 3 (8%) Ambidextrous: 2 (5%)
BCTQ	3.0 +/- 0.9	3.2 +/- 0.8	2.8 +/- 0.9
CISS	43.4 +/- 20.0	45.4 +/- 21.2	40.9 +/-18.2
Baseline Characteristics of the Study Participants who Completed the Study			
	Overall n= 49 (%) +/- SD	**Surgical Arm n= 23 (%) +/-SD**	**Splinting Arm n= 26 (%) +/- SD**
Age (Years)	55.7 +/- 12.5	58.1 +/- 13.4	53.5 +/- 11.5
Sex = Female	36 (74%)	15 (65%)	21 (81%)
Comorbidities	12 (25%)	6 (26%)	6 (23%)
Smoking	9 (18%)	5 (22%)	4 (15%)
Handedness	Right: 42 (86%) Left: 5 (10%) Ambidextrous: 2 (4%)	Right: 18 (78%) Left: 4 (17%) Ambidextrous: 1 (4%)	Right: 24 (92%) Left: 1 (4%) Ambidextrous: 1 (4%)
BCTQ	3.0 +/- 0.8	3.2 +/- 0.7	2.9 +/- 0.9
CISS	42.9 +/- 20.4	42.5 +/- 22.2	43.2 +/- 19.1

BCTQ: Boston Carpal Tunnel Questionnaire. CISS: Cold Intolerance Symptom Severity Questionnaire

Table 2: Associations with Cold Sensitivity (CISS Scores) in Patients with CTS

Variable	Difference	Beta	95% CI	P-value
BCTQ	1	10.33	6.09 to 14.58	<0.0001 *
Age	10	-0.05	-2.58 to 2.48	0.97
Smoking	NA	2.36	-8.19 to 12.91	0.66
Sex (Male)	NA	-2.63	-9.75 to 4.49	0.46
Comorbidities	NA	1.59	-5.53 to 8.71	0.66
Cold-induced Pain	NA	8.30	1.67 to 14.94	0.01 *
Cold-induced Numbness	NA	9.51	2.81 to 16.22	0.006 *
Cold-induced Weakness	NA	7.48	0.25 to 14.70	0.04 *

BCTQ: Boston Carpal Tunnel Questionnaire. CISS: Cold Intolerance Symptom Severity Questionnaire. Dependent Variable = Baseline CISS.

Table 3: Adjusted Analysis for Between-Group Comparisons Following Treatment for CTS

Variable	Difference	Beta	95% CI	P-value
Baseline BCTQ	1	-0.06	-7.39 to 7.28	0.99
Baseline CISS	10	3.02	0.20 to 5.84	0.036
Group = Splint	NA	28.01	17.60 to 38.42	<0.0001
Age (Years)	10	1.05	-3.08 to 5.17	0.61
Sex = Male	NA	-0.51	- 12.41 to 11.39	0.93

BCTQ: Boston Carpal Tunnel Questionnaire. CISS: Cold Intolerance Symptom Severity Questionnaire. Dependent Variable = Post-Intervention CISS.

References:

1. Lawrence RC, Felson DT, Helmick CG, Arnold LM, Choi H, Deyo RA, et al. Estimates of the prevalence of arthritis and other rheumatic conditions in the United States. Part II. Arthritis Rheum. 2008;58(1):26-35.
2. Stapleton MJ. Occupation and carpal tunnel syndrome. ANZ J Surg. 2006;76(6):494-6.
3. Irwin MS, Gilbert SE, Terenghi G, Smith RW, Green CJ. Cold intolerance following peripheral nerve injury. Natural history and factors predicting severity of symptoms. J Hand Surg Br. 1997;22(3):308-16.
4. Novak CB, Anastakis DJ, Beaton DE, Mackinnon SE, Katz J. Cold intolerance after brachial plexus nerve injury. Hand (N Y). 2012;7(1):66-71.
5. Carlsson IK, Edberg AK, Wann-Hansson C. Hand-injured patients' experiences of cold sensitivity and the consequences and adaptation for daily life: a qualitative study. J Hand Ther. 2010;23(1):53-62.
6. Novak CB, Anastakis DJ, Beaton DE, Mackinnon SE, Katz J. Biomedical and psychosocial factors associated with disability after peripheral nerve injury. J Bone Joint Surg Am. 2011;93(10):929-36.
7. Saggaf M, Evangelista JV, Novak CB, Anastakis DJ. Evaluation of Cold Sensitivity in Patients with Upper Extremity Nerve Compression Syndromes: A Scoping Review. American Society for Peripheral Nerve (ASPN) Annual Meeting 2021.
8. Novak CB, Mackinnon SE. Evaluation of Cold Sensitivity, Pain, and Quality of Life After Upper Extremity Nerve Injury. Hand (N Y). 2016;11(2):173-6.
9. Ruijs AC, Jaquet JB, van Riel WG, Daanen HA, Hovius SE. Cold intolerance following median and ulnar nerve injuries: prognosis and predictors. J Hand Surg Eur Vol. 2007;32(4):434-9.
10. Levine DW, Simmons BP, Koris MJ, Daltroy LH, Hohl GG, Fossel AH, et al. A self-administered questionnaire for the assessment of severity of symptoms and functional status in carpal tunnel syndrome. J Bone Joint Surg Am. 1993;75(11):1585-92.
11. Carlsson I, Cederlund R, Hoglund P, Lundborg G, Rosen B. Hand injuries and cold sensitivity: reliability and validity of cold sensitivity questionnaires. Disabil Rehabil. 2008;30(25):1920-8.
12. Carlsson IK, Rosen B, Dahlin LB. Self-reported cold sensitivity in normal subjects and in patients with traumatic hand injuries or hand-arm vibration syndrome. BMC Musculoskelet Disord. 2010;11:89.
13. Carlsson IK, Dahlin LB. Self-reported cold sensitivity in patients with traumatic hand injuries or hand-arm vibration syndrome - an eight year follow up. BMC Musculoskelet Disord. 2014;15:83.
14. Cesim OB, Oksuz C. More severe cold intolerance is associated with worse sensory function after peripheral nerve repair or decompression. J Hand Surg Eur Vol. 2020;45(3):231-6.
15. Novak CB. Cold intolerance after nerve injury. J Hand Ther. 2018;31(2):195-200.
16. Magistroni E, Ferriero G, Peri E, Parodi G, Massazza G, Franchignoni F. Psychometric properties of the Italian version of the Cold Intolerance Symptom Severity questionnaire in upper-extremity nerve repair. Eur J Phys Rehabil Med. 2019;55(5):627-33.

I am pleased to submit our manuscript/extended abstract entitled “The Clinical Predictors of Cold Sensitivity and the Impact of Carpal Tunnel Release in Patients with Carpal Tunnel Syndrome”. I am currently in the Surgeon-Scientist Training Program in the Division of Plastic and Reconstructive Surgery at the University of Toronto.

The work that I am submitting is closely related to my thesis. I confirm that the submitted work is the work of our research team. I am the Principal Investigator, and I am the lead on all the aspects of the study, including the design, conduct, analysis, interpretations, and manuscript preparation. I am also the PI on the grant that funded this original research from the Plastic Surgery Foundation and the American Society for Peripheral Nerve.

Dr. Anastakis is my research supervisor. Drs. Anastakis and Novak assisted in the study design. Drs. Robinson and Drucker provided expertise in some of the methodological challenges in the conduct of the study. All the authors reviewed the submitted manuscript. The current work was conducted at Toronto Western Hospital and Sunnybrook Health Sciences Centre from July 2019 to date.

I look forward to the outcome of the selection process. Thank you for your consideration.

Sincerely,

Moaath Saggaf, MD

Disclosure:
This study was funded by the Plastic Surgery Foundation/ American Society for Peripheral Nerve

RACIAL AND SOCIOECONOMIC DISPARITIES IN BREAST CANCER DIAGNOSIS, TREATMENT, AND PROGNOSIS: A SEER-BASED POPULATION STUDY

Houman Tahmasebi[1], Arash Azin[1,2], Amanpreet Brar[1,2], Gary Ko[1,2], Sam Azin[3], Andrea Covelli[1,2,4], Tulin Cil[1,2, 5]

[1] Faculty of Medicine, University of Toronto, Ontario, Canada
[2] Department of Surgery, University of Toronto, Toronto, Ontario, Canada
[3] Department of Mathematics and Statistics, Queen's University, Kingston, Ontario, Canada
[4] Division of Surgical Oncology, Marvelle Koffler Breast Centre, Mount Sinai Health System, Toronto, Ontario, Canada
[5] Sprott Department of Surgery, Princess Margaret Cancer Centre, University Health Network, Toronto, Ontario, Canada

Introduction:

Breast cancer is the most common non-skin cancer and the second leading cause of death from cancer in United States (US) women (1). Regardless of continuous advances in breast cancer treatment and prognosis, there is a large body of evidence demonstrating racial/ethnic and socioeconomic disparities in breast cancer diagnosis, treatment and prognosis (2). For instance, patients from lower socioeconomic backgrounds have higher odds of being diagnosed at later stages of breast cancer (3–8). Compared to Non-Hispanic White (NHW) patients, Hispanic and non-Hispanic Black (NHB) patients are more likely to be diagnosed at a later stage of breast cancer (3,9–11) and to not receive immediate breast reconstruction following mastectomy (12–15). NHB patients also tend to have higher breast cancer mortality rates (16–24), yet they are less likely to receive breast cancer surgical interventions (5,16,25–27), compared to NHW patients. These disparities are often multifaceted and are propagated by institutional and national-level policies.

Nevertheless, a limited number of available studies have analyzed the interaction of race/ethnicity, socioeconomic status (SES) and insurance status, and their compounded impact on breast cancer outcomes. Thus, currently, there is a limited understanding around the impact of SES on ethnic/racial differences in breast cancer outcomes. Such gaps in the literature provide inadequate knowledge about underlying reasons responsible for the observed disparities and therefore provide challenges in reducing inequities faced by minorities. Furthermore, to approximate SES, the majority of current studies have used county level measures, household income, or Medicaid insurance status alone (4,6–8). None of these measures provide adequate data to measure significant factors contributing to the observed disparities.

The objective of the study was to determine the influence of race/ethnicity, SES, and insurance status on breast cancer diagnosis, treatment, and survival using large nationally representative data. Our study was unique for using multi-dimensional SES calculations, as well as identifying the compounded impact of variables on outcomes.

Methods:

The Surveillance, Epidemiology, and End Results (SEER) 18 registry database was used to obtain demographic and cancer-specific data. SEER represents approximately 28% of the US population (32); thus, it is considered to be nationally representative. All NHB, NHW, and Hispanic female patients diagnosed with non-metastatic breast cancer between 2007 and 2016 were selected. All patients with non-primary cancers or missing important demographic or oncological information were excluded. Yost Index (29), a combined score of seven variables (i.e. median household income, percent working class, percent unemployed, median rent,

median house value, percent below 150% of poverty line, and Education Index), was used to calculate SES. SES was then divided into tertiles: upper, middle and lower.

The three independent variables were race/ethnicity, SES, and insurance status. Five primary outcomes consisted of: stage of cancer at diagnosis, access to primary oncologic surgery, access to post-mastectomy immediate breast reconstruction (IBR), as well as cancer-specific and overall survival. Pearson chi-squared and Kruskal-Wallis test were used to compare categorical and continuous variables, respectively. Survival data were estimated and compared via Kaplan-Meier method and log-rank test, respectively. Binary logistic regression and Cox proportional hazards regression analysis were used to calculate univariate and multivariate survival analyses. A Bonferroni correction was applied to account for the five variables and $p< 0.01$ implied significant differences. R (v 4.0.02) and SPSS (v 23.0) were used to perform statistical analyses.

Results:

A total of 382,975 patients were identified. The median age was 60 (IQR: 51-70) years. 75.5% (n=289,074) were NHW, 12% (n=45,821) were NHB, and 12.6% (n=48,080) were Hispanic. Most patients were diagnosed with stage I (50.2%), ER positive (80.8%), PR positive (70.3%), and HER2 negative (57.6%) breast cancer. The most common surgical procedure was lumpectomy (56.6%).

Compared to NHW patients, Hispanic and NHB patients were associated with a more advanced presentation (i.e. stage II/III) of breast cancer in multivariate analysis (OR 1.20 [1.17-1.22] and OR 1.18 [1.15-1.20], respectively). Patients of lower and middle SES were also more likely to present later (i.e. stage II/III). NHB and Hispanic patients without insurance and in the lowest SES had a mush higher rate of stage II/III cancer than NHW patients with insurance and in the upper SES tertile (OR 1.94 [1.84-2.05] and OR 1.97 [1.87-2.07], respectively). While these racial/ethnic differences decreased with improving SES and insurance status, they persisted for all sub-categories (**Figure 1**).

In multivariate analysis, Hispanic and NHB patients were more likely to not undergo primary oncologic surgery (OR 1.41 [1.34-1.48] and OR 1.56 [1.49-1.64], respectively) and post-mastectomy IBR (OR 1.60 [1.54-1.66] and OR 1.07 [1.03-1.11]), compared to NHW patients. NHB and Hispanic patients without insurance and in the lowest SES, compared to NHW patients with insurance and in the highest SES, were associated with significantly higher odds of not undergoing primary oncologic surgery (OR 2.14 [1.94-2.45] and OR 2.45 [2.23-2.69], respectively). These differences decreased, but still remained, after NHB and Hispanic patients had insurance coverage and were in the highest SES tertile (**Figure 2A**). Furthermore, there were racial/ethnic differences in access to post-mastectomy IBR across SES and insurance status categories; Hispanic patients had lowest access in the majority of categories (**Figure 2B**).

Out of 47,476 patients (12.4%) who died between 2007 and 2016, 7,590 (16.6%) were NHB, 4,612 (9.6%) were Hispanic, and 35,274 (12.2%) were NHW. Five-year overall survival was significantly different across races: 80.8% [80.4%-81.3%] for NHB, 87.1% [86.9%-87.2%] for NHW, and 87.9% [87.6%-88.3%] for Hispanic patients. Five-year overall and cancer-specific mortality were significantly different across races and SES categories. NHW patients and those of the highest SES tertile had higher overall and cancer-specific survival. NHB patients had higher hazard of overall (HR: 1.13, 95%CI: 1.10-1.16) and breast cancer-specific (HR: 1.20, 95%CI: 1.16-1.24) mortality, while Hispanic patients had lower hazard of overall (HR: 0.89, 95%CI: 0.85-0.90) and breast cancer-specific (HR: 0.94, 95%CI: 0.90-0.98) mortality, compared to NHW patients. Although the Hazard of cancer-specific and overall mortality decreased with improving SES and access to insurance, higher hazard of cancer-specific and overall mortality remained for NHB patients in the highest SES and insurance category (**Figures 3A** and **3B**).

Discussion:

This is the first study that uses SEER database to analyze the compounded impact of race/ethnicity, SES (via Yost Index), and insurance status on breast cancer diagnosis, treatment, and survival. Our findings demonstrate that ethnic and racial minorities are more likely to present with a more advanced disease presentation, and decreased access to primary oncologic surgery and post-mastectomy IBR. NHB patients were also associated with worse overall and cancer-specific survival. These disparities were generally found to increase with lower SES and lack of insurance coverage.

Consistent with our findings, other studies have demonstrated a more advanced breast cancer diagnosis in NHB and Hispanic patients (3,9–11) and patients of lower SES (3–8). Furthermore, our results are unique for demonstrating that minorities have an approximately double the odds of later disease presentation (i.e. stage II/III) and that these disparities remain within SES and insurance categories after adjusting for demographic and oncological factors. Such disparities are likely multifactorial, such as reduced access to breast centers and mammography by NHB and Hispanic patients (30,31). Screening guidelines that do not recommend mammography for low risk patients may disadvantage NHBs, as they tend to develop breast cancer earlier than NHWs (32,33). Thus, there is a need for policy adjustments to reduce such inequities and to advocate for minorities and marginalized populations.

Several studies also confirm our finding regarding NHB patients having reduced access to primary oncologic surgery and post-mastectomy IBR (8-16) compared to NHW patients. However, our finding regarding reduced access in Hispanic patients is unique. Our variable interaction analysis found that Hispanic and NHB patients have approximately 7-fold and 5.5-fold decrease in access to IBR following mastectomy, respectively, a finding that had not been sufficiently established in the past. Racial/ethnic differences, although smaller, remained for patients with insurance and in the highest SES tertile. Racial and socioeconomic differences in access to surgery could be explained by structural racism, economic deprivation, and implicit bias against marginalized communities. Long-term efforts are needed to reduce the impact of such disparities, such as introducing policy changes to reduce financial burden of medical costs on patients, and expanding the number of physicians from marginalized communities.

Similar to our findings, other studies have reported cancer-specific and overall mortality rates in NHB compared to NHW patients (16–18,23,24). On the other hand, evidence for Hispanic patients (17–19,23,24,34) and the impact of SES and insurance status (20–22,35,36) is inconsistent and unclear. Conflicting findings regarding SES and insurance status could either be due to the failure to analyze the interaction between variable or the use of county level data, which do not provide adequate number of variables to measure SES. Furthermore, our findings suggest graded increases in overall and cancer-specific mortality across lower SES tertiles. Similar to the other outcomes, systemic racism and socioeconomic inequities that have been engrained in healthcare throughout the years may be contributing to racial/ethnic differences in mortality rates.

This study used large nationally representative data to analyze the impact of race/ethnicity, SES and insurance status on breast cancer diagnosis, treatment, and survival. Compared to NHW patients, NHB and Hispanic patients were found to be diagnosed at a later stage of cancer, and had decreased access to primary oncologic surgery and post-mastectomy IBR. Findings also demonstrated that NHB patients have a higher hazard of overall and cancer-specific mortality compared to NHW patients. These disparities increased in lower SES tertiles and with decreased insurance coverage. Further studies are encouraged to identify underlying reasons for such disparities and the role of structural injustices in diagnosis, treatment and prognosis of minority patients with breast cancer.

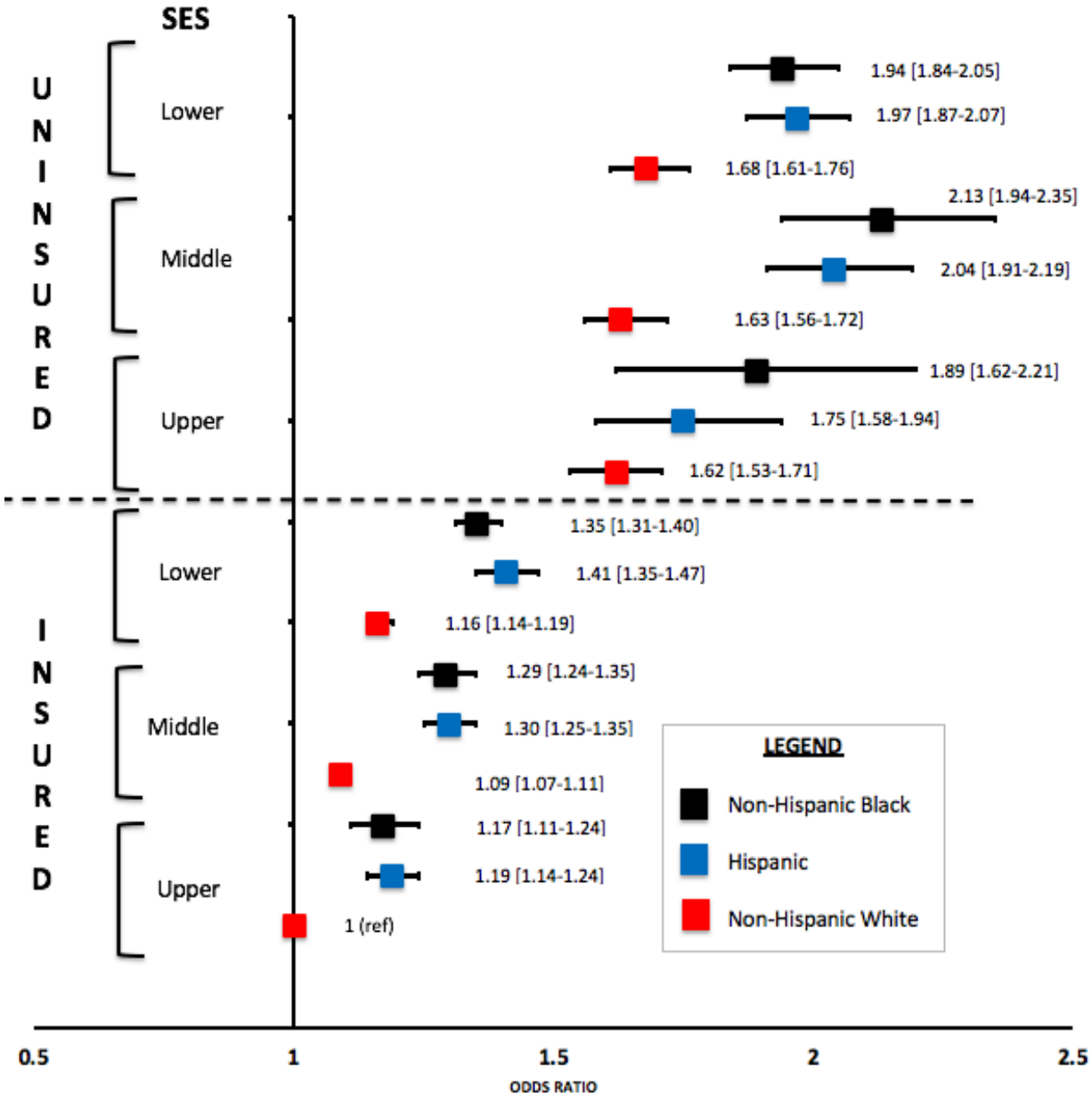

Figure 1: Multivariate analysis of the predictors of advanced disease presentation (stage II/III vs. stage I). Odds ratio refers to odds of advanced disease presentation.

A.

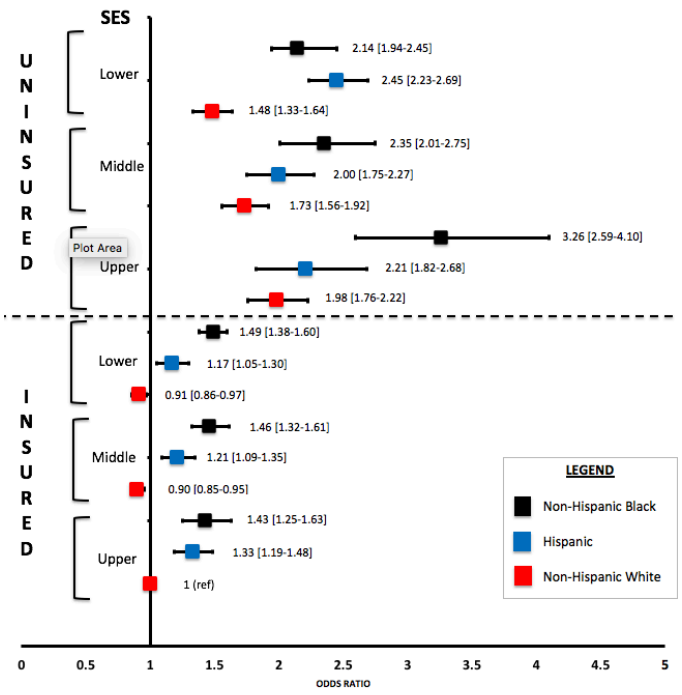

B.

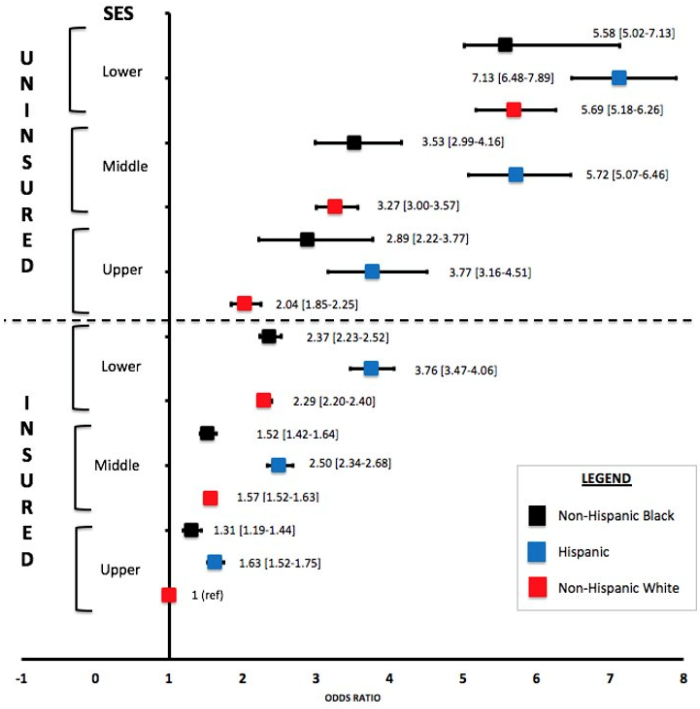

Figure 2: Multivariate analysis of the predictors of primary oncologic surgery (A) and post-mastectomy immediate breast reconstruction (B). Odds ratio refers to odds of not receiving surgery (i.e. higher odds indicate decreased rate of surgical intervention).

A.

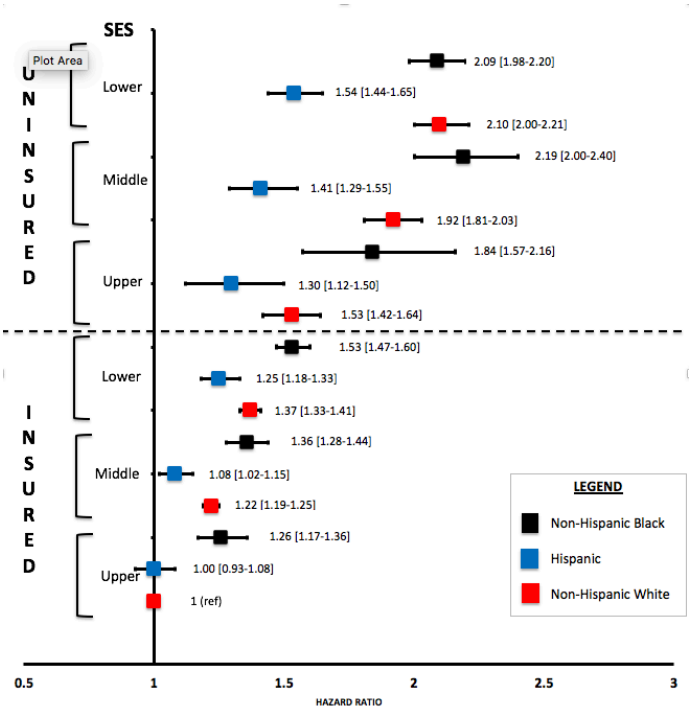

B.

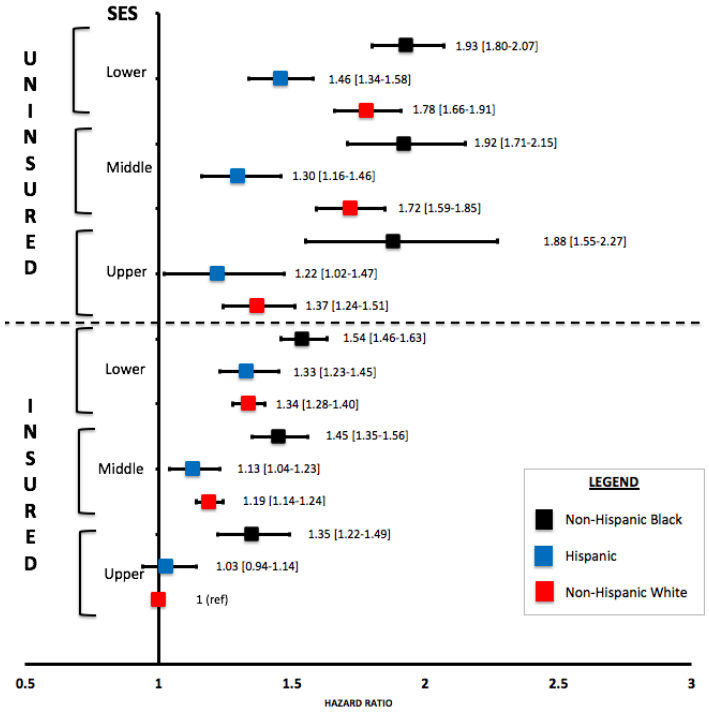

Figure 3: Multivariate analysis of the predictors of overall (A) and breast cancer-specific (B) mortality. Hazard ratio refers to hazard of mortality.

References:

1. Siegel RL, Miller KD, Jemal A. Cancer statistics, 2020. CA Cancer J Clin. 2020;70(1):7–30.

2. Yedjou CG, Sims JN, Miele L, Noubissi F, Lowe L, Fonseca DD, et al. Health and Racial Disparity in Breast Cancer. Adv Exp Med Biol. 2019;1152:31–49.

3. Ko NY, Hong S, Winn RA, Calip GS. Association of Insurance Status and Racial Disparities With the Detection of Early-Stage Breast Cancer. JAMA Oncol. 2020 Mar 1;6(3):385–92.

4. Williams F, Thompson E. Disparities in Breast Cancer Stage at Diagnosis: Importance of Race, Poverty, and Age. J Health Disparities Res Pract. 2017;10(3):34–45.

5. Bradley CJ, Given CW, Roberts C. Race, socioeconomic status, and breast cancer treatment and survival. J Natl Cancer Inst. 2002 Apr 3;94(7):490–6.

6. Merkin SS, Stevenson L, Powe N. Geographic socioeconomic status, race, and advanced-stage breast cancer in New York City. Am J Public Health. 2002 Jan;92(1):64–70.

7. MacKinnon JA, Duncan RC, Huang Y, Lee DJ, Fleming LE, Voti L, et al. Detecting an association between socioeconomic status and late stage breast cancer using spatial analysis and area-based measures. Cancer Epidemiol Biomark Prev Publ Am Assoc Cancer Res Cosponsored Am Soc Prev Oncol. 2007 Apr;16(4):756–62.

8. Dianatinasab M, Mohammadianpanah M, Daneshi N, Zare-Bandamiri M, Rezaeianzadeh A, Fararouei M. Socioeconomic Factors, Health Behavior, and Late-Stage Diagnosis of Breast Cancer: Considering the Impact of Delay in Diagnosis. Clin Breast Cancer. 2018 Jun;18(3):239–45.

9. Warner ET, Tamimi RM, Hughes ME, Ottesen RA, Wong Y-N, Edge SB, et al. Time to diagnosis and breast cancer stage by race/ethnicity. Breast Cancer Res Treat. 2012 Dec;136(3):813–21.

10. Lantz PM, Mujahid M, Schwartz K, Janz NK, Fagerlin A, Salem B, et al. The influence of race, ethnicity, and individual socioeconomic factors on breast cancer stage at diagnosis. Am J Public Health. 2006 Dec;96(12):2173–8.

11. Shoemaker ML, White MC, Wu M, Weir HK, Romieu I. Differences in breast cancer incidence among young women aged 20-49 years by stage and tumor characteristics, age, race, and ethnicity, 2004-2013. Breast Cancer Res Treat. 2018 Jun;169(3):595–606.

12. Sergesketter AR, Thomas SM, Lane WO, Orr JP, Shammas RL, Fayanju OM, et al. Decline in Racial Disparities in Postmastectomy Breast Reconstruction: A Surveillance, Epidemiology, and End Results Analysis from 1998 to 2014. Plast Reconstr Surg. 2019 Jun;143(6):1560–70.

13. Wirth LS, Hinyard L, Keller J, Bucholz E, Schwartz T. Geographic variations in racial disparities in postmastectomy breast reconstruction: A SEER database analysis. Breast J. 2019 Jan;25(1):112–6.

14. Onega T, Weiss J, Kerlikowske K, Wernli K, Buist DS, Henderson LM, et al. The influence of race/ethnicity and place of service on breast reconstruction for Medicare beneficiaries with mastectomy. SpringerPlus. 2014;3:416.

15. Lang JE, Summers DE, Cui H, Carey JN, Viscusi RK, Hurst CA, et al. Trends in post-mastectomy reconstruction: a SEER database analysis. J Surg Oncol. 2013 Sep;108(3):163–8.

16. Hardy D, Du DY. Socioeconomic and Racial Disparities in Cancer Stage at Diagnosis, Tumor Size, and Clinical Outcomes in a Large Cohort of Women with Breast Cancer, 2007-2016. J Racial Ethn Health Disparities. 2020 Sep 10;

17. Han Y, Miao Z-F, Lian M, Peterson LL, Colditz GA, Liu Y. Racial and ethnic disparities in 21-gene recurrence scores, chemotherapy, and survival among women with hormone receptor-positive, node-negative breast cancer. Breast Cancer Res Treat. 2020 Dec;184(3):915–25.

18. Akinyemiju T, Moore JX, Ojesina AI, Waterbor JW, Altekruse SF. Racial disparities in individual breast cancer outcomes by hormone-receptor subtype, area-level socio-economic status and healthcare resources. Breast Cancer Res Treat. 2016 Jun;157(3):575–86.

19. Feinglass J, Rydzewski N, Yang A. The socioeconomic gradient in all-cause mortality for women with breast cancer: findings from the 1998 to 2006 National Cancer Data Base with follow-up through 2011. Ann Epidemiol. 2015 Aug;25(8):549–55.

20. Markossian TW, Hines RB, Bayakly R. Geographic and racial disparities in breast cancer-related outcomes in Georgia. Health Serv Res. 2014 Apr;49(2):481–501.

21. Ji P, Gong Y, Jiang C-C, Hu X, Di G-H, Shao Z-M. Association between socioeconomic factors at diagnosis and survival in breast cancer: A population-based study. Cancer Med. 2020 Mar;9(5):1922–36.

22. Lu G, Li J, Wang S, Pu J, Sun H, Wei Z, et al. The fluctuating incidence, improved survival of patients with breast cancer, and disparities by age, race, and socioeconomic status by decade, 1981-2010. Cancer Manag Res. 2018;10:4899–914.

23. Warner ET, Tamimi RM, Hughes ME, Ottesen RA, Wong Y-N, Edge SB, et al. Racial and Ethnic Differences in Breast Cancer Survival: Mediating Effect of Tumor Characteristics and Sociodemographic and Treatment Factors. J Clin Oncol Off J Am Soc Clin Oncol. 2015 Jul 10;33(20):2254–61.

24. Han Y, Moore JX, Langston M, Fuzzell L, Khan S, Lewis MW, et al. Do breast quadrants explain racial disparities in breast cancer outcomes? Cancer Causes Control CCC. 2019 Nov;30(11):1171–82.

25. Poulson MR, Beaulieu-Jones BR, Kenzik KM, Dechert TA, Ko NY, Sachs TE, et al. Residential Racial Segregation and Disparities in Breast Cancer Presentation, Treatment, and Survival. Ann Surg. 2021 Jan 1;273(1):3–9.

26. Yu XQ. Socioeconomic disparities in breast cancer survival: relation to stage at diagnosis, treatment and race. BMC Cancer. 2009 Oct 14;9:364.

27. Curtis E, Quale C, Haggstrom D, Smith-Bindman R. Racial and ethnic differences in breast cancer survival: how much is explained by screening, tumor severity, biology, treatment, comorbidities, and demographics? Cancer. 2008 Jan 1;112(1):171–80.

28. Abualkhair WH, Zhou M, Ahnen D, Yu Q, Wu X-C, Karlitz JJ. Trends in Incidence of Early-Onset Colorectal Cancer in the United States Among Those Approaching Screening Age. JAMA Netw Open. 2020 Jan 3;3(1):e1920407.

29. Yu M, Tatalovich Z, Gibson JT, Cronin KA. Using a composite index of socioeconomic status to investigate health disparities while protecting the confidentiality of cancer registry data. Cancer Causes Control CCC. 2014 Jan;25(1):81–92.

30. Rauscher GH, Allgood KL, Whitman S, Conant E. Disparities in screening mammography services by race/ethnicity and health insurance. J Womens Health 2002. 2012 Feb;21(2):154–60.

31. Ahmed AT, Welch BT, Brinjikji W, Farah WH, Henrichsen TL, Murad MH, et al. Racial Disparities in Screening Mammography in the United States: A Systematic Review and Meta-analysis. J Am Coll Radiol JACR. 2017 Feb;14(2):157-165.e9.

32. Dobson R. Black women have a higher risk of breast cancer than white women. BMJ. 2008 Jan 19;336(7636):116.2-116.

33. Gerend MA, Pai M. Social Determinants of Black-White Disparities in Breast Cancer Mortality: A Review. Cancer Epidemiol Biomarkers Prev. 2008 Nov;17(11):2913–23.

34. Hung M-C, Ekwueme DU, Rim SH, White A. Racial/ethnicity disparities in invasive breast cancer among younger and older women: An analysis using multiple measures of population health. Cancer Epidemiol. 2016 Dec;45:112–8.

35. Shariff-Marco S, Yang J, John EM, Sangaramoorthy M, Hertz A, Koo J, et al. Impact of neighborhood and individual socioeconomic status on survival after breast cancer varies by race/ethnicity: the Neighborhood and Breast Cancer Study. Cancer Epidemiol Biomark Prev Publ Am Assoc Cancer Res Cosponsored Am Soc Prev Oncol. 2014 May;23(5):793–811.

36. Obeng-Gyasi S, Bhattacharyya O, Li Y, Eskander M, Tsung A, Oppong B. The implications of neighborhood socioeconomic status on surgical management and mortality in malignant phyllodes patients in the Surveillance, Epidemiology, and End Results program. Surgery. 2020 Dec;168(6):1122–7.

This research study was completed under the supervision of Dr. Tulin Cil, who is a breast surgical oncologist at Princess Margaret Cancer Centre. The study was performed between September 2020 and February 2021. Data acquisition and analysis were performed away from the hospital. Data were obtained from Surveillance, Epidemiology, and End Results (SEER) database. This study was compliant with the SEER Research Data Use Agreement and was exempt from institutional ethics review at the University Health Network.

DNA METHYLATION BASED PROGNOSTIC SUBTYPES OF CHORDOMA TUMORS IN TISSUE AND PLASMA

Jeffrey A. Zuccato (SSTP),[1,2] Vikas Patil,[1] Sheila Mansouri,[1] Jeffrey C. Liu,[1] Farshad Nassiri (SSTP),[1,2] Yasin Mamatjan,[1] Ankur Chakravarthy,[3] Shirin Karimi,[1] Joao Paulo Almedia,[2] Anne-Laure Bernat,[4] Mohammed Hasen,[5,6] Shahbaz Khan,[3] Thomas Kislinger,[3,7] Namita Sinha,[8] Sébastien Froelich,[4] Homa Adle-Biassette,[9] Kenneth D. Aldape,[10] Daniel D. De Carvalho,[3,7] Gelareh Zadeh[1,2]

[1]MacFeeters Hamilton Neuro-Oncology Program, Princess Margaret Cancer Centre, University Health Network and University of Toronto, Toronto, Ontario, Canada.

[2]Division of Neurosurgery, Department of Surgery, University of Toronto, Toronto, Ontario, Canada.

[3]Princess Margaret Cancer Centre, University Health Network, Toronto, Ontario, Canada.

[4]Neurosurgery Department, Hôpital Lariboisiere, APHP, Université Paris Diderot, Paris, France

[5]Section of Neurosurgery, Division of Surgery, Rady Faculty of Health Science, University of Manitoba, Winnipeg, Canada.

[6]Department of Neurosurgery, King Fahad University Hospital, Imam Abdulrahman Bin Faisal University, Dammam, Saudi Arabia.

[7]Department of Medical Biophysics, University of Toronto, Toronto, Ontario, Canada.

[8]Department of Pathology, Shared Health, HSC, University of Manitoba, Winnipeg, Manitoba, Canada.

[9]Department of Pathology, Lariboisière Hospital, Assistance Publique - Hôpitaux de Paris, Université de Paris, Paris, France.

[10]Laboratory of Pathology, Center for Cancer Research, National Cancer Institute, Bethesda, MD, USA.

Abstract: Chordomas are rare malignant bone sarcomas of the skull-base and spine with significant variability in patient survival that cannot be reliably predicted using clinical factors or genomic alterations. Here, we show, for the first time, two distinct epigenetic chordoma subtypes with clear differences in prognosis. We characterize the subtype with a poorer disease-specific survival as *Immune-infiltrated* as it shows a higher abundance of immune cells within tumors. In comparison, the subtype with a better survival, termed the *Cellular* type, has a higher tumor cellularity and an enrichment of extracellular matrix and cell-to-cell interaction pathways that are hypomethylated at gene promoters. More notably, we demonstrate that plasma methylome-based non-invasive biomarkers can be used for chordoma diagnosis and prognostic subtyping, which can transform patient treatment by guiding surgical planning decisions. Accordingly, individualized treatment approaches depending on prognostic subtype may balance aggressiveness in extent of resection with the risk for treatment-induced neurological deficits.

Introduction: The identification of molecular tumor subtypes has changed management approaches for many cancers. Bone and central nervous system (CNS) tumors remain an exception, to a large extent, including chordomas. Although chordomas are rare bone sarcomas of the skull-base and spine comprising 1-4% of primary aggressive bone cancers, they cause devastating quality of life impacts due to neurological morbidities, metastasize to other organs in 30-40%, and have a relatively high mortality with 10-year survival being 40%.[1,2] Despite treatment with surgery and radiotherapy according to global consensus guidelines,[1,3] outcomes range extensively with up to 10% surviving under 1 year and one-third living over 20 years.[2]

There are currently no major prognostic factors to identify high-risk patients histopathologically or clinically, apart from treatment details including extent of resection and quality of radiotherapy.[1,3] Genomic[4] and transcriptomic[5] studies have not identified prognostic biomarkers. DNA methylation signatures can accurately diagnose CNS tumors[6] and also prognosticate meningiomas of the CNS.[7] There are a few existing chordoma methylation studies, however, with very small sample sizes and they do not resolve prognostic subtypes.[6,8,9] Here, using samples from multi-institutional sources to generate a larger cohort of chordomas, we identified

methylation-based prognostic subtypes that may allow clinicians to tailor treatment aggressiveness to patient risk.

Furthermore, identifying non-invasive preoperative biomarkers for chordoma diagnosis and prognostication could transform treatment by guiding surgical planning to balance aggressiveness in extent of surgical resection with morbidities associated with loss of neurological function.[1] Here, we also leverage our group's novel liquid biopsy approach to explore whether plasma methylated circulating cell-free tumor DNA (cfDNA) obtained by immunoprecipitation and high-throughput sequencing (cfMeDIP-seq) can serve as a reliable biomarker.[10-13]

Methods: DNA methylation profiles were obtained using the Illumina EPIC array on 68 chordoma samples collected over a 22-year period with comprehensive clinical annotation. Consensus clustering of tumors using the top 15,000 most variably methylated CpG sites was performed in the full cohort and in a randomly separated training set (N=37). The most variably methylated CpGs in the training subcohort were used for consensus clustering of the independent testing subcohort for validation. A multivariate Cox analysis with all prognostic variables was performed. Gene-set enrichment analyses (GSEA) assessed genes differentially methylated at promoters to characterize methylation clusters and compare tumors by location. A cell deconvolution analysis using methylCIBERSORT assessed tumor immune cell compositions. Leukocytes unmethylation for purity (LUMP) estimates evaluated tumor purity.

A total of 36 plasma cfDNA methylomes were obtained from matched chordoma patients (with tumor methylation profiles) together with meningioma and spine metastasis patients that have clinical entities commonly included in chordoma differential diagnoses. Samples were randomly split into fifty 80% training and 20% testing sets. The top 300 differentially methylated regions (DMRs) in each pairwise comparison between tumor types in training sets were combined for multidimensional scaling (MDS) plotting. Fifty negative-binomial generalized linear models for each tumor type were built using DMRs derived from training sets. Models were evaluated in corresponding independent testing sets with areas under receiver operating characteristic curves (AUROC) to assess discriminative capacity in distinguishing tumor types.[10,11] For representative cases having this clinical differential diagnosis, class probabilities from all one-class-versus-other models that included the tumor of interest in the testing set were calculated to assess model accuracy.

To evaluate whether plasma methylation signals are representative of the methylation patterns in chordoma tumors, Pearson's correlation coefficients were computed for each patient between normalized cfMeDIP-seq read counts at each region and averaged EPIC array beta values for CpGs in the region.

Results

Prognostic methylation subtypes - This cohort represents a range of clinical presentations with 55% females included, all adult ages represented (18-80 years), and a balance between skull-base (64%) and spinal (36%) tumor locations. Patient treatment included a gross-total resection (GTR) in 39%, subtotal resection (STR) in 61%, and adjuvant radiotherapy in 69%. Consensus clustering of tumors identified two stable clusters shown in Figure 1a; cluster 1 with a statistically significant poorer disease-specific survival than cluster 2 (Figure 1b, median 6.0 vs. 17.3 years, log-rank p=0.0062). Consensus clustering of both randomly divided training and testing sets using features derived in the training set identified prognostic clusters in each (Supplementary Figure 1a-b, training: p=0.011, testing: p=0.0081). In a multivariate analysis combining prognostic clinical factors with methylation-based clusters (Supplementary Figure 1c), cluster 1 (hazard ratio (HR)=16.5, 95% confidence interval (CI)=2.8-96.1, p=0.0018), subtotal resection (HR=8.9, 95% CI=1.2-67.1, p=0.0336), and non-receipt of adjuvant

radiotherapy (HR=9.5, 95% CI=1.7-52.8, p=0.0103) all independently predicted poorer survival with statistical significance.

Subtype characterization - A GSEA of genes differentially methylated at promoters (Supplementary Figure 1d) identified significant pathways with hypomethylated gene promoters, typically resulting in transcription, for each cluster (Figure 1c). Cluster 1 pathways were mainly immune- and transcription/translation-related while those in cluster 2 included cell-to-cell interaction, extracellular matrix, and angiogenesis pathways. Accordingly, cluster 1 was termed the *Immune-infiltrated* subtype and cluster 2 the *Cellular* subtype. Although tumor location was not predictive of disease-specific survival (univariate Cox p=0.1593), the GSEA in Supplementary Figure 1e revealed pathways with treatment-related implications[14] including both kinase activity (encompassing *PDGFR* and *KIT* genes) and vascular proliferation hypomethylated pathways that are enriched in spinal chordomas.

A greater abundance of neutrophils (7.0 fold, p<0.0001), B lymphocytes (2.5 fold, p=0.002), and natural killer cells (1.6 fold, p=0.045) was observed in cluster 1 chordomas (Figure 1d). Cytotoxic T lymphocytes with known anti-tumor activity[15] were not differentially abundant between subtypes (Supplementary Figure 1f). Furthermore, tumor purity estimates in Figure 1e are higher in cluster 2, supporting the *Cellular* nature of this subtype (median 0.66 vs. 0.45, p<0.0001).

Non-invasive diagnosis and subtyping - An MDS plot of DMRs between chordomas, meningiomas, and spine metastases obtained from plasma cfDNA methylomes depicts class separation of chordomas from representative clinical differential diagnoses (Figure 2a). The fifty iterations of chordoma-versus-other models differentiated chordomas from meningiomas and spinal metastases with a high discriminative capacity in testing sets (mean AUROC=0.84, 95%CI=0.52-1.00) as shown in Figure 2b.

A high correlation between chordoma tumor tissue methylation values and plasma cfMeDIP-seq signals was observed. Figure 2c displays a representative correlation plot and Pearson coefficients from all correlation plots portrayed in Figure 2d show high tumor-to-plasma correlations for both Immune-infiltrated (median r=0.69, 95%CI=0.66-0.72, $p<2.2x10^{-16}$ for all) and Cellular chordomas (median r=0.67, 95%CI=0.62-0.72, $p<2.2x10^{-16}$ for all). The top 7000 DMRs between subtypes distinguish them by hierarchical clustering (Figure 2e).

We illustrate two clinical cases in Figure 2f-g where two expert neuroradiologists provided top differential diagnoses of a skull-base meningioma (f) and a spinal metastasis (g). Histopathology confirmed chordoma diagnoses in these patients and the cfMeDIP-seq based models accurately diagnosed both cases.

Discussion: In this study we demonstrate, for the first time, two distinct methylation subtypes of chordoma, which we term *Immune-infiltrated* and *Cellular.* These subtypes have prognostic value independent of clinical factors and resolve the range of chordoma patient outcomes that are not explained by clinical, genomic, or transcriptomic features. We show that non-invasive diagnosis and prognostic subtyping of chordomas using plasma methylomes is possible with high accuracy and a discriminative capacity comparable to what we have shown previously for non-invasive identification of other cancers.[10,11]

We believe non-invasive chordoma prognostication will transform practice by allowing for individualized preoperative treatment planning for patients. Surgery and radiation for chordoma have significant risks due to proximity and involvement of critical neurovascular structures and so avoidance of overtreatment in less aggressive chordomas and more aggressive maximal safe resection in high-risk lesions holds promise for improving patient care.

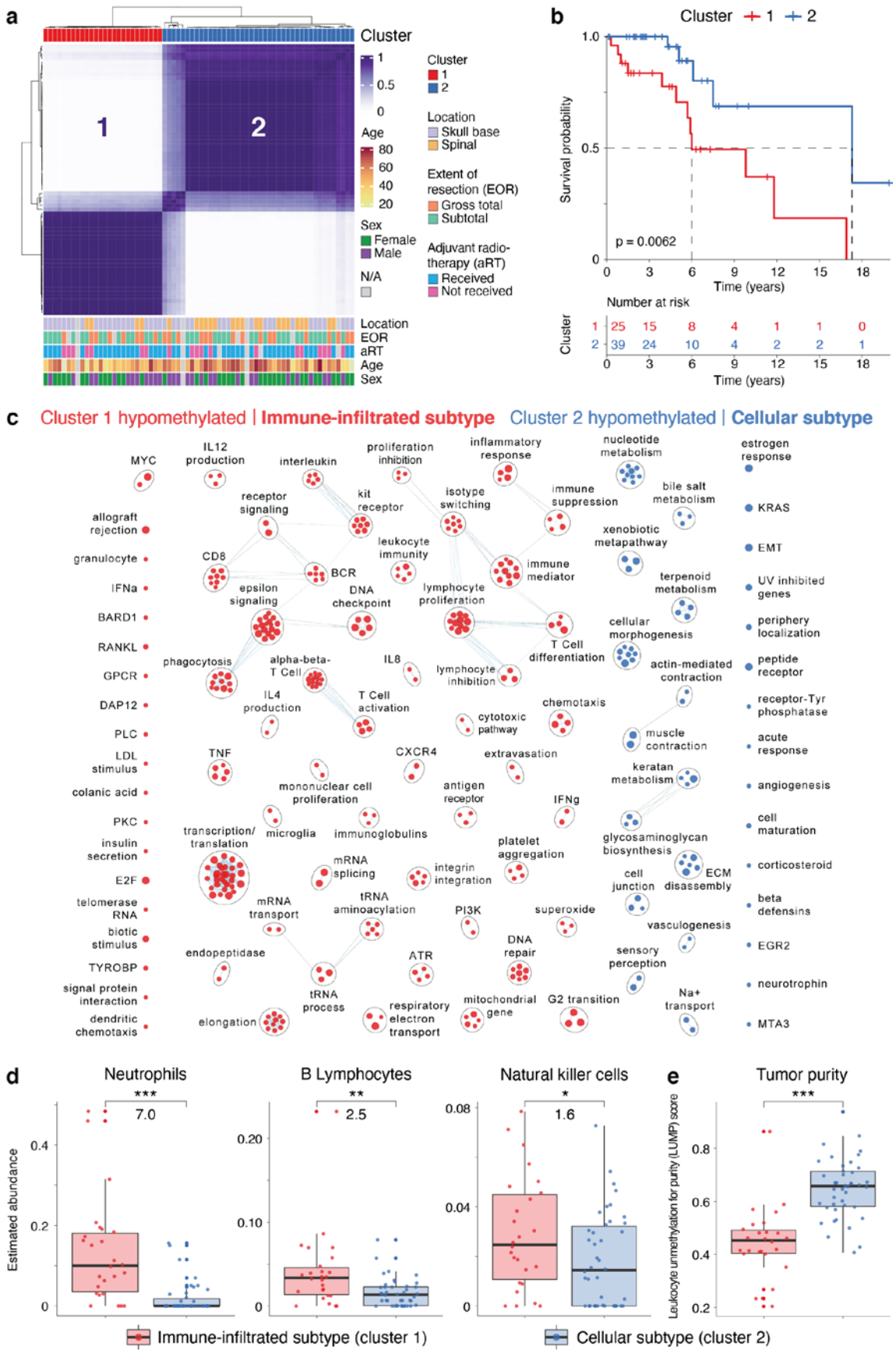
a
Cluster
1
0.5
0
Age
80
60
40
20
Sex
Female
Male
N/A
Location
EOR
aRT
Age
Sex
Cluster
1
2
Location
Skull base
Spinal
Extent of resection (EOR)
Gross total
Subtotal
Adjuvant radio-therapy (aRT)
Received
Not received
b
Cluster 1 2
Survival probability
p = 0.0062
Time (years)
Number at risk
Cluster
1 25 15 8 4 1 1 0
2 39 24 10 4 2 2 1
Time (years)
c
Cluster 1 hypomethylated | Immune-infiltrated subtype
Cluster 2 hypomethylated | Cellular subtype
MYC
IL12 production
interleukin
proliferation inhibition
inflammatory response
nucleotide metabolism
estrogen response
receptor signaling
kit receptor
isotype switching
immune suppression
bile salt metabolism
KRAS
allograft rejection
xenobiotic metapathway
EMT
granulocyte
CD8
BCR
leukocyte immunity
immune mediator
terpenoid metabolism
UV inhibited genes
IFNa
epsilon signaling
DNA checkpoint
lymphocyte proliferation
BARD1
cellular morphogenesis
periphery localization
RANKL
T Cell differentiation
phagocytosis
alpha-beta-T Cell
IL8
lymphocyte inhibition
actin-mediated contraction
peptide receptor
GPCR
IL4 production
T Cell activation
chemotaxis
receptor-Tyr phosphatase
DAP12
cytotoxic pathway
muscle contraction
PLC
TNF
CXCR4
extravasation
acute response
LDL stimulus
keratan metabolism
colanic acid
mononuclear cell proliferation
antigen receptor
IFNg
angiogenesis
PKC
microglia
immunoglobulins
glycosaminoglycan biosynthesis
cell maturation
transcription/ translation
platelet aggregation
insulin secretion
mRNA splicing
integrin integration
ECM disassembly
corticosteroid
E2F
cell junction
telomerase RNA
mRNA transport
tRNA aminoacylation
PI3K
superoxide
beta defensins
biotic stimulus
vasculogenesis
endopeptidase
DNA repair
EGR2
TYROBP
ATR
sensory perception
signal protein interaction
tRNA process
respiratory electron transport
mitochondrial gene
G2 transition
Na+ transport
neurotrophin
dendritic chemotaxis
elongation
MTA3
d
Neutrophils
***
7.0
B Lymphocytes
**
2.5
Natural killer cells
*
1.6
Estimated abundance
e
Tumor purity
***
Leukocyte unmethylation for purity (LUMP) score
Immune-infiltrated subtype (cluster 1)
Cellular subtype (cluster 2)

Fig. 1 | **Tumor DNA methylation signatures identify two prognostic chordoma subtypes.** **a**, Consensus clustering of chordomas using the 15,000 most variably methylated CpG sites. **b**, Disease-specific survival is statistically significantly poorer in cluster 1 than 2. **c**, GSEA showing enrichment of immune pathways with genes hypomethylated at promoters in cluster 1 ("Immune-infiltrated subtype") and cell interaction combined with extracellular matrix pathways in cluster 2 ("Cellular subtype"). **d**, Boxplots of deconvoluted tumor cell compositions, with fold changes between clusters displayed, showing greater immune cell abundance in Immune-infiltrated (cluster 1) tumors. **e**, Boxplots showing higher tumor purity estimates in Cellular chordomas (cluster 2). ***p<0.00005, **p<0.005, *p<0.05.

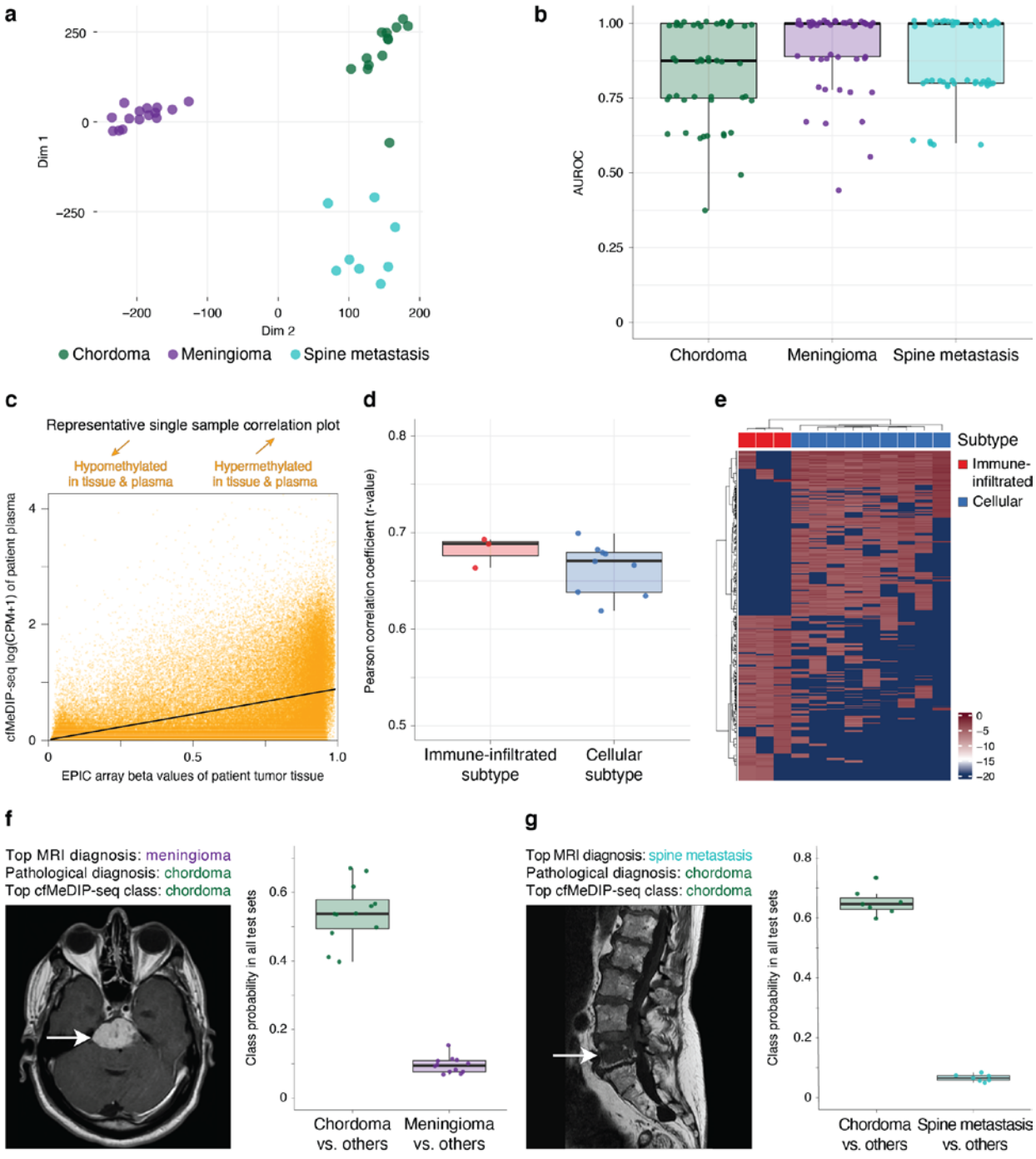

Fig. 2 | **Plasma cfDNA methylomes distinguish chordomas from other clinical differential diagnoses and detect chordoma subtypes. a**, MDS plot using DMRs between chordomas and differential diagnoses. **b**, Boxplots of AUROC values across 50 iterations of one-class-versus-other models show accurate discrimination of chordomas from differential diagnoses. **c**, Representative single-patient scatterplot showing correlation between tumor methylation and plasma methylome signals. **d**, Boxplots of Pearson coefficients from all patient scatterplots show strong tumor-to-plasma methylation signal correlations in both subtypes. **e**, Hierarchical clustering using 7000 DMRs between subtypes. **f-g**, Representative clinical cases where neuroimaging suggested skull-base meningioma (**f**) or spine metastasis (**g**) diagnoses. Top plasma methylome classes were consistent with final neuropathological diagnoses of chordoma.

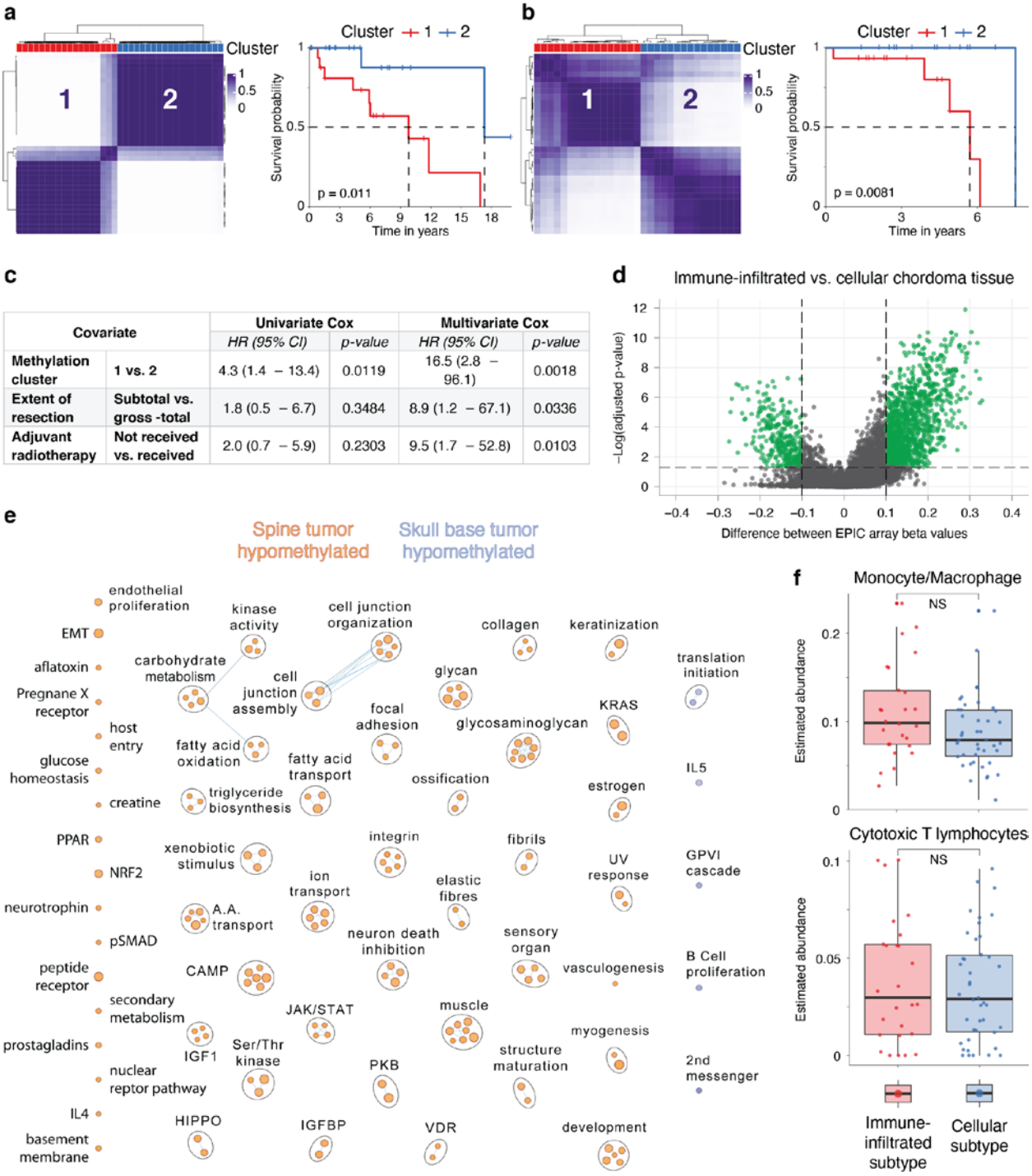

Supplementary Fig. 1 | **Validation of chordoma subtypes and location-specific signatures. a**, Consensus clustering of 37 chordoma tissue samples in a randomly selected training subcohort using the top 15,000 most variably methylated CpG sites identifies two prognostic clusters. **b**, Clustering of 31 testing subcohort samples using CpGs from **a** similarly shows prognostic clusters. **c**, Multivariate Cox analysis identifies methylation cluster as well as extent of resection and adjuvant radiotherapy use as independently prognostic factors. **d**, Volcano plot of 1601 genes with differentially methylated promoters between clusters. **e**, GSEA showing main pathways with hypomethylated gene promoters between skull-base and spinal chordomas. **f**, Boxplots of deconvoluted tumor immune cell compositions with similar abundance between clusters. HR, hazard ratio; CI, confidence interval; NS, not significant.

References

1. Stacchiotti S, Sommer J. Building a global consensus approach to chordoma: a position paper from the medical and patient community. *Lancet Oncol.* 2015; 16(2):e71-83.
2. Smoll NR, Gautschi OP, Radovanovic I, Schaller K, Weber DC. Incidence and relative survival of chordomas: the standardized mortality ratio and the impact of chordomas on a population. *Cancer.* 2013; 119(11):2029-2037.
3. Stacchiotti S, Gronchi A, Fossati P, et al. Best practices for the management of local-regional recurrent chordoma: a position paper by the Chordoma Global Consensus Group. *Ann Oncol.* 2017; 28(6):1230-1242.
4. Tarpey PS, Behjati S, Young MD, et al. The driver landscape of sporadic chordoma. *Nat Commun.* 2017; 8(1):890.
5. Bell AH, DeMonte F, Raza SM, et al. Transcriptome comparison identifies potential biomarkers of spine and skull base chordomas. *Virchows Arch.* 2018; 472(3):489-497.
6. Capper D, Jones DTW, Sill M, et al. DNA methylation-based classification of central nervous system tumours. *Nature.* 2018; 555(7697):469-474.
7. Olar A, Wani KM, Wilson CD, et al. Global epigenetic profiling identifies methylation subgroups associated with recurrence-free survival in meningioma. *Acta Neuropathol.* 2017; 133(3):431-444.
8. Alholle A, Brini AT, Bauer J, et al. Genome-wide DNA methylation profiling of recurrent and non-recurrent chordomas. *Epigenetics.* 2015; 10(3):213-220.
9. Rinner B, Weinhaeusel A, Lohberger B, et al. Chordoma characterization of significant changes of the DNA methylation pattern. *PLoS One.* 2013; 8(3):e56609.
10. Shen SY, Singhania R, Fehringer G, et al. Sensitive tumour detection and classification using plasma cell-free DNA methylomes. *Nature.* 2018; 563(7732):579-583.
11. Nassiri F, Chakravarthy A, Feng S, et al. Detection and discrimination of intracranial tumors using plasma cell-free DNA methylomes. *Nat Med.* 2020; 26(7):1044-1047.
12. Nuzzo PV, Berchuck JE, Korthauer K, et al. Detection of renal cell carcinoma using plasma and urine cell-free DNA methylomes. *Nat Med.* 2020; 26(7):1041-1043.
13. Shen SY, Burgener JM, Bratman SV, De Carvalho DD. Preparation of cfMeDIP-seq libraries for methylome profiling of plasma cell-free DNA. *Nat Protoc.* 2019; 14(10):2749-2780.
14. Meng T, Jin J, Jiang C, et al. Molecular Targeted Therapy in the Treatment of Chordoma: A Systematic Review. *Front Oncol.* 2019; 9:30.
15. Kim S, Kim A, Shin JY, Seo JS. The tumor immune microenvironmental analysis of 2,033 transcriptomes across 7 cancer types. *Sci Rep.* 2020; 10(1):9536.

EVALUATING VARIATION IN PERIOPERATIVE RED BLOOD CELL TRANSFUSION FOR PATIENTS UNDERGOING ELECTIVE GASTROINTESTINAL CANCER SURGERY: A POPULATION-BASED ANALYSIS

Jesse Zuckerman (SSTP)[1,2], Natalie Coburn[1-4], Jeannie Callum[5,6], Alyson L Mahar[7], Yulia Lin[5,6], Alexis F Turgeon[8,9], Robin McLeod[10], Emily Pearsall[10], Guillaume Martel[11], Julie Hallet[1-4]

[1]Division of General Surgery, Department of Surgery, University of Toronto, Toronto, Ontario, Canada
[2]Institute of Health Policy, Management, and Evaluation, University of Toronto, Toronto, Ontario, Canada
[3]Division of General Surgery, Sunnybrook Health Sciences Centre, Toronto, Ontario, Canada
[4]Evaluative Clinical Sciences, Sunnybrook Research Institute, Toronto, Ontario, Canada
[5]Department of Laboratory Medicine and Molecular Diagnostics, Sunnybrook Health Sciences Centre, Toronto, Ontario, Canada
[6]Department of Laboratory Medicine and Pathobiology, University of Toronto, Toronto, Ontario, Canada
[7]Manitoba Centre for Health Policy, Department of Community Health Sciences, University of Manitoba, Winnipeg, Manitoba, Canada
[8]CHU de Québec – Université Laval Research Centre, Population Health and Optimal Health Practices Research Unit (Trauma - Emergency - Critical Care Medicine), Université Laval, Québec City, Quebec, Canada
[9]Department of Anesthesiology and Critical Care Medicine, Division of Critical Care Medicine, Faculty of Medicine, Université Laval, Québec City, Quebec, Canada
[10]Department of Surgery, University of Toronto, Toronto, Ontario, Canada
[11]Department of Surgery, University of Ottawa, Ottawa, Ontario, Canada

INTRODUCTION - Patients undergoing surgery to remove gastrointestinal cancer often receive red blood cell (RBC) transfusions.[1-3] Anemia caused by their underlying malignancy, previous chemotherapy, or poor nutrition may be exacerbated by major operations with the potential for significant blood loss.[4,5] While perioperative anemia itself carries risks of postoperative morbidity and mortality, there is evidence that correcting anemia with RBC transfusions is not necessarily associated with better patient outcomes and that transfusions can actually worsen outcomes.[6] Several studies have demonstrated associations between RBC transfusions and increased postoperative morbidity, such as infections, cardiac events and respiratory failure, short-term mortality, cancer recurrence, and shortened survival.[3,7-9] Balancing both the risks of anemia and transfusions with the potential benefits of transfusions is difficult. This is especially pertinent in cancer patients as avoiding postoperative complications may improve their prognosis.

Reducing transfusion use has the potential to improve patient outcomes while minimizing resource costs.[10] Efforts to limit transfusion use with restrictive transfusion strategies and patient blood management programs have therefore grown.[11] Yet, considerable variation in transfusion practice has been reported among different settings and patient populations.[12-21] While many studies have documented that variation exists, few address the factors that underlie this variation nor quantify the importance of both non-modifiable and modifiable patient, physician, and hospital factors. Furthermore, no studies have evaluated variation in transfusion use in a contemporary cohort of patients undergoing gastrointestinal cancer surgery. Given the evolution of the evidence base and transfusion guidelines over the past two decades, transfusion practice is changing.[2,22] Lastly, most studies exploring and understanding transfusion variation have been performed in the United States healthcare system; there are few studies that have explored transfusion variation in Canada, none of which focused specifically on patients undergoing gastrointestinal surgery.[16-21] Yet, previous work has demonstrated that transfusion use varies between countries.[12,23,24] Given changes in transfusion practice over time and differences in transfusion practice across countries, it is important to assess the extent of and factors underlying this variation in more recent practice in patients undergoing gastrointestinal cancer surgery in Canada.

Minimizing transfusion variation is an actionable target to better transfusion practices and patient outcomes. Defining the factors that underlie practice variation will help identify and target opportunities for improvement. Given that RBC transfusion overutilization is a burden for patients, healthcare institutions, and the health system, we aimed to measure the extent and importance

of variation in perioperative RBC transfusion use across surgeons and hospitals among gastrointestinal cancer surgery patients with an ultimate goal of instigating change and improving patient care.

METHODS - This retrospective, population-based cohort study included adults who underwent elective resection for gastrointestinal cancer between January 1, 2007 and March 31, 2019 in Ontario, Canada. We used several routinely collected administrative healthcare datasets stored and analyzed at ICES (formerly the Institute for Clinical Evaluative Sciences) that were linked using unique and encoded identifiers. Use of the data was approved by the Sunnybrook Health Sciences research ethics board and was authorized under section 45 of Ontario's Personal Health Information Act.

We identified all individuals ≥ 18 years old in the Ontario Cancer Registry with a diagnosis of gastrointestinal cancer (esophageal, gastric, small bowel, colon, rectal, hepatic, biliary, or pancreatic) and retained those who had a documented surgical resection (esophagectomy, gastrectomy, small bowel resection, colectomy, proctectomy, hepatobiliary resection, pancreatectomy, or multivisceral resection) in the Canadian Institute for Health Information Discharge Abstract Database (CIHI-DAD) between 3 months prior and 6 months after diagnosis. Patients were then linked to individual surgeons and admitting hospitals.

The outcome of interest was perioperative RBC transfusions, defined as the receipt of 1 or more unit of allogeneic RBCs from the date of hospital admission to discharge. RBC transfusion provision is documented in CIHI-DAD as a dichotomous variable, either transfused or not. Documentation of transfusion provision is mandatory in CIHI-DAD.[25]

Several variables were considered as potential factors influencing the use of and variation in RBC transfusion use. Patient-, surgeon-, and hospital-level factors were chosen for examination using a modified Donabedian conceptual framework for health services, which examines the components of quality health care.[26,27] Putative risk factors were selected *a priori* if: based on existing literature they represented a clinically-relevant antecedent condition, structure of care, or process of care; occurred prior to transfusion; and represented a unique conceptual domain, thus mitigating against collinearity.

Descriptive statistics evaluated patient, surgeon, and hospital characteristics. To measure the extent of variation across surgeons and hospitals, we calculated crude and adjusted proportions of transfused patients for surgeons and hospitals with indirect standardization adjusting for patient-level risk factors.[28] Variation was graphically represented using funnel plots in which surgeons' and hospitals' adjusted proportions were plotted against their median annual gastrointestinal resection volume.[29] To estimate the adjusted association between patient, surgeon, and hospital factors and transfusion, we used three-level hierarchical logistic regression with surgeons and hospitals as random intercepts. Estimates were described as odds ratios (OR) and 95% confidence intervals (CI). To characterize the contribution of individual surgeons and hospitals to variation in transfusion use, we used the covariance test and calculated the variance partition coefficients (VPC) and median ORs for each level. The VPC represents the proportion of the total observed variation in the outcome that is attributable to systematic differences between surgeons or hospitals.[30] The median OR is a measure that quantifies the magnitude of heterogeneity and represents the median value of all possible ratios of the odds of transfusion in 2 patients with the same covariates treated by or admitted to 2 randomly selected distinct surgeons or hospitals.[30] To characterize the contribution of patient-level factors to variation in transfusion use, we calculated an R^2-type measure created for hierarchical models that quantifies the proportion of the total observed variation explained by factors included in the model.[31] To evaluate how variation may differ among procedures, we performed subgroup analyses in four procedure type subgroups. Given significant missingness of hemoglobin levels, we analyzed the contribution of pre-operative anemia only among patients with recorded values who had surgery in recent study years. We conducted analyses using SAS Enterprise Guide 7.1 (SAS Institute,

Cary, NC, USA) and created graphics using R software (v4.0.2). Two-sided p-values < 0.05 were considered statistically significant.

RESULTS - There were 59,964 patients included who underwent elective gastrointestinal cancer resection. Median patient age was 69 years (IQR 59-77) and the majority of patients were male (56.8%). Patients most commonly underwent either colectomy (49.2%) or proctectomy (26.6%). Of patients who had pre-operative hemoglobin levels captured (n=31,958, 53.3%), 56.1% were anemic in the pre-operative period. A roughly equal distribution of patients had surgery over the study years. Patients were treated by 616 surgeons and admitted to 81 hospitals.

Perioperative RBC transfusions were given to 18.0% (n=10,768) of the study cohort. There was marked variation in transfusion use observed across surgeons and hospitals before adjusting for patient case-mix: the crude proportion of transfused patients for individual surgeons ranged from 0% to 70% (median 17.9%, IQR 12.2-24.5%) and from 5.8 to 34.2% for individual hospitals (median 16.5%, IQR 14.2-21.3%). After adjustment for patient factors, the surgeon- and hospital-level proportions of transfused patients for still varied widely (surgeon: 0 to 67.9%; hospital: 5.0 to 44.5%). Funnel plots demonstrated that the variation in transfusion use was in excess of what would be expected by chance alone, as shown by many surgeons and several hospitals that are found outside the 95% confidence limits (**Figure 1**).

After adjustment for patient demographics, comorbidities, procedural details, and surgeon and hospital characteristics, several patient-level factors were associated with increased odds of RBC transfusion use, whereas both physician and hospital factors did not have important associations with transfusion use (**Figure 2**). Patient-level factors with the strongest association with transfusion use were increased age, cardiac comorbidity, neoadjuvant therapy, complex procedure types (esophageal, gastric, hepato-pancreato-biliary, and multivisceral resections), and an open resection approach.

Patient demographics, comorbidities, and procedural factors explained 12.8% of the variation in transfusion use (R^2 0.128). Moreover, both the individual treating surgeons and admitting hospitals contributed significantly to the variation in transfusion use ($p < 0.001$) and were determinants of patients' likelihood of transfusion. Of the residual variation in transfusion use that existed after adjusting for patient factors, 2.8% was due to systematic differences between physicians (VPC 0.28) and 2.1% was due to systematic differences between hospitals (VPC 0.21). This translated to a surgeon-level median OR of 1.35 (95% CI 1.30-1.40) and hospital-level median OR of 1.30 (95% CI 1.23-1.42), suggesting that, after adjusting for patient case-mix, there is an approximately 30% difference in the odds of transfusion for 2 similar patients treated by distinct surgeons or admitted to distinct hospitals (**Table 1**). In comparison with other determinants of transfusion, the treating surgeon and admitting hospital were as important as patient factors such as sex and comorbidity burden and more strongly associated with transfusion use than any specific physician or hospital factor (**Figure 2**).

We observed comparable effects across procedure-type subgroups (**Table 1**). In a sub-cohort of patients with recorded hemoglobin concentrations, pre-operative anemia had the strongest association with transfusion relative to all other risk factors after adjusting for patient-, surgeon-, and hospital-level factors (OR 3.99, 95% CI 3.38-4.71). A model including pre-operative anemia explained a larger amount of variation in transfusion use (R^2 0.213), such that pre-operative anemia alone incrementally explained 9.0% of the variation. Adjusting for pre-operative anemia, however, did not meaningfully alter the previously observed median odds of transfusion attributable to individual physicians (median OR 1.41, 95% CI 1.29-1.67) or hospitals (median OR 1.48, 95% CI 1.34-1.82).

CONCLUSIONS - This goal of our study was to describe and understand the variation in RBC transfusion use among physicians and hospitals who treated patients that underwent gastrointestinal cancer surgery. We observed a wide variation in surgeon and hospital transfusion practices. While transfusion provision is patient-dependent, the impact of the treating surgeon

and hospital on variation relative to other factors is important and reflects opportunities to target modifiable structures and processes to optimize perioperative care. By measuring the extent of between-physician and between-hospital variation in RBC transfusion use and exploring factors that may explain this variation, this work has contributed clinically important foundational information to help guide future transfusion-related research and policy decisions both in the provincial context and beyond. Improving transfusion use is crucial to help better patient outcomes and manage scarce resources and costs. Understanding individual or institutional transfusion practices is paramount to the development of effective, meaningful quality improvement programs with a goal of standardizing perioperative transfusion practices to improve outcomes for gastrointestinal cancer patients.

References

1. Lucas DJ, Schexneider KI, Weiss M, et al. Trends and risk factors for transfusion in hepatopancreatobiliary surgery. *J Gastrointest Surg.* 2014;18(4):719-728.
2. Ecker BL, Simmons KD, Zaheer S, et al. Blood Transfusion in Major Abdominal Surgery for Malignant Tumors: A Trend Analysis Using the National Surgical Quality Improvement Program. *JAMA Surg.* 2016;151(6):518-525.
3. Elmi M, Mahar A, Kagedan D, et al. The impact of blood transfusion on perioperative outcomes following gastric cancer resection: an analysis of the American College of Surgeons National Surgical Quality Improvement Program database. *Canadian journal of surgery Journal canadien de chirurgie.* 2016;59(5):322-329.
4. Weber RS, Jabbour N, Martin II RC. Anemia and transfusions in patients undergoing surgery for cancer. *Annals of surgical oncology.* 2008;15(1):34-45.
5. Munoz M, Laso-Morales M, Gomez-Ramirez S, Cadellas M, Nunez-Matas M, Garcia-Erce J. Pre-operative haemoglobin levels and iron status in a large multicentre cohort of patients undergoing major elective surgery. *Anaesthesia.* 2017;72(7):826-834.
6. Shander A, Fink A, Javidroozi M, et al. Appropriateness of allogeneic red blood cell transfusion: the international consensus conference on transfusion outcomes. *Transfus Med Rev.* 2011;25(3):232-246.e253.
7. Hill GE, Frawley WH, Griffith KE, Forestner JE, Minei JP. Allogeneic blood transfusion increases the risk of postoperative bacterial infection: a meta-analysis. *The Journal of trauma.* 2003;54(5):908-914.
8. Bernard AC, Davenport DL, Chang PK, Vaughan TB, Zwischenberger JB. Intraoperative transfusion of 1 U to 2 U packed red blood cells is associated with increased 30-day mortality, surgical-site infection, pneumonia, and sepsis in general surgery patients. *Journal of the American College of Surgeons.* 2009;208(5):931-937, 937.e931-932; discussion 938-939.
9. Amato A, Pescatori M. Perioperative blood transfusions for the recurrence of colorectal cancer. *Cochrane Database Syst Rev.* 2006(1):Cd005033.
10. LaPar DJ, Crosby IK, Ailawadi G, et al. Blood product conservation is associated with improved outcomes and reduced costs after cardiac surgery. *J Thorac Cardiovasc Surg.* 2013;145(3):796-803; discussion 803-794.
11. Mueller MM, Van Remoortel H, Meybohm P, et al. Patient Blood Management: Recommendations From the 2018 Frankfurt Consensus Conference. *Jama.* 2019;321(10):983-997.
12. Bennett-Guerrero E, Zhao Y, O'Brien SM, et al. Variation in use of blood transfusion in coronary artery bypass graft surgery. *Jama.* 2010;304(14):1568-1575.
13. Qian F, Osler TM, Eaton MP, et al. Variation of blood transfusion in patients undergoing major noncardiac surgery. *Ann Surg.* 2013;257(2):266-278.
14. Aquina CT, Blumberg N, Probst CP, et al. Large Variation in Blood Transfusion Use After Colorectal Resection: A Call to Action. *Dis Colon Rectum.* 2016;59(5):411-418.

15. Surgenor DM, Wallace EL, Churchill WH, Hao SH, Chapman RH, Poss R. Red cell transfusions in total knee and total hip replacement surgery. *Transfusion.* 1991;31(6):531-537.
16. Hutcheon JA, Chapinal N, Skoll A, Au N, Lee L. Inter-hospital variation in use of obstetrical blood transfusion: a population-based cohort study. *BJOG.* 2020;127(11):1392-1398.
17. Hébert PC, Wells G, Martin C, et al. Variation in red cell transfusion practice in the intensive care unit: a multicentre cohort study. *Crit Care.* 1999;3(2):57-63.
18. Qiang JK, Thompson T, Callum J, Pinkerton P, Lin Y. Variations in RBC and frozen plasma utilization rates across 62 Ontario community hospitals. *Transfusion.* 2019;59(2):545-554.
19. Cote C, MacLeod JB, Yip AM, et al. Variation in transfusion rates within a single institution: exploring the effect of differing practice patterns on the likelihood of blood product transfusion in patients undergoing cardiac surgery. *J Thorac Cardiovasc Surg.* 2015;149(1):297-302.
20. Karkouti K, Wijeysundera DN, Beattie WS, et al. Variability and predictability of large-volume red blood cell transfusion in cardiac surgery: a multicenter study. *Transfusion.* 2007;47(11):2081-2088.
21. Hutton B, Fergusson D, Tinmouth A, McIntyre L, Kmetic A, Hébert PC. Transfusion rates vary significantly amongst Canadian medical centres. *Canadian Journal of Anaesthesia.* 2005;52(6):581-590.
22. Zuckerman J, Coburn N, Callum J, et al. Declining Use of Red Blood Cell Transfusions for Gastrointestinal Cancer Surgery: A Population-Based Analysis. *Annals of surgical oncology.* 2020.
23. Vincent JL, Jaschinski U, Wittebole X, et al. Worldwide audit of blood transfusion practice in critically ill patients. *Crit Care.* 2018;22(1):102.
24. *Global status report on blood safety and availability 2016.* Geneva: World Health Organization;2017.
25. DAD Data Elements 2018–2019. https://www.cihi.ca/sites/default/files/document/dad-data-elements-2018-en-web.pdf. Accessed Feb 15, 2020.
26. Donabedian A. *An Introduction to Quality Assurance in Health Care.* New York, NY: Oxford University Press; 2003.
27. Coyle YM, Battles JB. Using antecedents of medical care to develop valid quality of care measures. *Int J Qual Health Care.* 1999;11(1):5-12.
28. Schwartz M, Ash A, Iezzoni L. Comparing outcomes across providers. In: LI I, ed. *Risk adjustment for measuring healthcare outcomes.* Chicago, IL: Health Administration Press; 1997.
29. Spiegelhalter DJ. Funnel plots for comparing institutional performance. *Stat Med.* 2005;24(8):1185-1202.
30. Austin PC, Merlo J. Intermediate and advanced topics in multilevel logistic regression analysis. *Stat Med.* 2017;36(20):3257-3277.
31. Snijders T, Bosker R. *Multilevel Analysis: An Introduction to Basic and Advanced Multilevel Modeling.* London: Sage Publications; 2012.

Disclaimers: This study was supported by ICES, which is funded by an annual grant from the Ontario Ministry of Health and Long-Term Care (MOHLTC). Parts of this material are based on data and/or information compiled and provided by CIHI. However, the analyses, conclusions, opinions and statements expressed in the material are those of the author(s), and not necessarily those of CIHI. Parts of this material are based on data and information provided by Cancer Care Ontario (CCO). The opinions, results, view, and conclusions reported in this paper are those of the authors and do not necessarily reflect those of CCO. No endorsement by CCO is intended or should be inferred.

FIGURE 1: FUNNEL PLOTS DEMONSTRATING VARIATION IN TRANSFUSION PRACTICE AMONG INDIVIDUAL SURGEONS AND HOSPITALS ADJUSTED FOR PATIENT CASE-MIX

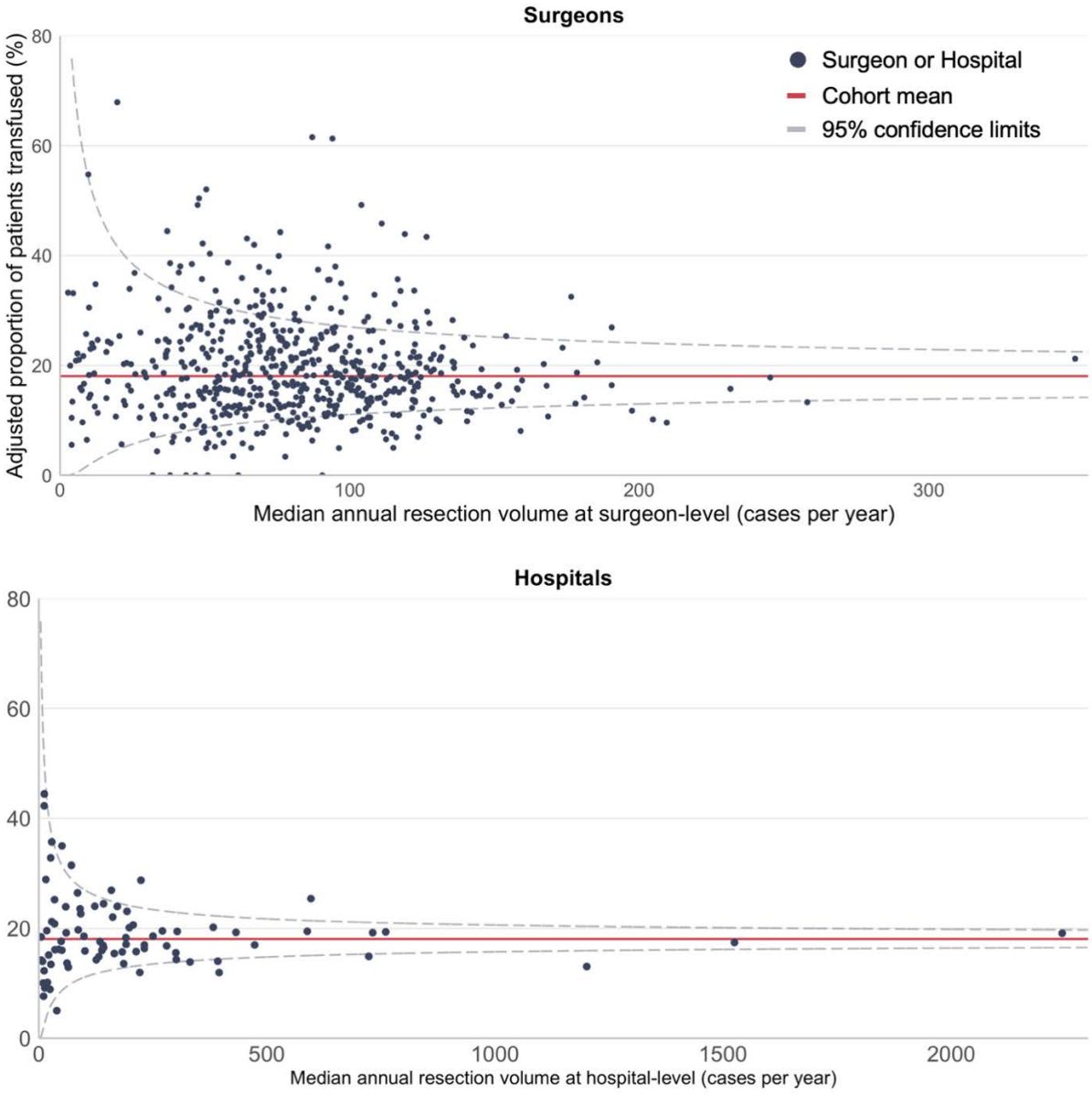

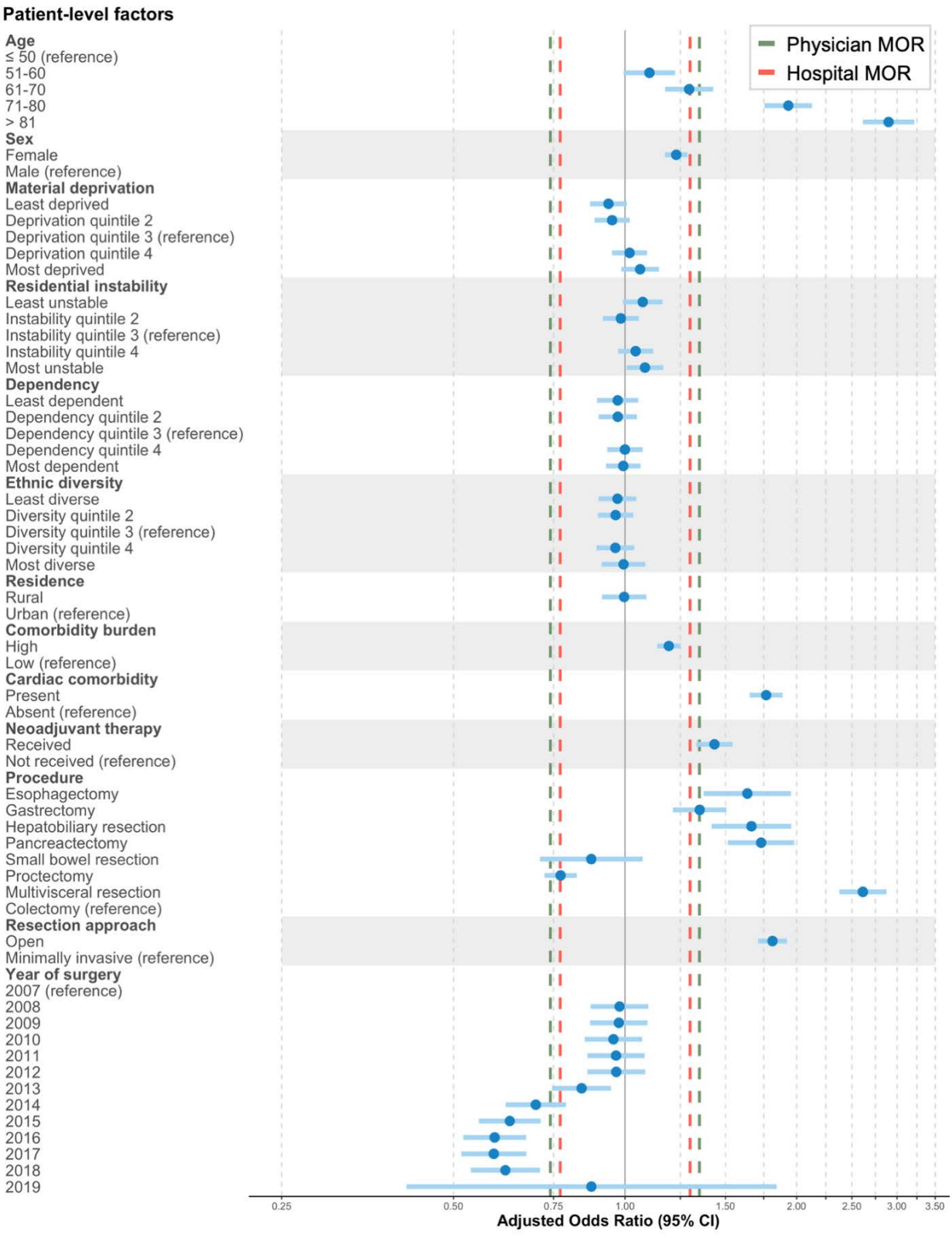
Patient-level factors
Age
≤ 50 (reference)
51-60
61-70
71-80
> 81
Sex
Female
Male (reference)
Material deprivation
Least deprived
Deprivation quintile 2
Deprivation quintile 3 (reference)
Deprivation quintile 4
Most deprived
Residential instability
Least unstable
Instability quintile 2
Instability quintile 3 (reference)
Instability quintile 4
Most unstable
Dependency
Least dependent
Dependency quintile 2
Dependency quintile 3 (reference)
Dependency quintile 4
Most dependent
Ethnic diversity
Least diverse
Diversity quintile 2
Diversity quintile 3 (reference)
Diversity quintile 4
Most diverse
Residence
Rural
Urban (reference)
Comorbidity burden
High
Low (reference)
Cardiac comorbidity
Present
Absent (reference)
Neoadjuvant therapy
Received
Not received (reference)
Procedure
Esophagectomy
Gastrectomy
Hepatobiliary resection
Pancreactectomy
Small bowel resection
Proctectomy
Multivisceral resection
Colectomy (reference)
Resection approach
Open
Minimally invasive (reference)
Year of surgery
2007 (reference)
2008
2009
2010
2011
2012
2013
2014
2015
2016
2017
2018
2019
Physician MOR
Hospital MOR
0.25
0.50
0.75
1.00
1.50
2.00
2.50
3.00
3.50
Adjusted Odds Ratio (95% CI)

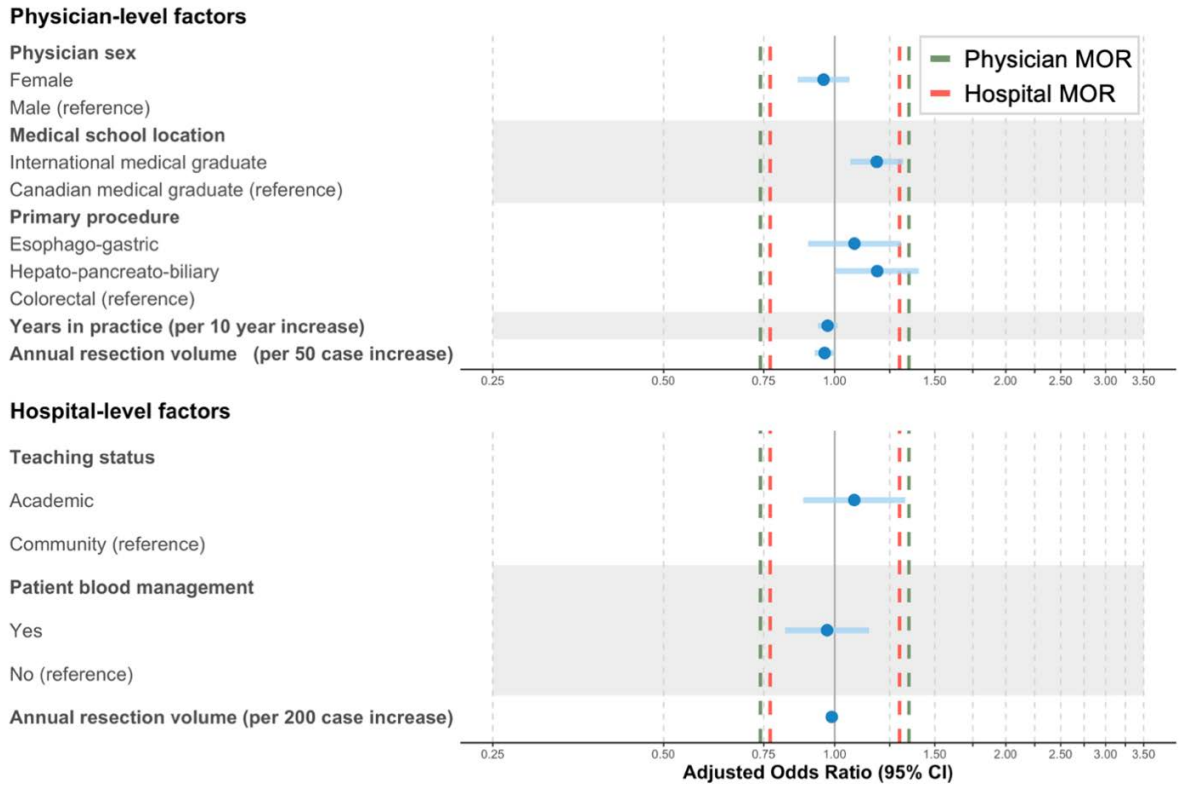

Figure 2: Comparison of the adjusted odds of transfusion associated with patient-, physician-, and hospital-level determinants of transfusion use and the median odds ratio (MOR) of transfusion associated with treating physicians and admitting hospitals

Table 1: Measures of variation in transfusion use among physicians and hospitals for all procedures and procedure type subgroups

	All procedures	Esophago-gastric	Hepato-pancreato-biliary	Entero-colorectal	Multivisceral resection
			Covariance test p-value		
Physician	< 0.001	0.014	0.046	< 0.001	0.018
Hospital	< 0.001	0.030	0.032	< 0.001	0.011
			Variance partition coefficient (%)		
Physician	2.80	2.12	1.28	3.03	3.35
Hospital	2.13	2.07	4.69	1.92	4.12
			Median odds ratio (95% confidence interval)		
Physician	1.35 (1.30-1.40)	1.29 (1.20-1.58)	1.22 (1.14-1.58)	1.36 (1.31-1.44)	1.39 (1.25-1.83)
Hospital	1.30 (1.23-1.42)	1.29 (1.18-1.68)	1.47 (1.29-2.21)	1.28 (1.21-1.41)	1.44 (1.29-1.87)